Numerical Analysis of Installation Faults in Plastic Heave Screens and Their Influence on Piping

Evaluating defects with the use of 2D and 3D numerical models

Koen Heijmans

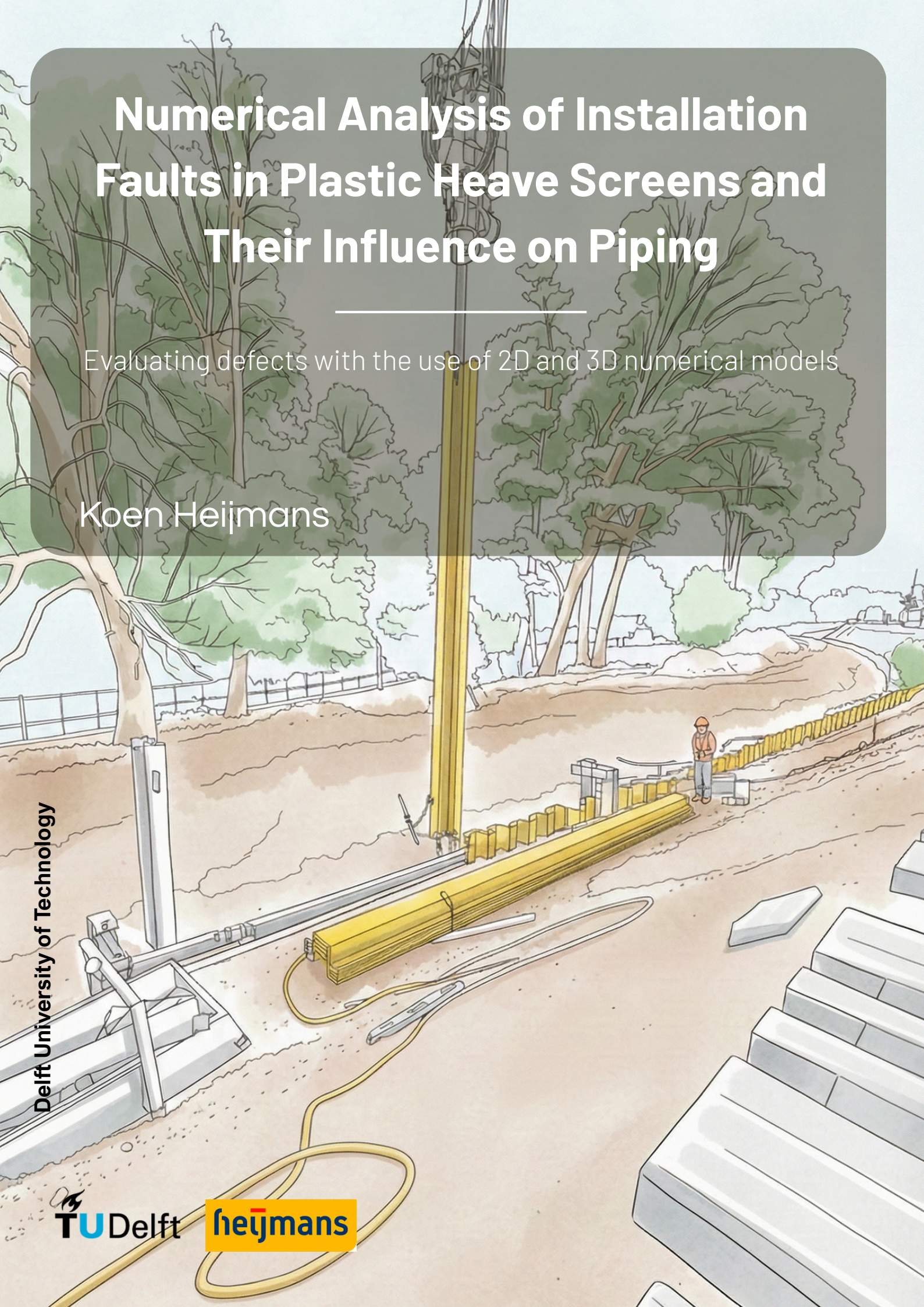

Delft University of Technology

TU Delft heijmans

Technical University Delft

Civil Engineering and Geoscience
CIEM0400 - Master Thesis

NUMERICAL ANALYSIS OF INSTALLATION FAULTS IN PLASTIC HEAVE SCREENS AND THEIR INFLUENCE ON PIPING

Evaluating defects with the use of 2D and 3D numerical models

Koen Heijmans
5009928

March 23, 2026

Committee members:
Mr. Dr. Ir. C. (Cong) Mai Van
Dr. Ir. E. (Vagelis) Kementzetzidis

Supervisor Heijmans:
Ir. H. (Harm) van Oorschot

Preface

This thesis marks the completion of my Master's degree in Civil Engineering and Geosciences at the Delft University of Technology. My decision for this specific research was driven by an interest in hydraulic structures and their critical role in protecting the Netherlands from flooding. The research presented in this report investigates the hydraulic effectiveness of plastic heave screens when subjected to realistic installation related defects. Specifically, it addresses the impact of mandrel extraction and interlock failure, challenges that arise when implementing these innovative and sustainable solutions in Dutch dike reinforcements. By comparing 2D and 3D numerical models, this work aims to provide insights into the reliability of these structures under complex seepage conditions.

I would like to express my gratitude to my committee members at TU Delft, Mr. Dr. Ir. C. (Cong) Mai Van and Dr. Ir. E. (Vagelis) Kementzetzidis, for their academic guidance and feedback throughout this process. I am also very grateful to Heijmans for providing the professional environment and practical resources necessary for the case study. In particular, I would like to thank my supervisor, Ir. H. (Harm) van Oorschot, for his support and help in the process of doing my research. Furthermore, I would like to thank Jaap Wierenga and Rens Servais for their contributions and help during my research.

This thesis is also the end of my studies which I enjoyed very much and gave me many memories. Finally, I want to thank my family and friends for their encouragement and support during my studies.

Koen Heijmans

February 22, 2026

Abstract

Large parts of the Netherlands are situated below sea level, making the country vulnerable to flooding. To prevent flooding, dikes form the most critical measure against flooding. Because of the rising water level and more extreme weather events dikes are being reinforced. One of the most important failure mechanisms of dikes is backward erosion piping (BEP). To prevent this failure mechanism from occurring, heave screens can be used as a vertical impermeable barrier at the inland toe of the dike. While traditional steel sheet piles have been the standard. Lately, plastic heave screens are more used as an innovative, sustainable, and cost effective alternative. However, the lower bending stiffness and strength of plastic require different installation techniques, often in the form of a steel mandrel to guide the piles to their design depth. This mandrel is a steel motherplate which is used to drive the plastic sheet pile safely into the ground. The installation process and the properties of plastic provide new challenges, such as mandrel induced soil disturbance and interlock failure, that are typically neglected in current assessment practice, which assumes ideal, continuous, and undamaged conditions.

The primary objective of this research is to examine how the installation process, or faults that occur during this process, influences the hydraulic effectiveness of plastic heave screens against BEP. Using a representative case study of a Dutch river dike section prone to piping, this study uses a numerical modelling strategy using PLAXIS 2D and 3D. The methodology evaluates the sensitivity of the system to localized defects by analysing key hydraulic indicators: groundwater head distribution for global heave safety, vertical flow velocity, and vertical hydraulic gradients.

Numerical results demonstrate that installation induced faults have a measurable impact on hydraulic performance. 2D analysis reveals that mandrel induced disturbed zones with higher permeability act as a local relief well. This leads to a reduction in hydraulic head at the screen tip, which increases the calculated safety factor for global heave. However, this venting significantly increases vertical flow velocities within the disturbed zone, heightening the risk of internal vertical erosion.

3D modelling is essential for capturing localized delocking, which triggers 3D flow towards the fault that 2D plane-strain models fail to represent. While global head remains largely unaffected by a single isolated delocked sheet pile, the local head at the gap increases significantly, causing local heave safety factors to drop below the required threshold. Furthermore, the study investigated multiple gaps and concluded that clustered defects pose a significantly greater risk than isolated imperfections, as their zones of influence overlap and amplify negative hydraulic consequences.

In conclusion, the hydraulic resistance of plastic heave screens is influenced by installation quality and three dimensional flow effects. It is recommended that future research focuses on the governing mechanisms of vertical fluidization and the development of more realistic 3D representations of pipe systems to bridge the gap between execution reality and safety assessment.

Contents

List of Tables

List of Figures

1 Introduction

In this chapter background information for this research is provided. Furthermore, the problem statement, the knowledge gaps, research scope and research questions are formulated.

1.1. Background information

Large parts of the Netherlands are situated below sea level, making the country vulnerable to flooding. For centuries, dikes have formed the most critical line of defence against the water. However, the task of maintaining this safety is becoming more complex. Climate change is leading to rising water levels and more extreme weather events, which significantly increase the hydraulic load on these defences.

Currently, a large number of Dutch dike sections have been rejected or marked for reinforcement because they no longer meet the safety standards. This is not only due to environmental changes but also a shift in safety assessment that now prioritizes a probabilistic approach, where failure probability of individual components contributes to the overall safety of a dike section. (This probabilistic approach is explained in appendix B. To address the rejection of dikes on safety, the Dutch government established the national High Water Protection Programme (HWBP). This program is the largest dike reinforcement operation since the Delta Works, aiming to reinforce over 1500 kilometers of dikes and 500 hydraulic structures by 2025 (IPM-team, 2021).

Dikes can fail through various mechanisms depending on hydraulic conditions, soil composition, and geometry. These mechanisms can be categorized in four groups: Hydraulic failure, Geo-hydraulic failure, Global stability failure, and External failure. Among these, geo-hydraulic failure is a critical concern for Dutch river dikes.

One of these geo-hydraulic failure modes in Backward Erosion Piping (BEP). This is frequently identified as a governing failure mechanism for dikes founded on permeable sandy aquifers. Piping occurs during periods of high water when a high hydraulic gradient is established between the river side and the land side. Water seeps through the aquifer, carrying small soil particles with it (Rosenbrand et al., 2019).

This process often initiates at the interface between the sand layer and the impermeable cover layer, eventually creating erosion channels or 'pipes'. If these pipes grown they can pose a threat to the stability of the dike. In current Dutch assessment practice, piping contributes to approximately 24% of the total failure space of dikes (see table 1.1), making it a primary focus for reinforcement projects.

Table 1.1: Failure mechanisms and probability factors (Knoeff and van Bree, 2016)

Failure mechanisms	Failure probability factor [-]
Heave and piping	0.24
Failure due to overtopping	0.24
Inner or outer slope failure	0.04
Revetment inner or outer slope	0.10
Construction failure	0.08
Other	0.30
Total	**1.00**

From the HWBP, the desire is constructed for innovative and sustainable dike piping reinforcement solutions (te Riele, 2021). Traditional solutions, such as widening dikes with large seepage berms or steel sheet piles have their disadvantages, like required space or environmental footprint. Consequently, there is a need for space efficient, cost effective and sustainable solutions like plastic heave screens.

Heave screens serve as a vertical barrier installed at the dike toe to block horizontal seepage and force water to follow a longer, vertical path (Wiggers et al., 2025). A schematization can be seen in figure 1.1. While steel sheet piles have been the standard for decades, plastic heave screens have recently emerged as a promising alternative. Plastic screens offer several advantages: they are made from recycled materials, emit less CO_2 during production, are more cost effective and are resistant to corrosion (Hakkers et al., 2023).

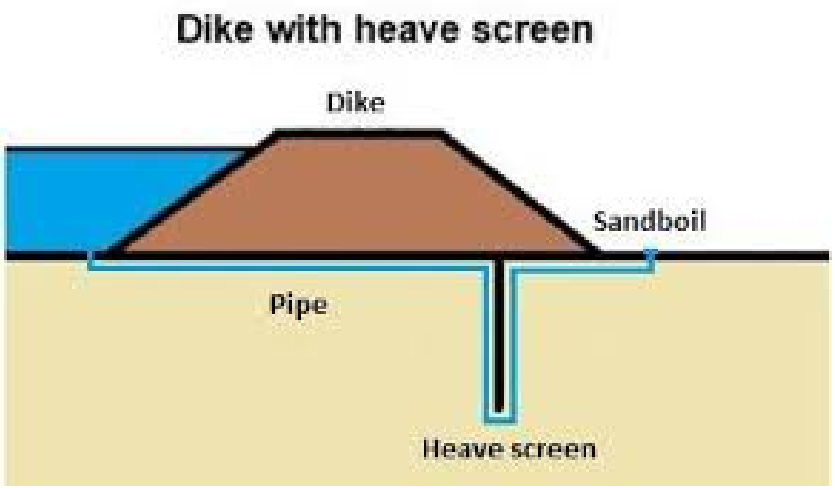

Figure 1.1: Working principle of a heave screen (Raadschelders and Lukas, 2023)

1.2. Problem statement

Despite their advantages, plastic heave screens differ fundamentally from steel sheet piles in terms of material properties. Plastic sheet piles exhibit significantly lower bending stiffness and strength, which limits their structural contribution to dike stability and restricts the installation methods that can be applied (te Riele, 2021). As a result, plastic heave screens cannot be driven using conventional hammering techniques and often require alternative installation procedures (Halter et al., 2025).

These material related limitations introduce additional uncertainties compared to steel. In current practice, the hydraulic performance of heave screens is commonly assessed under the assumptions of ideal installation conditions, meaning that the screen is continuous, undamaged, and fully embedded to the design depth. However, for plastic heave screens, achieving these ideal conditions is more challenging due to the installation risks (Zagema, 2023). The most common installation related problems are:

- Running out of the interlocking connection (delocking)

- Breaking during the installation process
- Long installation time
- Inability to extract sheet piles after installation

(te Riele, 2021, Wiggers et al., 2025, Zagema, 2023).

These installation issues can lead to defects in the heave screen, which directly impact the function of the total screen. In figure 1.2, different failure mechanisms that can occur due to a failing heave screen can be seen:

- Underpass: If the screen does not reach the required depth (IKAMI and MAEDA, 2021).
- Through-pass: If gaps or discontinuities exist, allowing water and soil particles to pass through (Wiggers et al., 2025).
- Overpass/Front pass: If the connection between the top of the screen and the overlying soil is inadequate or the overlying soil is not good enough, a bypass for piping can occur (Wiggers et al., 2025).

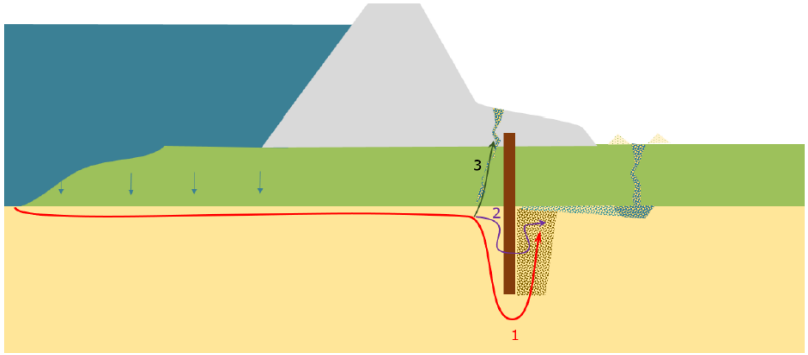

Figure 1.2: Failure mechanisms of broken heave screen. 1. Underpass, 2. Through-pass, 3. Front pass (Wiggers et al., 2025)

The overarching problem is the existence of knowledge gaps and uncertainties around the behaviour and reliability of plastic heave screens. There is little research on heave screens under dikes with cover layers, complexities in pipe formations around screens and challenges in assessing reliability after installation (Wiggers et al., 2025). Current assessment methods include a lot of assumptions, which could lead to a wrong conclusion on the safety of heave screens (te Riele, 2021). Furthermore, experience with long-term management and maintenance of plastic heave screens is limited (Halter et al., 2025).

1.3. Knowledge gaps

Although plastic heave screens are applied more and more in practice, large scale use is relatively recent. As a result, several knowledge gaps remain regarding their behaviour, reliability, and long-term performance (Wiggers et al., 2025).

One important knowledge gap concerns the installation process of plastic heave screens using a steel mandrel, which is a steel mother plate used to drive the plastic sheet pile safely into the ground (see figure 1.3). Due to the limited strength of plastic, a steel mandrel is often used to guide the pile into the ground. After the plastic pile reaches the required depth, the mandrel is extracted, potentially leaving behind a gap or zone of disturbed soil.

In current assessment practice, it is commonly assumed that if the mandrel is used in between the dike and the plastic sheet pile, the disturbed zone or gap left behind after extraction has a negligible effect on the hydraulic performance of the heave screen. However, this assumption has not been sufficiently validated, and the impact of such installation-induced disturbances on seepage flow and piping remains unclear.

Additional knowledge gaps include:

- The influence of local installation defects on the effectiveness of a heave screen along a dike section
- The limitations of 2D assessment models in representing inherently 3D piping processes
- Uncertainties related to spatial variability in subsoil conditions, particularly in older dikes (Halter et al., 2025).

These gaps indicate that both scientific understanding and practical assessment methods may be insufficient to accurately quantify the effects of installation related defects, which can lead to wrong design decisions.

Figure 1.3: Steel mandrel (Ploegam, 2020)

1.4. Research scope

This research focuses on the effects of using a mandrel during the installation of plastic heave screens under dikes and the gaps that occur when sheet piles delock. As the use of plastic sheet piles is a relatively new development, uncertainties remain regarding their long term performance.

The primary objective of this research can be seen below:

- Evaluating the potential failure mechanisms of dikes.
- Evaluating the piping mechanism in more detail.
- Investigating the hydraulic effects of the removal of the mother plate, particularly the formation of gaps or loosened soil and its implications on piping resistance.
- Investiging the hydraulic effect of delocking of a screen and the gap that occurs

The research will mainly focus on dikes and typical Dutch subsoil conditions. It aims to contribute to a better understanding of the behavior of plastic heave screens after installation and provide practical insights for improving the safety and reliability of this innovative solution.

1.5. Research question

The main research question is as follows:

”To what extent does the installation process of plastic heave screens influence their hydraulic effectiveness in preventing backward erosion piping?”

Furthermore, the sub-questions are formulated as follows:

Subquestion 1: How do different hydraulic indicators give insight into the effects of improper installation of plastic heave screens?

Subquestion 2: How do installation induced gaps or disturbed soil zones affect seepage flow patterns and hydraulic gradients?

Subquestion 3: How do multiple gaps in a heave screen influence the hydraulic behaviour in between each other?

To answer these questions first more information is gathered about piping and heave screens, after which the methodology is devised in chapter 4.

2

Dike failure and Backward Erosion Piping

This chapter reviews the existing literature relevant to backward erosion piping and the use of heave screens in dike reinforcement projects. The goal of this chapter is not only to describe existing knowledge, but also to assess current theories, design approaches, and modelling practices, and to identify limitations that motivate the research presented.

2.1. Failure mechanisms of dikes

Dikes can fail through different mechanisms depending on hydraulic loading conditions, soil composition, geometry, and construction quality. It is important to distinguish between failure and collapse: a dike is considered to fail when it no longer fulfils its water retaining function, even if a complete structural collapse does not occur (Technical Advisory Committe on Water Defences, 1998).

Common failure mechanisms include overflow, waver overtopping, slope instability, uplift, heave, and internal erosion. These mechanisms are often classified into hydraulic failure, geo-hydraulic failure, global stability failure, and externally induced failure (Vorogushyn et al., 2009). An overview of these mechanism can be seen in figure 2.1.

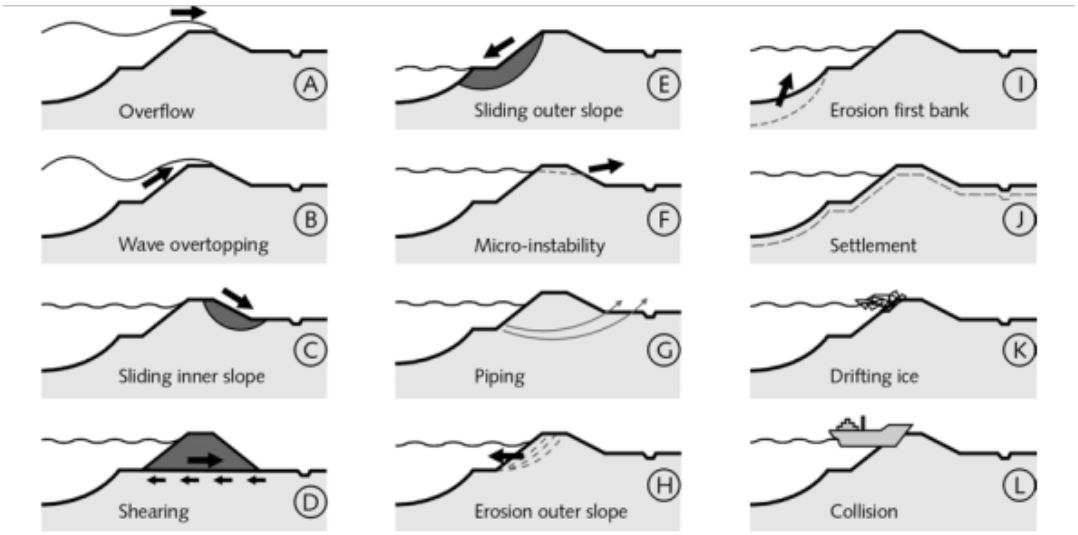

Figure 2.1: Failure mechanisms soil structures (Technical Advisory Committe on Water Defences, 1998)

Hydraulic failures, such as overflow and overtopping, occur when hydraulic loads exceed the dike crest level or surface protection capacity. Geo-hydraulic failures involve the interaction between groundwater flow and soil, including uplift, heave, and piping. Global stability failures are associated with slope instability and shear failure, while other failure mechanisms include external impacts such as ship collisions or ice loading.

For river dikes founded on permeable sandy aquifers, backward erosion piping is frequently identified as one of the governing failure mechanism. In such cases, piping often determines the required measures (Foster et al., 2000), making it a critical focus for both assessment and design. Other failure mechanisms, while relevant, are therefore not considered in detail in this thesis.

In the fault tree below an overview is given of the different failure mechanism, providing a clear overview of the connection between failure mechanisms and the subcategory they belong to.

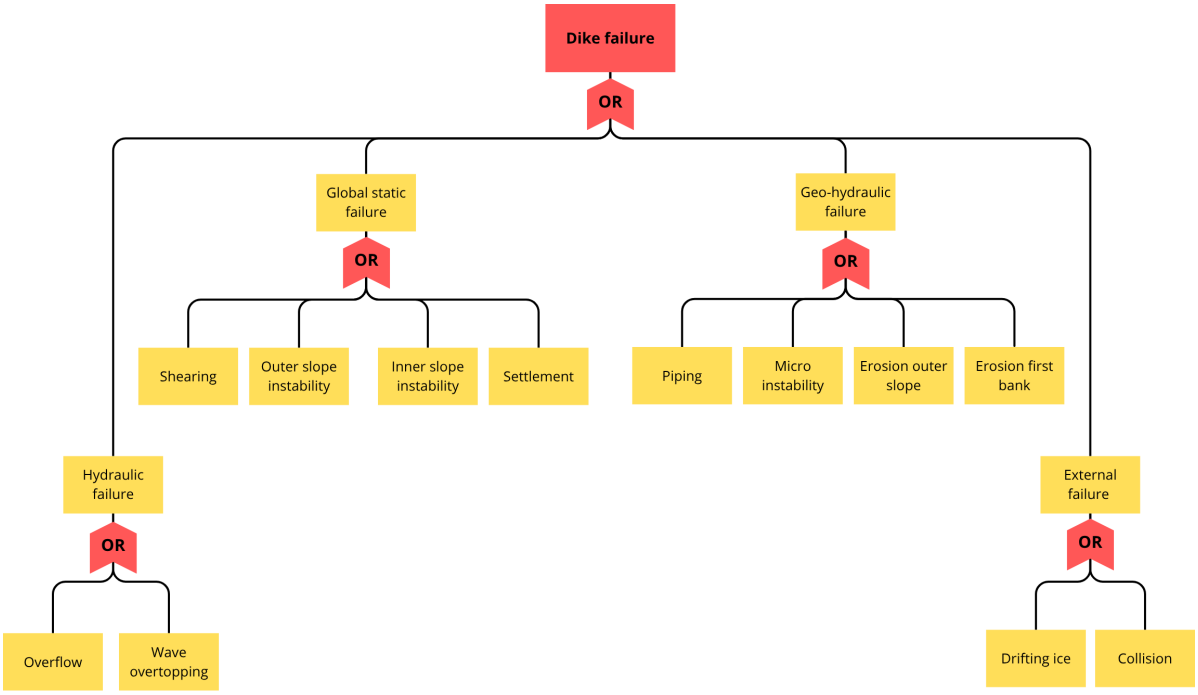

Figure 2.2: General fault tree dike failure

2.2. Backward erosion piping

Piping in dikes occurs when an excess of seepage flow in the permeable layer below a dike is forming, such that soil particles are entrained in this flow (Box and Vrouwenvel, 1987). Increased seepage flow initiates sand transport that can form a sandboil behind the dike core, an indicator of erosion (Vorogushyn et al., 2009). This sandboil is located at the exit point, which can be seen in figure 2.4. It occurs when the critical hydraulic head causes a stable pipe to turn into an unstable pipe that keeps growing (Sellmeijer et al., 2011).

Piping is mainly governed by the seepage length through the permeable layer and the high hydraulic gradient between the water side and the land side caused by high water. The permeable layer is typically situated between 2 impermeable layers (Vorogushyn et al., 2009). Furthermore, the pipes often form at the interface between the permeable sand layer and the impermeable layer above it, which acts as a 'roof' for the pipe. The exact soil composition can differ between locations of the dike, which has great influence on the probability of the occurrence of piping. A clear schematization of piping can be seen in figure 2.3 below.

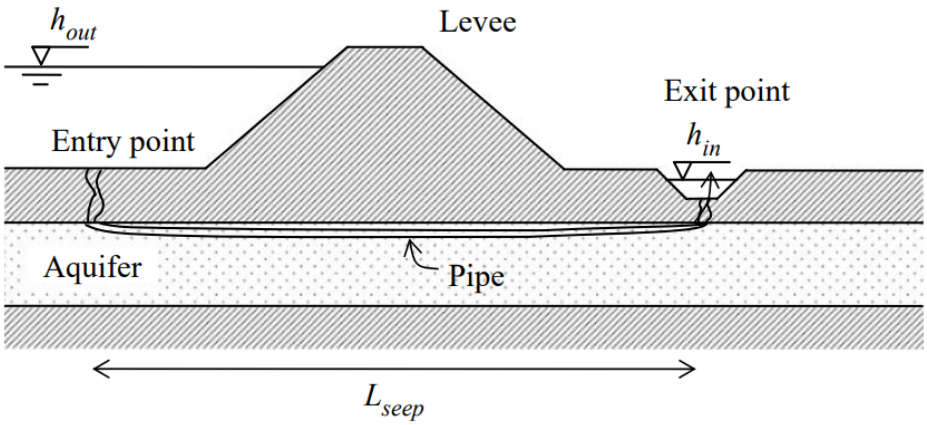

Figure 2.3: The piping failure mechanism: levee cross-section and relevant geometry parameters (Jongejan and Calle, 2013).

Schweckendiek et al., 2014 stated that the total piping mechanism exists out of more events that can be combined to one that causes failure. The process is interdependent and is explained below by taking each step of the process. The process can be seen in figure 2.4.

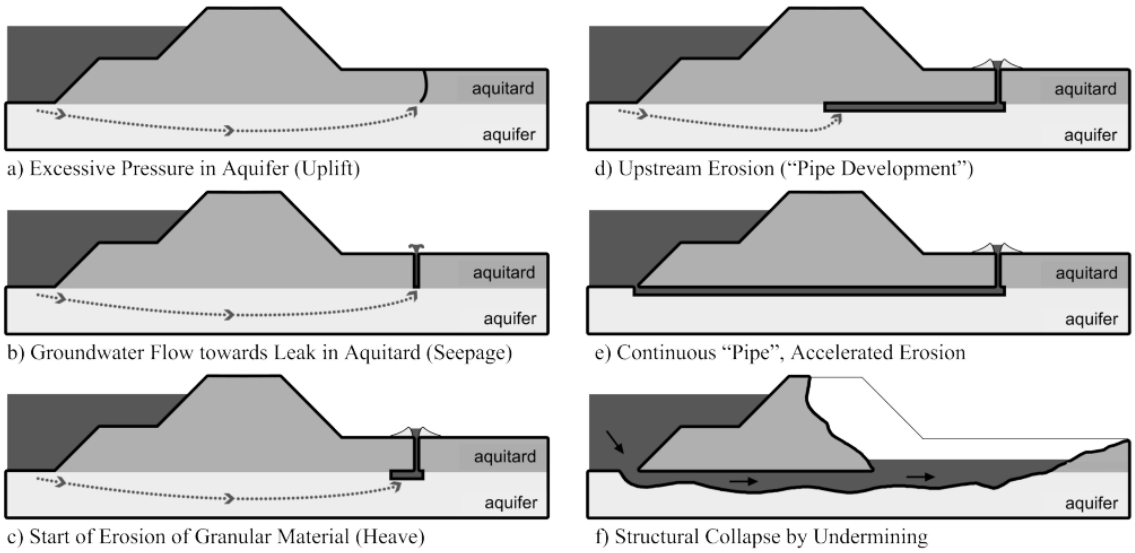

Figure 2.4: Stages of piping, (Schweckendiek et al., 2014)

1. **Increased hydraulic load:**
   Dike failure typically occurs due to extreme conditions like floods. The most important condition for piping to emerge is therefore high water. This situation causes high gradients, which is a requirement for piping.

2. **Uplift:**
   The first step is the start of uplift, closely related to heave or bursting, which is a geo-hydraulic failure mechanism. This occurs when a non permeable cover layer of a dike overlays a permeable sandy sub layer. High water levels on the water side of the dike, create high pore pressures in the aquifer beneath the dike. If these upward pressures exceed the effective weight of the overlying impermeable clay layer, this layer will be lifted upwards (Vorogushyn et al., 2009). This reduces the effective normal stresses in the soil and decreases friction between sand particles, which can lead to cracking and increased seepage flow. Uplift is a crucial condition for piping to occur (IPM-team, 2021). The Bergambacht field test, for instance, demonstrated how increased hydraulic

head led to the uplift of clay and peat layers (Zwanenburg and Patricia, 2018). In practice, if the overlaying clay layer is more than 4m thick it is assumed that uplift and cracking will not occur (Van Hoven et al., 2019). This step in the process is important because uplift is linked to the same variables as heave. Therefore, uplift is prevented with the use of heavescreens.

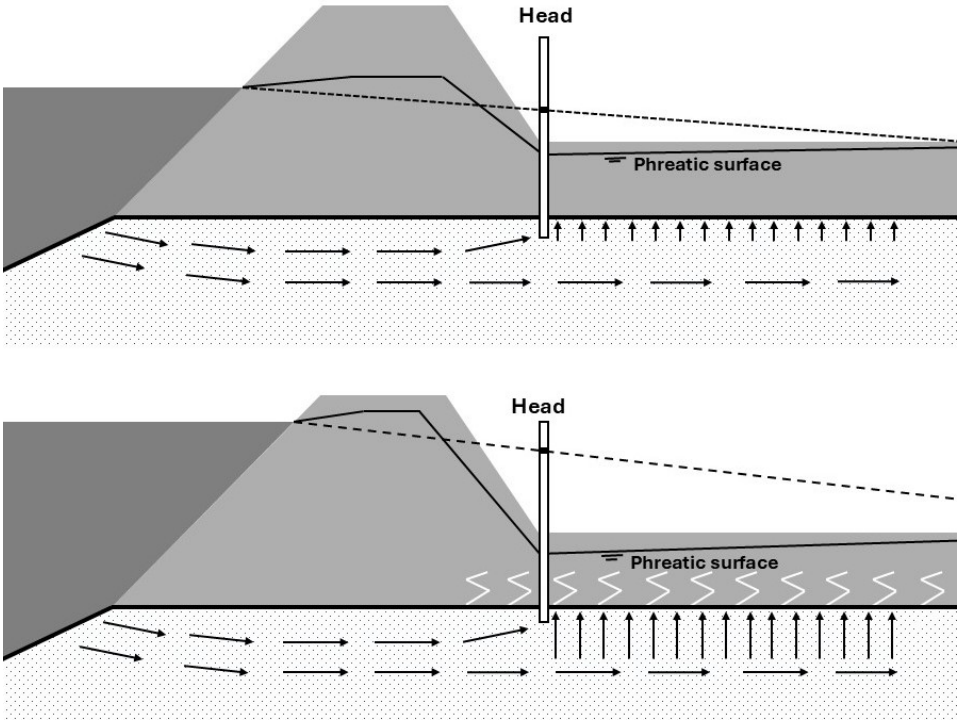

Figure 2.5: Schematic drawing uplift mechanism

3. **Seepage:**
   Following uplift, seepage refers to the flow of water under or through a flood defense, driven by a hydraulic head (Allsop et al., 2007). Uplift directly enhances the seepage flow through the dike foundation, as cracks formed during uplift reduce resistance and allow more water to pass. Seepage also reduces the effective normal stresses in the soil, which is a critical factor in slope instability (Vorogushyn et al., 2009). This process is a key component of geo-hydraulic failure.

4. **Erosion Initiation:**
   As seepage flow increases, particularly after uplift has created pathways, it can entrain soil particles. If the hydraulic gradient is high enough and the critical shear stress in the sandy material is exceeded, soil transport initiates (Vorogushyn et al., 2009). This internal erosion often creates sandboils behind the dike, which are a visible indicator of progressive erosion. This stage also relates to micro-instability, where small soil elements are washed out from the slope surface by groundwater seepage (Box and Vrouwenvel, 1987).

5. **Pipe Development:**
   As a consequence of this progressive erosion, localized channels or tunnels, referred to as pipes, begin to develop in the sandy dike foundation. These pipes progress from the landside dike toe towards the outer dike toe. Initially, this development might halt if an equilibrium state is reached (Vorogushyn et al., 2009). Piping is defined as an excess of seepage flow in a permeable layer below a dike, leading to the entrainment of soil particles. Pipes commonly form at the interface between the permeable sand layer and an impermeable layer above it, acting as a 'roof' (van Beek, 2015).

6. **Continuous Pipe Formation:**
   If the pressure difference across the dike, known as the critical head (H_{crit}), is exceeded beyond

the point where equilibrium can be maintained, the erosion becomes progressive. This leads to the development of extended pipes under the dike core that reach the riverside dike toe. This signifies that the piping has progressed to a ”critical length”. At this point, a direct water flow path is established between the river side and the landside, fundamentally compromising the dike’s integrity.

7. **Structural Collapse:**
   The consequence of a continuous pipe developing along the total length is structural collapse of the dike. When pipes fully penetrate the dike, the dike core can sag, which can then lead to other failure mechanisms like sliding. A conservative approach, that is used often, assumes complete dike failure once piping reaches the total length under the dike, in the absence of more detailed information (Lengkeek et al., 2019).

2.3. Event tree

A event tree is made to trace a specific event back to the causes and therefore a good tool to visually show the path and causes of failure of a dike. The event tree shown in figure 2.6 displays the piping events that can occur during high water, which will lead to failure due to piping. The diagram begins with high water. Once initiated, piping may progress to form a continuous pipe if the hydraulic gradient exceeds the critical threshold and if countermeasures are absent or ineffective.

The event tree shown in figure 2.6 displays the different events that can occur during high water, which will lead to failure due to piping. The diagram begins with high water. Once initiated, piping may progress to form a continuous pipe if the hydraulic gradient exceeds the critical threshold and if countermeasures are absent or ineffective.

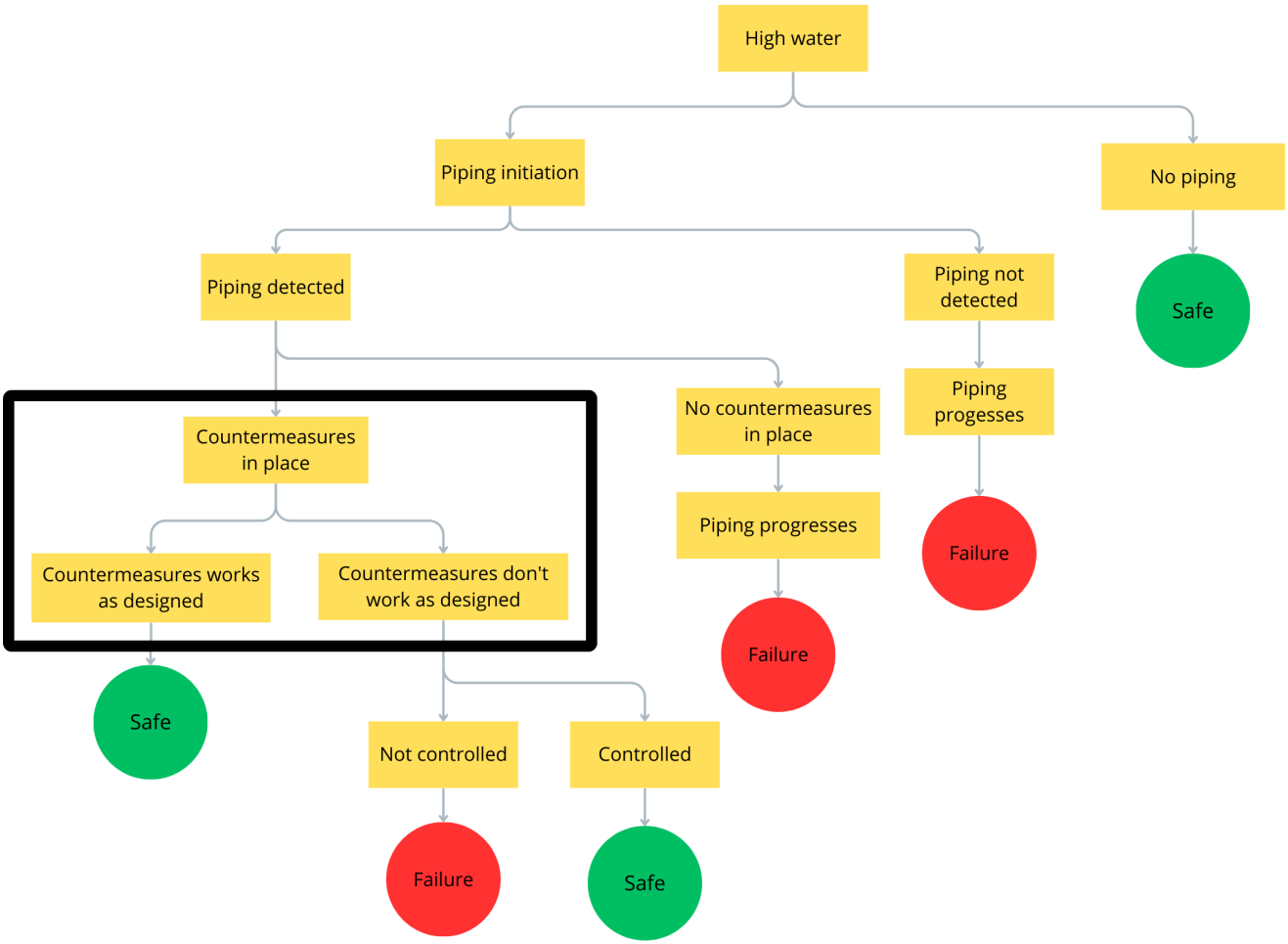

Figure 2.6: Event tree piping

This research focusses on the part in the rectangle. Different countermeasures are available to reduce the risk of backward erosion piping. Often applied measures include widening of the berm, installation of relief wells, application of filter screens, and the use of vertical cut-off walls such as heave screens (Oldhoff, 2013). Further explanation about the different countermeasures can be found in appendix A.

Each countermeasure addresses a different aspect of the piping mechanism. Berm widening increases the seepage length, relief wells reduce pore water pressures, and filter screens prevent transport of soil particles while allowing water to pass. Heave screens act as impermeable vertical barriers that both increase the seepage length and block sediment transport.

Compared to other countermeasures, heave screens are particularly effective in situations with limited space, as they can be installed without significantly increasing the footprint of the dike. However, their effectiveness depends on continuity, penetration depth, and installation quality.

2.4. Analytical and semi-empirical approaches

Over the past decades, several analytical and semi-empirical models have been made to assess the vulnerability of dikes to backward erosion piping. These models aim to relate hydraulic loading and geometric properties to a critical condition for piping initiation or progression. These analytical models give a good first indication and understanding of what parameters influence the resistance of a dike against piping. In this section Sellmeijer and Lane are discussed to provide these first insights.

Sellmeijer

Sellmeijer is an advanced analytical formulation for backward erosion piping. It is developed in 1988 and later refined and calibrated for engineering practice (Sellmeijer et al., 2011). The Sellmeijer model describes piping as a balance between driving hydraulic forces and resisting forces acting on soil particles within a developing pipe. It is used to determine the critical head at which piping occurs for a given dike geometry and soil conditions.

The Sellmeijer formulation is as follows:

$$F_p = \frac{\Delta H_c}{\Delta H - r_c D_{coverlayer}} \tag{2.1}$$

With:

$$\Delta H_c = L \cdot F_{resitance} \cdot F_{scale} \cdot f_{geometry} \tag{2.2}$$

$$F_1 = F_{resistance} = \frac{\gamma_p'}{\gamma_w}(\eta tan(\theta)) \tag{2.3}$$

$$F_2 = F_{scale} = \frac{d_{70m}}{\sqrt[3]{\kappa L}}\left(\frac{d_70}{d_{70m}}\right)^{0,4} \tag{2.4}$$

$$\kappa = \frac{\nu_{water}}{g} \cdot k \tag{2.5}$$

$$F_3 = F_{geometry} \overset{MSeep}{=} F(G) \overset{standarddike}{=} 0,91 \cdot \left(\frac{D}{L}\right)^{\frac{0,28}{\left(\frac{D}{L}\right)^{2,8}-1}} + 0,04 \tag{2.6}$$

In which:

F_p = Calculated stability factor for backward erosion piping

ΔH_c = critical hydraulic gradient

ΔH = head loss across the water barrier [m]

d = thickness of the cover layer [m]

γ_p' = unit weight of sand grains under water [kN/m^3]

γ_w = unit weight of water [kN/m^3]

θ = angle of repose of sand grains [°]

η = White's coefficient [-]

κ = intrinsic permeability of the piping-sensitive upper sand layer [m^2]

d_{70} = 70th percentile of the grain size distribution [m]

d_{70m} = average d_{70} in small-scale tests (2.08 × 10^{-4} m)

D = thickness of the sand layer [m]

L = horizontal length of the seepage path [m]

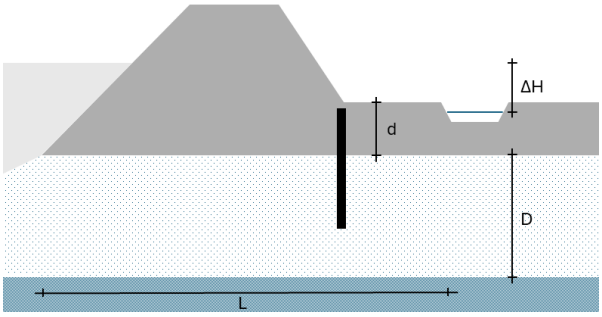

Figure 2.7: Sellmeijer's piping method

The Sellmeijer model explicitly incorporates soil properties and geometric parameters and reflects the nature of pipe development from the land site exit point towards the waterside. As stated before, the Sellmeijer formulation forms the basis for evaluating backward erosion piping in The Netherlands.

Nevertheless, the Sellmeijer model assumes homogeneous soil conditions, idealised geometry, and a continuous seepage path. Installation related disturbances are not explicitly represented in the analytical formulation.

Lane

One of the earliest approaches to piping assessment is Lane's weighted creep theory (Lane, 1935). Lane proposed that piping failure occurs when the ratio between head difference and the effective seepage path length exceeds a critical value. The effective seepage length accounts for both horizontal and vertical seepage paths, with vertical seepage weighted heavily due to its higher resistance.

$$h = \frac{\frac{1}{3}H + \sum V}{c_w} \tag{2.7}$$

h = Critical head that would initiate piping
c_w = Weighted seepage ratio
H = Horizontal seepage length
V = Vertical seepage length

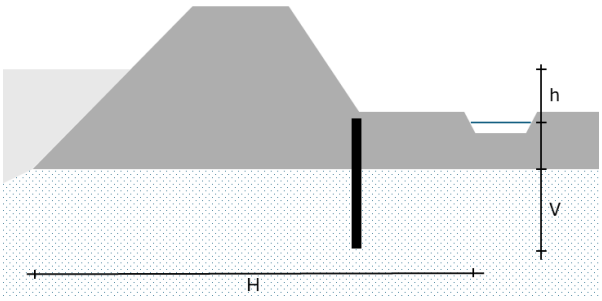

Figure 2.8: Lane's weighted creep theory

Lane's method provides a simple and intuitive assessment of piping risk and has historically been used in preliminary dike design because it is able to describe a vertical screen solution. However, the approach is purely empirical and does not explicitly account for soil mechanical properties, grain size distribution, or three dimensional seepage behaviour. Due to these limitations, Lane's weighted creep theory is generally considered conservative.

3

Heave Screens

This chapter examines the use of heave screens as a primary defence system against piping in dikes. By interrupting seepage flow and extending the hydraulic path, these screens reduce flow velocity and exit gradients to prevent internal erosion. The following sections show the working principles of heave screens, the specific design and installation requirements for plastic heave screens, and the analytical model (Lane) used to calculate their effectiveness.

3.1. Working principle

A heave screen, also referred to as a 'sheet pile wall', is a measure used to prevent piping. It can be described as a closed, vertical wall that prevents seepage through a water retaining structure, such as a dike. They are typically installed deep below the surface of the structures. Heave screens can be made of different impermeable materials, like steel or plastic (Oldhoff, 2013).

The primary purpose of a heave screen is to interrupt or modify the seepage flow path (Sivakugan and Das, 2010). Instead of allowing uninterrupted horizontal flow under the dike, the screen forces the flow to go deeper and around it as can be seen in figure 3.1. This prevents piping from occurring in different ways:

1. **Increasing seepage path length:** The primary function of a heave screen is to increase the resistance the seepage flow encounters by making the length of the flow it must travel, the length of the seepage path, longer (Oldhoff, 2013).

2. **Reduction of flow velocity and gradient:** Due to the longer seepage path, the seepage flow is reduced. A correctly installed heave screen lowers the hydraulic gradient across the dike. A lower flow velocity and gradient reduce the likelihood of erosion of the sand layer (Oldhoff, 2013).

3. **Prevention of heave:** A heave screen is also designed to prevent heave. Piping occurs when heave and uplift occur (J. C. Pol et al., 2021). When the heave screen is located on the inner side of the dike, the seepage flow near the exit point is forced vertically, and if drainage or a berm is present, the screen prevents heave on the inner side (Oldhoff, 2013). Heave occurs when seepage pressures equal the submerged weight of the sand and therefore a negative effective soil pressure. A sufficient screen length prevents complete fluidization behind the screen.

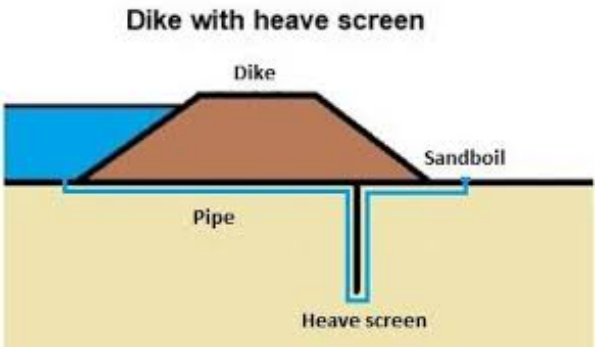

Figure 3.1: Flow path around heave screen (Raadschelders and Lukas, 2023)

3.2. Design of plastic sheet pile walls

For the design of the sheet pile walls not only the water safety is important. Different aspects can play a big role in the design, such as constructibility, spatial integration, manageability, sustainability, and expandability. Often additional control measures may be necessary to achieve a solution that is feasible.

It is important to gain good insights into control measures because they can become determining for the design choice and could influence the water safety. For example, consider pre-loosening the soil to install the sheet pile wall (Halter et al., 2025). The OBOR (Ontwerp-, Beoordelings- en Onderhoudsrichtlijn) explains different control measures and when they will be used.

These design steps can be seen in the flowchart in figure 3.2. The location of the sheet pile wall is dependent on the same different aspects as mentioned above.

It is assumed that if the screen extends for 3 meters or more into the aquifer, progressive fluidization and internal soil particle erosion is ignored (Wiggers et al., 2025) leaving heave as the important failure mechanism. For progressive fluidization no evidence is found that occurs before hydraulic heave is occurring, further research in this topic is done in the KIA research heave screens (J. Pol, 2020). Designing against heave can be done in two ways, vertical equilibrium according to Terzaghi and testing the average hydraulic gradient behind the screen.

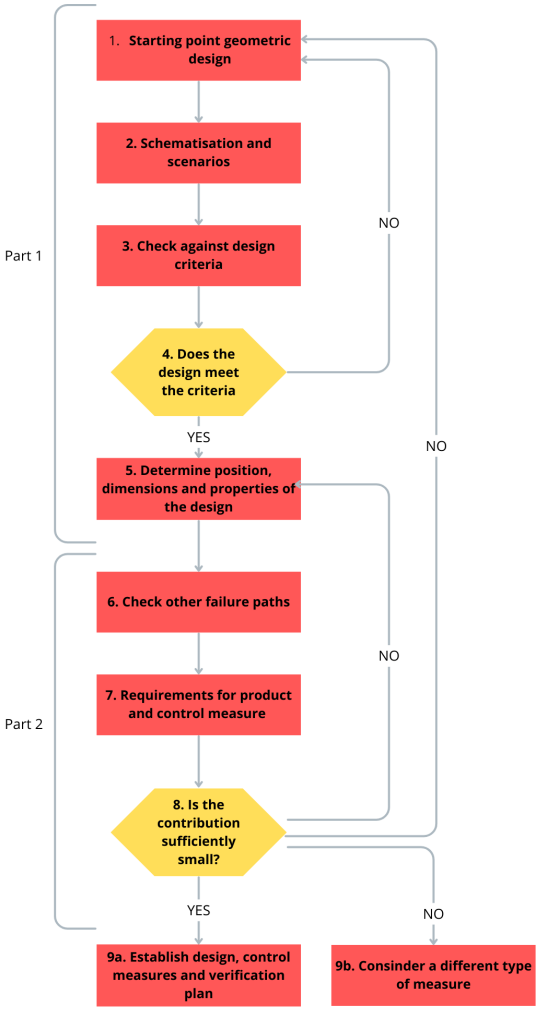

Figure 3.2: Flowchart sheet pile wall design

3.3. Installation plastic sheet pile walls

Heave screens are installed deep into the ground. This installation is a critical step in the process of reinforcing a dike with the use of heave screens, and different methods and considerations are involved.

The most common way of installing a plastic heave screen is driving. This is a typical method using traditional pile driving equipment. Sheet piles are aligned using templates or similar guiding structures. Driving can be done by pushing, vibrating, or hammering. (Gedeon, 1994)

Different types of hammers can be used to drive the sheet piles into the ground. Vibratory hammers are widely used because they are often faster, do not damage the top of the pile, and can easily extract piles if needed (Gedeon, 1994).

For installing plastic sheet piles, a steel support plank is often used, as can be seen in figure 1.3. This plank, named a mandrel, is a steel sheet pile plank with a piling cap matching the plastic plank profile. It is vibrated together with the plastic plank into the soil. This method transfers the vibration load directly to the mother plank, preventing damage to the plastic pile. At the bottom the plastic pile is connected to the mandrel with clamps to prevent sand accumulation between them. After reaching the required depth, the plastic plank is disconnected, and the mandrel is extracted (Hakkers et al., 2023).

The installation process is crucial for the functioning of the heave screen. Sheet piles are typically driven vertically into the water bearing layer and must extend into the sand layer to force groundwater flow vertically behind the screen. The top of the heave screen should be at least 0.5 meters into the clay cover layer (Halter et al., 2025).

For plastic sheet piles, which are more flexible than steel, installing them requires additional operations. The plastic sheet pile interlocks fail more quickly and therefore must be installed with more ease, preventing lock failure and the creation of gaps. An example of the locking mechanism can be seen in figure 3.3. The insertion speed is also important, a too low insertion speed can cause the plastic, and therefore the lock, to melt (Zagema, 2023).

(a) Plastic sheet pile wall left locking mechanism

(b) Plastic sheet pile wall right locking mechanism

(c) Plastic heave screen locking mechanism in the ground

Figure 3.3: Plastic heave screen locking mechanism

A trench is often excavated before installation for equipment access, which must be closed with clay afterward and sufficiently compacted to prevent groundwater flow.

For determining if the soil is suitable for plastic sheet pile walls the cone resistance is often used as the limiting factor. The hardest part is getting the piles into the sand. If the resistance measured by tests is to high there will be chosen for steel sheet pile walls instead of plastic. The following table shows the values for cone resistant connected to the installation of plastic sheet piles.

Table 3.1: Effects of installation pressure on execution at Wolferen–Sprok (Halter et al., 2025)

Pressure Range	Observed Effects	Implications for Execution
< 15 MPa	Minimal wear	Installation possible without pre-drilling or fluidization. If pressures remain below 20 MPa, a freely hanging block can be applied. Pressures exceeding 17 MPa require switching strategies depending on ground conditions and consideration of prestressing (compression or tension).
< 20 MPa	Limited wear	Pre-drilling is recommended. Pre-drilling significantly improves the quality of plastic cut-off walls and should be combined with compressive and tensile foundation verification.
20–30 MPa	Moderate wear	Pre-drilling is mandatory and must be combined with compressive and tensile foundation verification.
25–38 MPa	Severe wear	Significant wear observed; further research is required to assess impacts on execution and potential mitigation measures.
> 38 MPa	No experience	Insufficient field experience available; additional research is necessary.

As mentioned before the installation process has a big influence on the working of the screen. Detecting installation errors, such as interlocking, or uncertainties because of the installation, is crucial but can be complex and impractical after installation (Wiggers et al., 2025). A couple of detection methods exist that are listed below:

- **Visual inspection:** Checking if the sheet pile is undamaged before starting and observing if it is installed stably and quietly to depth. This is a low-cost method but has large uncertainties and is sensitive to subjectivity (Halter et al., 2025).
- **Lock indicators:** Devices used to detect if the sheet pile is properly locked along its length. For example, the lock indicator seen in figure 3.4 (Zagema, 2023).
- **Indirect measurements:** Focusing on the effects of sheet pile movement, such as water pressure differences or ground settlement, potentially using CPT (cone penetration test) measurements or permeability pumping tests (Zagema, 2023).
- **Monitoring insertion parameters:** Keeping an eye on insertion speed and plank skewness (Zagema, 2023).

It is important that detection and quality control are continuous and potentially performed by an independent party (Halter et al., 2025). Registration forms should be used to document the installation process for each plank, noting lock indicator tests and any deviations.

Lock indicators, as can seen at the right, are little plastic parts that slide over the locking mechanism as can be seen in figure 3.3a. This plastic part slides over this side of the plank when it is installed. The next sheet pile, seen in figure 3.3b, is sliding over the sheet pile already installed, taking this plastic part down into the ground. Connected to this plastic part a steel cable is connected with the length of the screen, plus 0.5 meter. If the the mandrel and sheet pile get to the required depth the cable should be taken down with the sheet pile, leaving 0.5m above the ground. If there is more than 0.5m cable left above ground, it is assumed that the sheet piles are delocked.

Figure 3.4: Lock indicator

3.4. Prototype explanation

Figure 3.5: Prototype explanation of the installation of plastic sheet pile walls

4

Research Methodology

This chapter describes the research methodology adopted in this thesis. The methodology is designed to address the research questions formulated in Chapter 1, based on the knowledge gaps identified in the literature from Chapter 2. The focus of this chapter is explaining why specific methodological choices are made, while the technical implementation of the numerical models is described in Chapter 5. This chapter establishes the logical connection between the identified limitations in existing piping assessment methods and the numerical modelling approach adopted in this research.

4.1. Research approach

Existing analytical and semi-empirical piping models, as discussed in chapter 2.4, are primarily intended for assessment under idealised conditions and are not capable of explicitly representing local defects or three dimensional flow behaviour. Numerical modelling allows for controlled modification of geometry, material properties, and boundary conditions.

This research adopts a numerical modelling approach to investigate the influence of installation induced defects in plastic heave screens on piping. Numerical modelling is selected because the defects, such as mandrel gaps or delocked screens, are difficult to isolate and study experimentally under controlled conditions.

4.2. Research framework

The research methodology follows a structured workflow consisting of four main steps which can be seen in figure 4.1:

- Definition of a representative reference model with an ideally installed plastic heave screen
- Definition of installation induced defect scenarios based on reported construction issues
- Numerical simulations of seepage flow using both two dimensional and three dimensional models
- Comparative analysis of model outputs to evaluate the influence of the installation defects

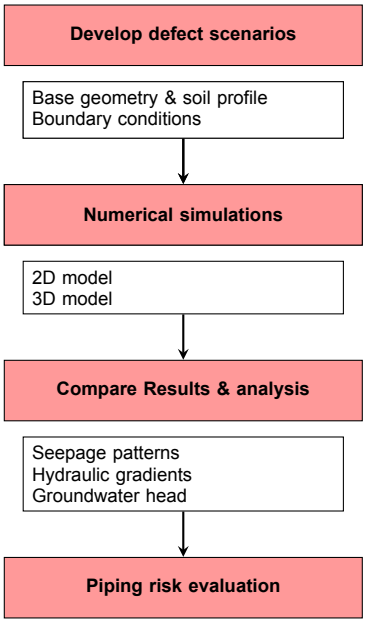

Figure 4.1: Research methodology flowchart.

4.3. Selection of modelling strategy

A numerical modelling strategy is adopted in this study. The primary goal is to find the hydraulic effects of installation faults, rather than to account for probabilistic variability in soil properties or loading conditions. The numerical analyses are performed using the finite element method (FEM), which allows for an accurate representation of groundwater flow through complex geometries and heterogeneous soil. FEM is particularly suitable for seepage problems involving localised disturbances, as it enables detailed resolution of hydraulic gradients and flow concentration around defects.

For the numerical modelling a specific real world case is selected. The use of a case study ensures that the developed scenarios and obtained results are relevant, credible, and applicable to practical engineering problems. Validation of the model requires that it represents reality as accurately as possible; therefore, the model is based on known geometry and site specific subsurface conditions. By using measured soil data derived from cone penetration tests (CPTs), the analysis avoids a purely theoretical approach and allows realistic input parameters to be applied in the model. To maintain discretion, the analysis focuses on a representative cross section rather than a precisely identifiable location.

A key characteristic of this dike section is that it is only vulnerable to piping. It satisfies all other flood safety requirements. This is due to the presence of a sand layer in the subsurface, which provides structural stability but also has a high permeability, a key factor governing the occurrence of piping.

PLAXIS 2D and PLAXIS 3D are selected as the numerical tools for this research. These software packages are widely applied in geotechnical engineering practice and provide validated FEM formulations for groundwater flow analysis in soil structure interaction problems.

4.4. Dimensionality of the numerical models

Both 2D and 3D numerical models are employed in this research. Two dimensional plane-strain models are used to represent current engineering assessment practice, in with dike cross sections are analysed assuming uniform conditions along the longitudinal direction. Three dimensional models are developed to investigate local installation induced defects that cannot be represented in 2D analyses. In particular, 3D modelling allows for the simulation of local flow concentration around defects, such as gaps behind the heave screen or locally increased permeability zones. The analytical methods discussed in chapter 2.4 are used to get an overview over how BEP works and how first estimations are made. In practice these analytical solution are not used any more. For determining if a dike section is prone to piping, Dgeoflow is used and to determine screen length, Plaxis is used.

4.5. Definition of reference and scenarios

A perfectly working heave screen configuration is defined as the reference scenario. This scenario represents ideal installation conditions and corresponds to a real time scenario. Furthermore it complies to the implicit assumptions made in current piping assessment practice.

Based on installation issues reported in literature and practice, several scenarios are defined. These include:

- Gaps behind the heave screen at the land side resulting from mandrel extraction
- Delocking, creating a vertical hole in the screen

The selected scenarios are intended to represent realistic installation related imperfections. The geometries and material properties are varied systematically to assess the sensitivity of the hydraulic response to size and extent.

An overview of all the different scenarios that will be modelled can be seen in the table below:

Table 4.1: Numerical modeling scenarios for evaluating installation-induced defects in plastic heave screens.

Scenario	Dim.	Assessment Criteria	Explanation	Model Parameters
No Intervention	2D	Piping (BEP)	Baseline evaluation of the existing dike section's safety against internal erosion.	Standard geometry derived from CPT data; validated using Sellmeijer analytical model.
Ideal Heave Screen	2D	Heave behind screen	Reference case for a perfectly installed screen. Required depth determined iteratively.	wide longitudinal pipe configuration.
Mandrel-induced Gap	2D	Heave behind screen, flow velocity, and hydraulic gradient	Simulation of disturbed zones on the downstream face of the screen following mandrel extraction.	Disturbed zone modelled as a high-permeability soil layer (e.g., $k = 300$ m/d).
Delocked Screen	3D	Heave behind screen and hydraulic gradient	localized defect (vertical hole) investigated to capture 3D flow concentration.	Depth taken from 2D results; converges flow from all directions towards the fault.
Pipe to hinterland	3D	Heave behind screen	Different models for pipe systems	Converges flow from all directions towards pipe.

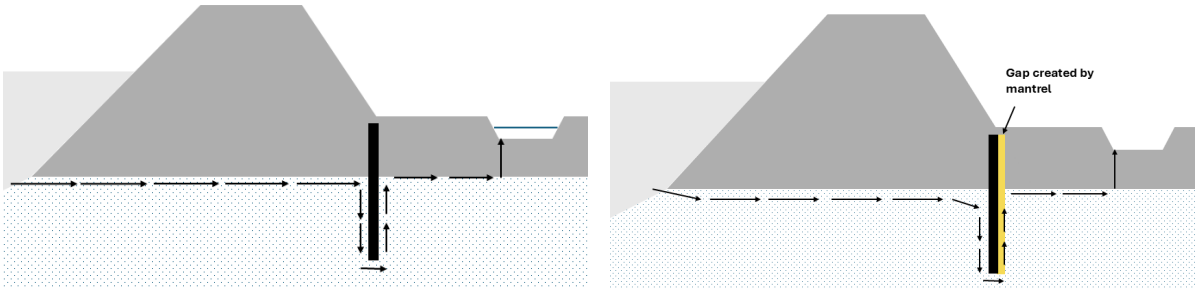

(a) Ideal heave screen

(b) Gap behind the screen induced by the mandrel

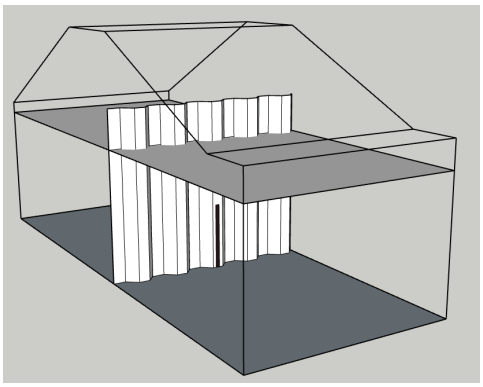

(c) Delocked heave screen creating a gap (black strip)

Figure 4.2: Different modelling scenarios

4.6. Evaluation criteria and output parameters

The effectiveness of the heave screen is evaluated using hydraulic indicators that are directly related to the initiation of backward erosion piping. The primary output parameters include:

- Hydraulic head
- Vertical hydraulic gradients at and around the heave screen
- Seepage velocities at and around the heave screen

These parameters are used to compare reference and disturbed scenarios The selected indicators focus on the governing mechanisms of piping, uplift, and heave initiation and do not represent full structural failure criteria.

Based on these indicators, three distinct failure mechanisms are evaluated, depending on the presence and condition of countermeasures. In the absence of a heave screen, the dominant failure mechanism is backward erosion piping beneath the dike. In this case, horizontal pipe development towards the river is assessed, assuming that uplift and heave of the cover layer in the hinterland have occurred as conditions.

When a heave screen is present, two other failure mechanisms are considered. The first is heave behind the screen, where the loss of effective stress behind the screen becomes the dominant node. It can also occur through vertical erosion. The second mechanism is uplift or overflow in front of the screen, which is evaluated to determine whether sufficient soil weight is present at the waterside of the screen to prevent uplift under high hydraulic loading. All four different failure mechanisms can be seen in figure 4.3.

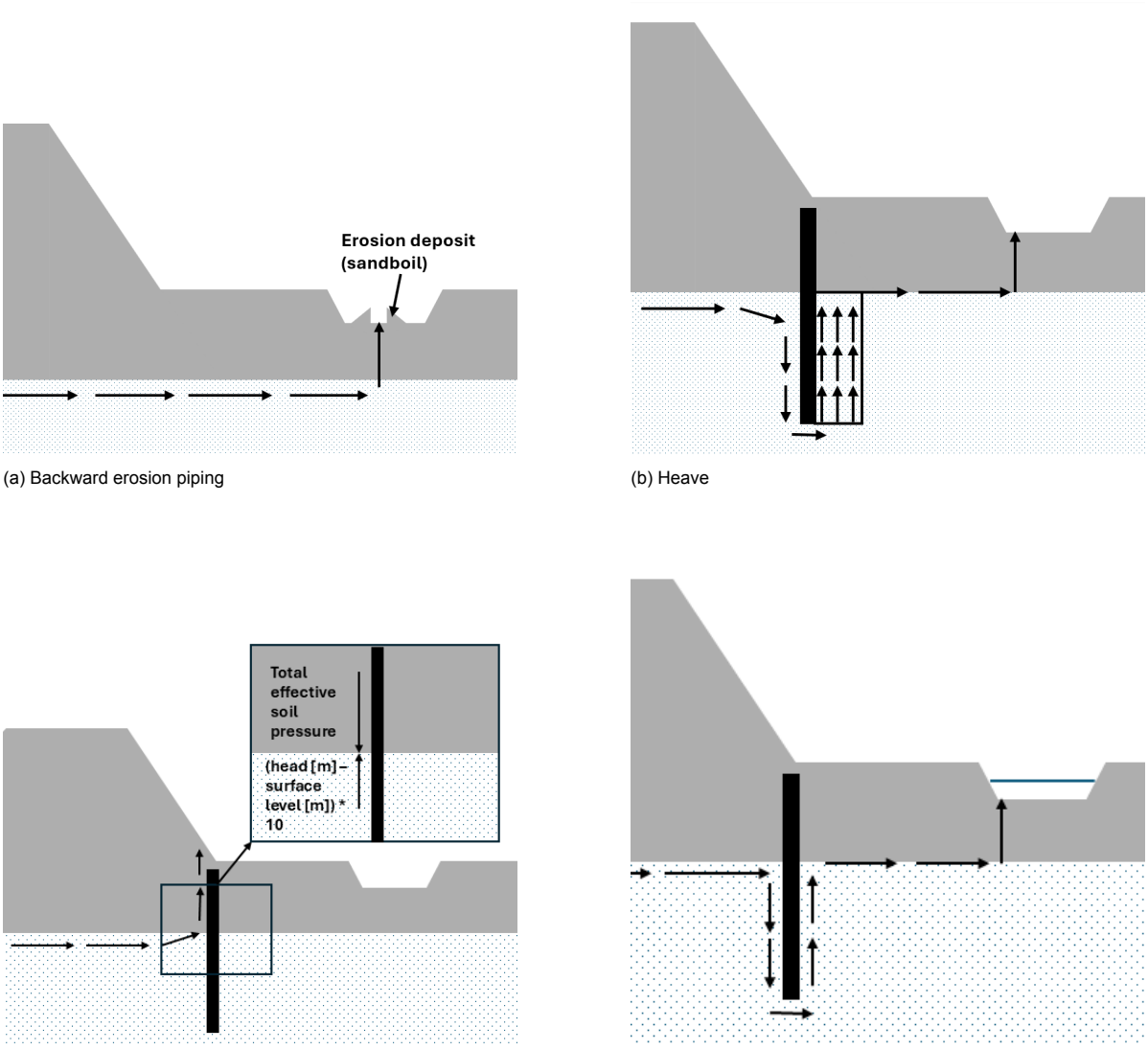

(a) Backward erosion piping

(b) Heave

(c) Front seepage

(d) Vertical fluidization

Figure 4.3: Different testing criteria for piping

For the reference case without intervention, piping is expected to govern failure. For intact heave screens subjected to the design flood level, it is anticipated that it suffices for both heave behind the screen and uplift in front of the screen. For scenarios involving installation induced defects such as mandrel induced gaps, delocking between screen elements, the models are expected to show increasing safety problems, potentially resulting in failure.

4.6.1. Evaluation of global heave

As can be seen in table 4.1, the assessment criteria for most of the installation induced defects is heave behind the screen. The HWBP has developed a guideline that is followed in practice which will be explained below (Wiggers et al., 2025).

The figure below, illustrates the application of the vertical equilibrium method to a sand layer topped by a cover layer and a dike. The method is fundamentally related to Terzaghi, 1943 his approach. The top surface of the considered prism is located at the underside of the cover layer, where a pipe system is present, which means the hydraulic head at this point is equivalent to the hydraulic head in the rest of the pipe going to the hinterland. The hydraulic head is the total energy of water at a specific point, calculated as being the sum of its elevation and pressure, expressed as a height above a reference datum. In this thesis the reference datum is the NAP. The dimensions of this prism are chosen based on the normative pipe system that can form further explained in appendix D. At the interface between the cover layer and the sand layer, the effective weight of the cover layer acts on the prism (Wiggers et al., 2025).

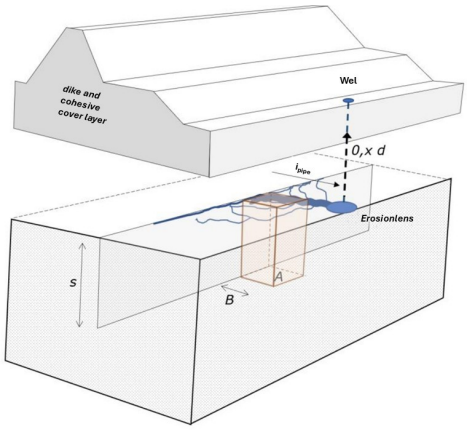

(a) Calculation of resistance against heave

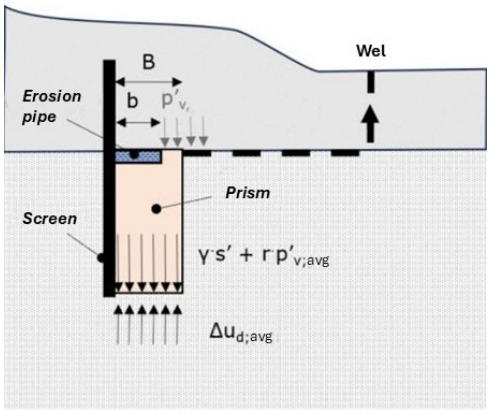

(b) Calculation of resistance against heave 2D (Wiggers et al., 2025)

Figure 4.4: Heave test in the Netherlands

For global heave, an equilibrium equation can be formulated for hydraulic heave occurring at a depth s beneath the cover layer. The pressures acting on the top and base of the prism are averaged over the surface area A of the prism. The resulting equilibrium condition is given by:

$$\Delta u_{d,\mathrm{avg}} = s \cdot \gamma' + r \cdot p'_{v,\mathrm{avg}} \tag{4.1}$$

In which:

$\Delta u_{d,\mathrm{avg}}$ is the difference between the pore water pressure under groundwater flow conditions and the hydrostatic pore pressure, averaged over the base area of the considered prism (at level z_s) [kPa]

γ' is the effective unit weight, without any excess upwards water pressures, of the soil within the considered prism [kN/m^3]

γ_w is the volumetric weight of water [kN/m^3]

s is the embedment depth of the screen in the water-bearing sand layer [m]

$p'_{v,\mathrm{avg}}$ is the average effective vertical stress exerted by the cover layer and the dike at the top surface of the considered prism, i.e. at the underside of the cover layer [kPa]

r is a reduction factor representing the fraction of the effective surcharge $p'_{v,\mathrm{avg}}$ that is transferred to the base of the prism [–]. At $r = 1$, the full effective weight of the cover layer acts on the base of the prism, whereas at $r = 0$ no surcharge effect is present. In practice r=$\frac{1}{4}$ is used, the reason for this is explained in appendix C in figure C.4.

For the assessment no set of partial safety factors have been derived yet. This is because the contributions of model and schematization uncertainties to the overall uncertainty are currently unclear. A probabilistic analysis has not yet been carried out due to a lack of fundamental research on this mechanism, particularly for hydraulic heave in situations with a cover layer (Wiggers et al., 2025). Therefore, the use of partial safety factors is considered premature, and for the time being an overall safety factor is applied:

$$\frac{s \cdot \gamma' + r \cdot p'_{v,avg}}{\Delta u_{d,avg}} = SF \geq 2.0 \tag{4.2}$$

4.6.2. Local hydraulic gradient

If there is no surcharge from soil weight above the prisma ($p'_v = 0kPa$), which is not realistic because the cover layer will act as a surcharge, formula 4.1 can be rewritten as:

$$\Delta\varphi \cdot \gamma_w = s \cdot \gamma' \tag{4.3}$$

and

$$i = \frac{\Delta\varphi}{s} \tag{4.4}$$

When the ground water head gets high or the seepage length gets low, the gradient i gets so high that heave occurs this gradient becomes the critical hydraulic gradient. These gradients can be used for testing on local heave occurring.

$$i_c = \frac{\gamma'}{\gamma_w} \tag{4.5}$$

In which the relation between the soil properties and the hydraulic gradient is made. Nevertheless, the current way of evaluating heave in a dike system includes the weight of the cover layer and therefore this method cannot be used (Wiggers et al., 2025).

However, an analytical solution proposed by Li and Fannin (2012) is found, see equation 4.6. It provides a method for determining the critical hydraulic gradient when a surcharge loading is present. For an internally stable soil, as said before instability is triggered when the effective stress at the base of the soil element diminishes to zero. To account for the stabilizing effect of the cover layer's weight, taking into account the reduction factor r, the critical hydraulic gradient can be expressed as:

$$i_c = \frac{r \cdot p'_{v,avg}}{\gamma_w \Delta z} + \frac{\gamma'}{\gamma_w} \tag{4.6}$$

In which:

γ_w = Volumetric weight of water
γ' = Submerged unit weight of the soil
Δz = Thickness of the sand layer being considered

This equation will be used to determine if the local hydraulic gradients surpass the critical gradient, taking into account that the cover layer does have a stabilizing effect. Only the vertical hydraulic gradient will be looked at, because heave is a vertical failure mechanism. The stabilizing effect of the cover layer is also vertical, and the upward water pressure will also act vertically.

5

Model Definition

This chapter provides the definition of the numerical models used to evaluate the effectiveness of the plastic heave screens. It focusses on the specific schematization, parameter selection, technical setup and assumptions required to simulate the seepage flow of piping in Plaxis 2D and 3D. Firstly, a description of a case study on which the models will be based is given. Then, using analytical solution, a first insight into this specific dike section is given. After that, first the 2D models are discussed and thereafter, the 3D models.

5.1. Introduction Case Study

For confidentiality reasons, the exact location of the case study is not mentioned. However, the site is representative of typical Dutch river dikes founded on sandy aquifers overlain by a relatively thin clay cover layer. The case study forms part of a larger flood protection reinforcement project in which heave screens are considered as a mitigation measure to improve piping safety.

The selected dike section has been identified as prone to piping. This makes it suitable for studying both the effectiveness of an ideal heave screen and the sensitivity of the system to deviations introduced during installation. In particular this location is used because it is only prone to piping and no other safety problems. This because a old riverbed forms an ideal situation for piping, these sand pockets can be seen as the yellow parts of figure 5.1. The green and brown section showcase the cover layer and the gray is the aquifer, which is only prone to piping in the yellow, sandy, parts.

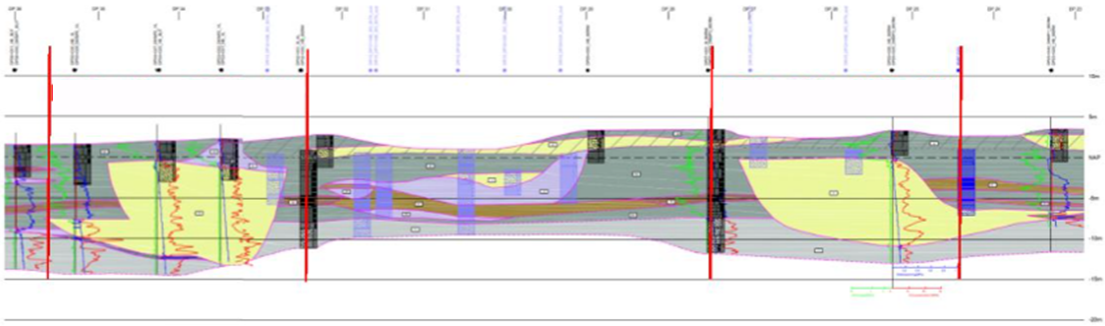

Figure 5.1: Cross section dike section case study (Wierenga et al., 2025)

To capture both global and local effects, the case study combines two dimensional and three dimensional numerical modelling. The 2D model is used to establish the baseline piping behaviour, to determine the required embedment depth of the heave screen under ideal conditions and to find out what the impact of the use of the mandrel is. A 3D model is used to assess the impact of localized installation imperfections that cannot be rightly represented using plane-strain assumptions.

5.2. Applicability models

The models presented in this chapter are developed to analyse the hydraulic performance of plastic heave screens in context of piping. They are applied to the representative dike cross-section mentioned in the previous paragraph and are intended to assess the influence of imperfections on the seepage behaviour, including computing the hydraulic head distribution, seepage velocities, and hydraulic gradients.

The modelling approach is suitable for a comparative analysis between the reference scenarios and defect scenarios. The 2D models, based on plane-strain conditions, are applicable for assessing the overall seepage behaviour along a continuous dike section, while the 3D models enable the representation of local defects. As such, the models are suited to identify trends, quantify relative differences between scenarios, and determine which types of defects have the most significant impact on piping related parameters.

At the same time, the applicability of the models is subject to limitations. The subsurface is schematized into homogeneous soil layers, and natural variability, anisotropy, and small scale heterogeneities are not included. The representation of the mandrel induced disturbed zone and delocking is idealised and does not capture the full complexity and therefore do not account for transient conditions such as varying hydraulic loads. Furthermore, mechanical processes, including soil deformation and potential damage or degradation of the plastic heave screen over time, are not considered.

Consequently, the model results should be interpreted as indicative of the relative influence of installation defects on the seepage behaviour, rather than as exact predictions. The models are most applicable as a tool to support understanding, comparison, and sensitivity analysis within the framework of piping assessments, and to provide insight into the implications of defects of the plastic heave screens.

5.3. Analytical Solutions

The analytical solutions in this section give a first insight in the dike section its vulnerability for piping and the need for a heave screen to make it safe against piping. Firstly the Sellmeijer rule is used and thereafter the method of Lane The Sellmeijer rule is not used to do calculation on the use of heave screens, this because no vertical flow is incorporated in the formula. It is only used to determine if the dike section is prone to piping. Taking the Sellmeijer rule explained in paragraph 2.4, often used in Dutch dike design, you will get the following conclusion for the need of piping measures:

Sellmeijer

The following variables are known from the dike section:

Table 5.1: Input parameters for Sellmeijer piping assessment

Parameter	Value
ΔH (hydraulic head difference) [m]	6.79
d (top layer thickness) [m]	2
γ_p' (submerged unit weight of soil) [kN/m^3]	18
γ_w (unit weight of water) [kN/m^3]	10
θ (friction angle) [°]	37
η (White coefficient) [-]	0.25
d_{70} (grain size) [μm]	265
d_{70m} (reference grain size) [μm]	208
D (aquifer thickness) [m]	50
L (seepage path length) [m]	73.5

This gives:

$$\Delta H_c = 3.76$$
$$F_p = 0.6$$
$$F_p < 1$$

This means that the dike section is prone to piping and a measure needs to be taken.

Lane

To determine the resistance against piping with a vertical element blocking the seepage flow is numerically done using Lane, 1935. The method of Lane is an analytical way of computing the critical head. The method can be seen below:

$$h = \frac{\frac{1}{3}H + \sum V}{c_w} \tag{5.1}$$

$h =$ Critical head that would initiate piping
$c_w =$ Weighted seepage ratio
$H =$ Horizontal seepage length
$V =$ Vertical seepage length

The sheet pile wall increases the numerator and therefore the value of the critical head that would initiate piping.

Table 5.2: Input values used for Lane's weighted creep calculation.

Variable	Value
h (Critical head difference)	6.79 m
H (Horizontal seepage length)	73.9 m
c_w (Weighted seepage ratio)	5 (coarse sand)

$$\sum V = h \cdot c_w - \frac{1}{3} \cdot H = 6.79 \cdot 5 - \frac{1}{3} \cdot 73.9 = 9.32$$

This means a needed length of:

$$\frac{9.32}{2} = 4.66\,\text{m}$$

Table 5.3: Lane's coefficient and safe hydraulic gradient for different soil types (based on Lane, 1935).

Type of Soil	Lane's Coefficient C_w	Safe Hydraulic Gradient ($< 1/C_w$)
Very fine sand or silt	8.5	$< 1/8.5$
Fine sand	7.0	$< 1/7$
Coarse sand	5.0	$< 1/5$
Gravel and sand	3.5 to 3.0	$< 1/3.5$ to $1/3$
Boulders, gravels and sand	2.5 to 3.0	$< 1/2.5$ to $1/3$
Clayey soils	3.0 to 1.6	$< 1/3$ to $1/1.6$

The needed screen height is the length of the screen into the aquifer, this because the clay layer acts as a roof for the pipe. It is known that Lane's method gives an conservative length for the screen, in practice it can be shorter than this computed length.

5.4. 2-Dimensional Models

The 2-dimensional (2D) models reflect standard engineering practice by analysing dike cross sections under plane strain assumptions. These models provide a computationally efficient way to establish a baseline for the performance of the dike and the heave screen. This section defines the parameters for simulating the mandrel induced disturbed zones as regions of increased permeability to find out what the influence is on seepage characteristics.

5.4.1. 2D; Reference Scenario

In practice, the length of the heave screen is determined iteratively using numerical models. The screen needs to comply to different conditions. No heave behind the screen may occur, no front seepage may occur and no vertical fluidization may occur. For the first two calculation criteria are made which can be seen in paragraph 4.6. For the latter one, according Wiggers et al. (2025), it can be assumed that, if the embedment depth is at least 3 meters, vertical fluidization does not occur. Vertical fluidization, however, does need more research to gain knowledge about the exact working of this mechanism. This means that if the criteria of heave and front seepage require a shorter length than 3 meters, still a length of 3 meters is used. This is important because the reference model explained later would be satisfy heave conditions with a shorter sheet pile.

Using the geometry of the existing dike trajectory discussed in paragraph 5.1, a Plaxis 2D model is made, this can be seen in figure 5.2. The first iteration is done by taking the minimum needed length of 3 meters into the aquifer. Using the calculation method explained in figure 4.4 it is determined that the minimum length of 3 meters is sufficient to meet the heave criteria. As can be seen the method of Lane is a conservative way of determining the required length of the heave screen.

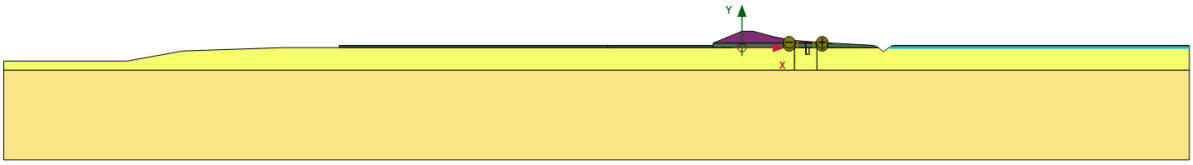

Figure 5.2: 2D model dike section case study

In figure 5.3 the dike section with its properties can be seen. Further characteristics are mentioned below:

- The model dimensions range is from x = -330, x = 200 and y = -50, y = 7.3.
- The longitudinal pipe is 1.5m wide, based on the 3m penetration depth of the screen into the aquifer.
- The groundwater flow boundary condition at the water side is based on the high water level of +6.79 NAP
- The groundwater flow boundary conditions at the screen and in the ditch are the same for imposing the head in the schematic pipe.

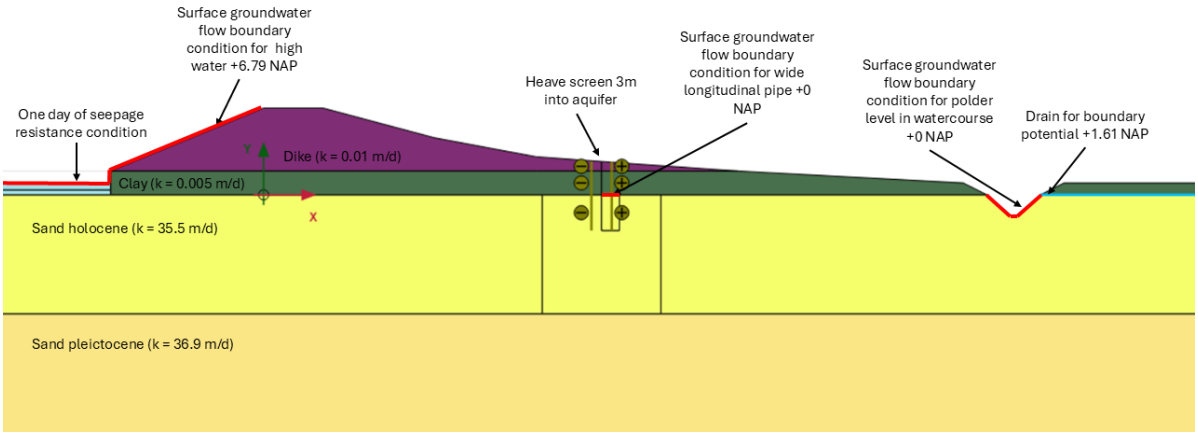

Figure 5.3: 2D model dike section with properties

A zoomed in detail of the groundwater flow boundary condition can be seen in figure 5.4.

Table 4.1 shows that this 2D model is used for determining the scenarios of no intervention, the ideal heave screen and the mandrel-induced gap. The situation with no intervention is used for determining the needed screen length, the ideal heave screen works as a reference for the 3D model and the results on the effect of the mandrel-induced gap.

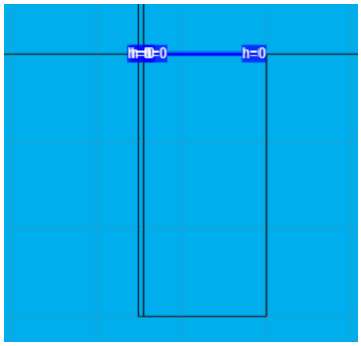

Figure 5.4: Hydraulic condition top of the prism

The model implies a couple of assumptions, to get a clear overview of they are listed below. The impact of each of the assumptions on the outcome will be discussed in the discussion.

- Soil layers are homogeneous and isotropic
- Only flow calculations are done, no soil stresses or deformations are taken into account.
- Plane strain (ϵ_z = 0), this means this section will go on infinitely in longitudinal direction.
- Only 2D streamlines; parallel flow in the xy-plane

5.4.2. 2D; Mandrel Induced Disturbed Zone

The first focus of this research is the impact of the disturbed zone created when the steel mandrel is extracted after the plastic sheet pile reaches its design depth. While current engineering practice assumes this disturbance had a negligible effect on seepage, the following model will be able to quantify the sensitivity of the system to these installation induced changes.

To determine the sensitivity three different indicators are computed. These are the hydraulic head at the bottom of the prism for checking heave, the hydraulic gradient through the disturbed zone, and the flow velocity through the disturbed zone. Important for the interpretation of the results is that in the model it is assumed backward erosion piping has occurred until the screen. This is modelled by using a hydraulic head at the top of the prism equivalent to the head in the pipe, in this case 0. The condition can be seen in figure 5.4. This is based on a wide longitudinal pipe system being the normative scenario, further explained in appendix D. It is not clear if this is also the normative scenario in the case of a gap created by the mandrel. Therefore, also the narrow longitudinal pipe is modelled. This means the width of the prism is smaller. The difference, in 3D, is shown in figure 5.5. This difference can also be modelled in 2D.

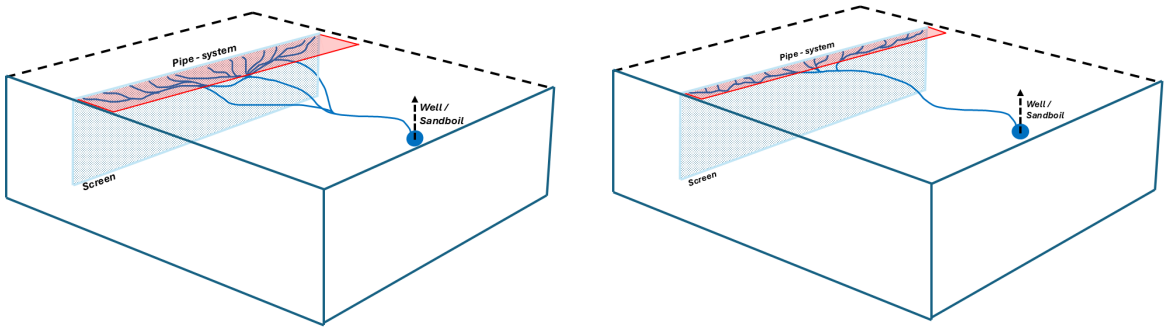

(a) Wide longitudinal pipe

(b) Narrow longitudinal pipe

Figure 5.5: Difference narrow and wide longitudinal pipe in 3D

In figure 5.6 can be seen how the gap is modelled. The red rectangle displays the disturbed zone. This zone is adjusted to different sizes and different permeabilities to see what the effect is on the three indicators mentioned above. The thickness of the mandrel in this case study is 10mm. The mandrel combined with the plastic screen are vibrated into the ground and therefore there is chosen for 20mm and 50mm of disturbed zones, of which the 50mm is an extreme situation. The different dimensions will give a trend out of which conclusions can be taken. For the permeability there is chosen for a denser configuration with 10 m/d until, almost, a ten fault of the permeability with 300 m/d. Again these values are chosen to show a trend. The actual soil behaviour requires in-situ testing. The scenarios computed can be seen in table 5.4 including the reference scenario which describes a ideally working heave screen.

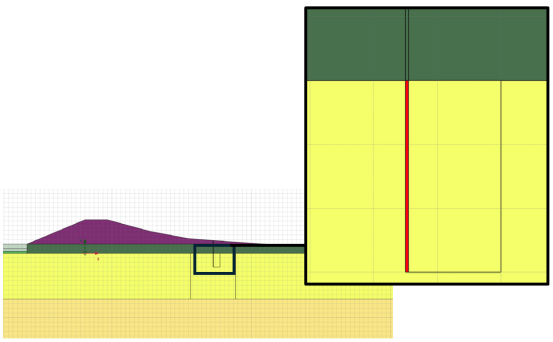

Figure 5.6: Mandrel induced zone of disturbed soil

Table 5.4: Different scenarios for gap created by retracting the mandrel

Scenario	k [m/day]	Width [m]
Reference	-	-
Scenario 1	10	0.02
Scenario 2	70	0.02
Scenario 3	70	0.05
Scenario 4	140	0.02
Scenario 5	140	0.05
Scenario 6	300	0.02
Scenario 7	300	0.05

For this model the most important assumption is the dimensions and characteristics of the disturbed zone. This is based on a prediction of what will happen and not based on actual soil tests. This could be based on soil tests or with the use of a model setting that takes into account soil behaviour. Also, no pipe forming to the hinterland, only a wide or narrow longitudinal pipe. Furthermore, the same assumptions as for the reference model apply.

5.4.3. 2D; Pipe to the Hinterland

To get an insight in the influence of 2 dimensional simplification against the 3 dimensional, more extensive, model there is looked at how pipe systems behave in reality compared to how it is modelled in 2D. In reality the piping system will not only occur at the screen as modelled in 2D, also a pipe formation in the direction of the exit point is necessary. If this is modelled in 2D, because of the plane strain assumption, it means that a complete pipe field will be realised from the screen until the exit point. This is not a realistic situation. Therefore, this situation will later be compared to the 3D situation with, or without a pipe running back to the hinterland. First, the two scenarios for 2D are explained below:

- 2D without line drain: this is the scenario used in engineering practice. To be seen in figure 5.7a.
- 2D with line drain: this means that a drain runs from the screen until the well at the hinterland. To be seen in figure 5.7b.

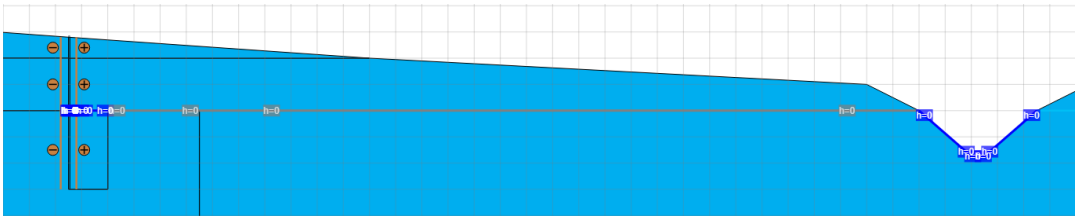

(a) No pipe to hinterland 2D

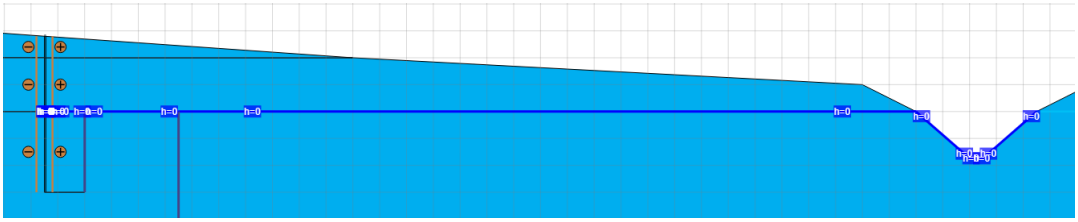

(b) Pipe to hinterland 2D

Figure 5.7: Different scenarios with or without pipe to hinterland 2D

5.5. 3-Dimensional Models

This section describes the development of 3-dimensional (3D) models to capture flow behaviours that 2D analyses can not represent. 3D modelling is used for evaluating localized installation faults, such as a sheet pile delocking, which trigger radial flow and high local hydraulic gradients. The technical setup includes various scenarios for isolated and clustered defects.

5.5.1. 3D; Reference Scenario

For the 3D scenarios only a 3D numerical model is used. Plaxis 3D is capable of computing 3D groundwater flow. In analytical solution often the simplification to a 2D situation is made. Therefore, no analytical solutions are made.

While piping is often simplified in models as a 2D mechanism for reasons of simplicity and computational efficiency, this is a significant concession. In reality, piping is an three dimensional process, involving 3D flow paths, potential meandering and the branching of channels (J. C. Pol et al., 2024). 2D calculations rely on the plane strain assumption, which requires uniform distribution along the dike its longitudinal axis. This assumption is generally valid for long, homogeneous dike sections. However, it becomes a limitation when the objective is to investigate the localized effects of errors in the installation process, as this uniformity no longer exists.

The primary function of the heave screen is to interrupt horizontal seepage flow and increase the seepage length, thereby reducing the hydraulic gradient. A 2D model cannot represent the installation related faults such as a gap in the screen due to delocking. The plane-strain assumption makes sure this single point defect is treated as a continuous linear fault extending perpendicular to the cross section.

A 3D model can solve more difficult spatial behaviour. It can more realistically simulate how seepage lines run. This simulation provides flow streamlines, which are parallel and uniform in a homogeneous 2D model, now converging from all directions towards the localized fault. This flow concentration leads to high localized hydraulic gradients which is a critical factor for initiating piping. As written by van Beek, 2015, 2D and 3D models can provide significantly different solutions for these critical gradients.

An example of the difference between 2D or 3D modelling can be observed if a gap in the screen is modelled. In a 2D model it will essentially be a screen not reaching the required depth, while in 3D the horizontal flow will be blocked at the sides of the hole. The prediction is that in 2D it will lead to failure while in 3D the screen will still hold. For the 3D model, the 2D model is extended in x-direction, to create volumes. Important to note is the change in reference system compared to the 2D model.

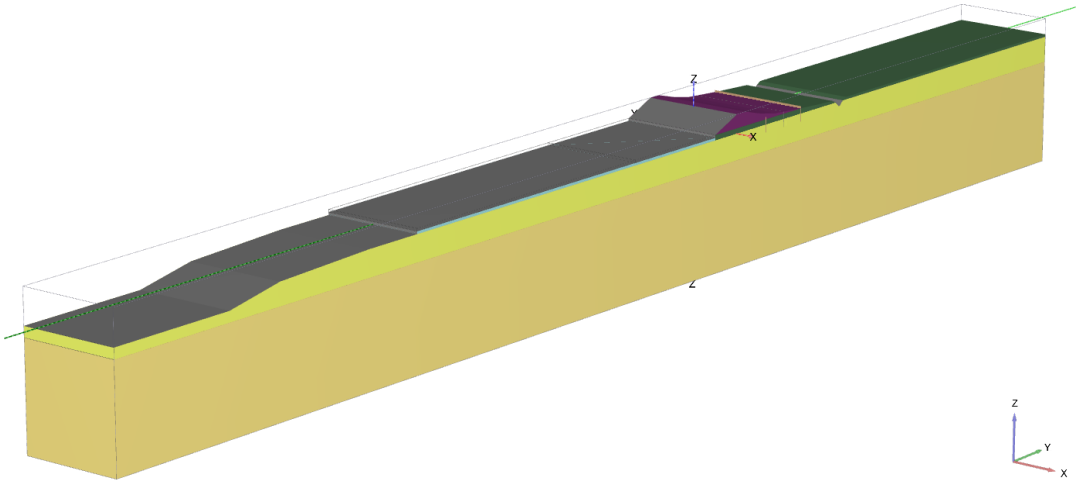

Figure 5.8: 3D model dike section case study

In figure 5.9 the 3D dike section with its properties can be seen. The model characteristic are similar to the 2D model but extended in longitudinal direction. Only the model dimensions change to: x = -50, x = 50, and y = -330, y = 200, and z = -50, z = 7.3

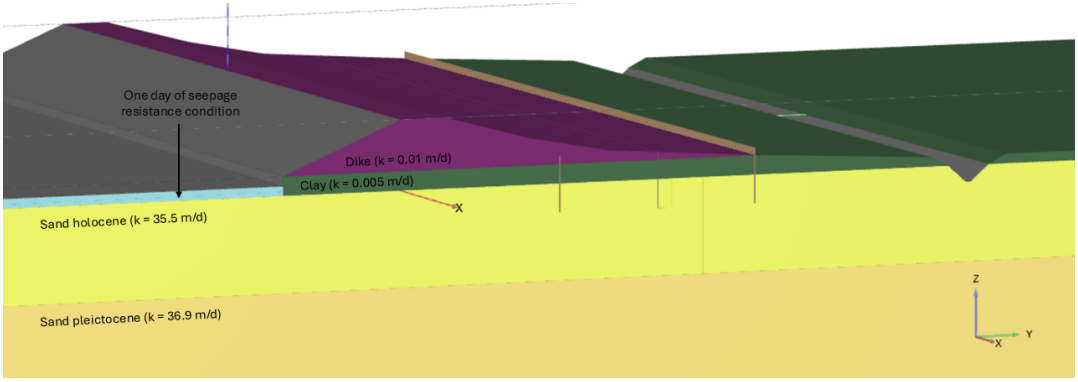

(a) 3D model with soil properties

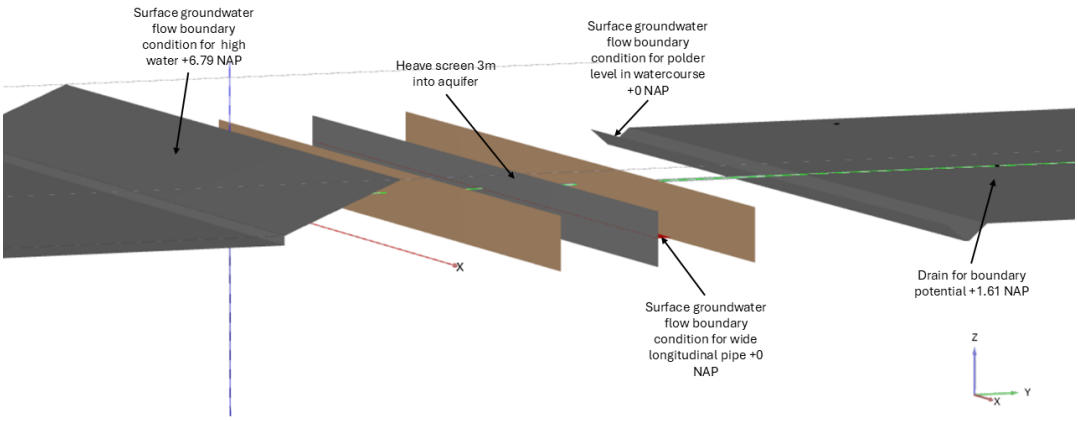

(b) 3D model with boundary conditions

Figure 5.9: 3D model with properties and boundary conditions

Similar to the 2D model, the 3D model relies on a couple assumptions that are mentioned below:

- Soil layers are homogeneous.
- Only flow calculations are done, no soil stresses or deformations are taken into account.

5.5.2. 3D; Pipe to the Hinterland

As said at the 2D; Pipe to the Hinterland paragraph this model is used to get an insight in the influence of 2 dimensional simplification against the 3 dimensional, more extensive, model. In figure 5.10 two scenarios are displayed. One with a pipe running back to the hinterland and one without.

- 3D with planar drain: A complete pipe field running from the screen to the hinterland. This means that there is a fixed head between the cover layer and the aquifer from the screen to the well or ditch in the hinterland.
- 3D with a line drain: this is the scenario that describes reality the most. It can be compared to the situation described in figure 5.10b.

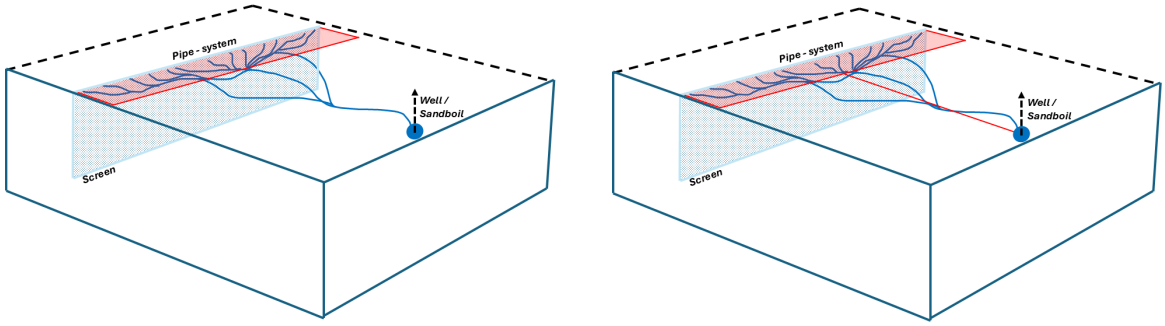

(a) Wide longitudinal pipe

(b) Wide longitudinal pipe with pipe going to the hinterland

Figure 5.10: With or without pipe running back to the hinterland

In the figure you can see a soil body, the heave screen and a schematization of how pipe systems form. In red the simplification used in the model can be seen. A wide longitudinal pipe system is modelled as a rectangle behind the screen in which the hydraulic head is equal to the hydraulic head in the pipe going back to the hinterland. The model has a width of 100m, and if over the full length of this section a wide longitudinal pipe system is formed large quantities of soil are needed to be displaced towards the sand boil, in practice this would not be realistic. But taking the safety assessment method from 2D it is chosen to use the pipe system over the full width of the dike section.

In figure 5.11 the Plaxis 3D model is shown. The red rectangle is the heave screen. Covering the full width of the screen is a wide longitudinal pipe system in gray and highlighted with dots is the pipe running back towards the ditch, which is shown as well.

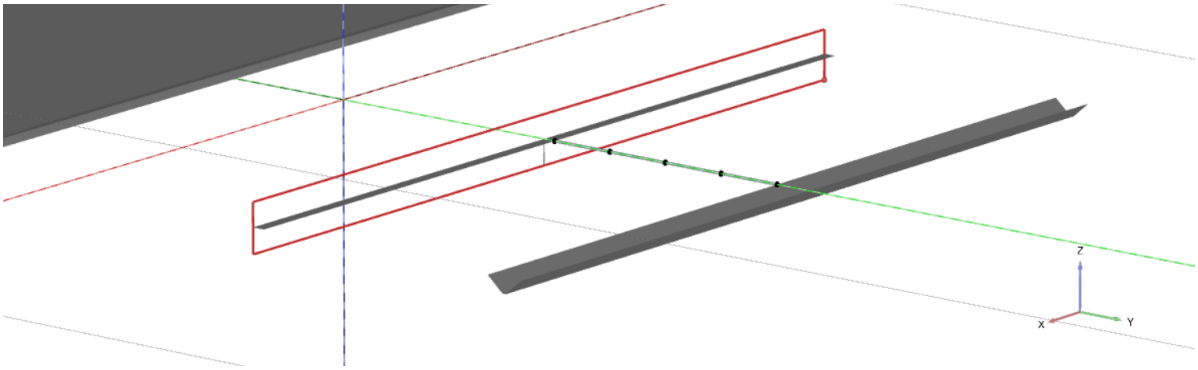

Figure 5.11: Wide longitudinal pipe with drain running back to the hinterland

The same assumptions are valid for this model as for the reference 3D model. An extra important assumption is that the wide longitudinal pipe is forming over the whole section width. This is not realistic. An extra model is made with a limited pipe width which can be seen in appendix D. This model is different to the 2D schematization and the model is not verified, therefore it needs more research. First findings are to be seen in the appendix but no conclusions can be drawn from it.

5.5.3. 3D; One Gap due to Delocking

In practice, the simplification to a 2D model is often made because of computation time and simplicity to model. However, local faults due to installation cannot always be correctly represented by a 2D

model. One of the most common local faults encountered when plastic heave screens are installed, is the delocking of two sheet piles. This will create a gap in the screen as can be seen in figure 5.12.

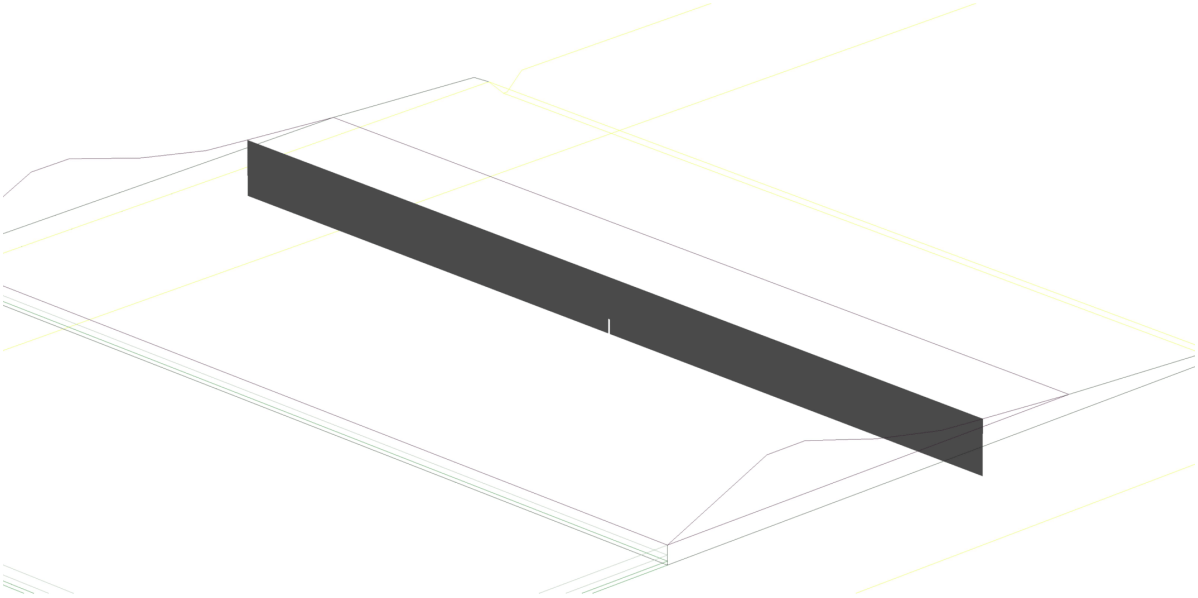

Figure 5.12: Gap in the screen in 3D

In the 3D model there is looked at two indicators, groundwater head and vertical hydraulic gradient. These indicators are first computed in the Plaxis 3D model for the reference scenario. Subsequently, different scenarios are analysed to account for installation induced defects, which are based on sheet pile interlock delocking.

Delocking refers to the separation of the interlock connection between two adjacent sheet piles, as illustrated in Figure 3.3. During installation, the use of a mandrel and the presence of clips that keep the sheet pile aligned with the mandrel ensure that, if delocking occurs, it does not take place under large gradients. As a result, any gaps formed due to delocking are expected to remain relatively small in size.

Furthermore, practical experience, supported by the use of delocking indicators, shows that sheet pile delocking typically occurs when significant resistance is encountered from the sand layer. Consequently, the resulting gap does not develop along the entire length of the sheet pile screen, but is instead limited to a section of the sheet piles.

Based on these considerations, a set of representative defect scenarios is defined and analysed. An overview of the simulated scenarios is presented in table 5.5.

Table 5.5: Different scenarios for gap created by delocking

Scenario	**Gap width [m]**	**Gap height in z-coordinates [m]**
Reference	-	-
Scenario 1	0.05	(-1.5; -3)
Scenario 2	0.05	(-0.75, -3)
Scenario 3	0.10	(-1.5; -3)
Scenario 4	0.10	(0, -3)
Scenario 5	0.20	(-1.5; -3)

The same assumptions are valid for this model as for the reference 3D model. An important assumption in this model is the dimensions of the gap that exists when the lock indicator detects de-

locking. No field tests are done where the surrounding soil is removed to show the delocked section. There is even a consideration that the lock indicators fail and not the locking mechanism of the sheet piles. Further research into delocking is necessary.

5.5.4. 3D; Multiple Gaps due to Delocking

In practice, delocking of screens happens multiple times in the installation of a complete heave screen. This model will give an insight on what distance between the gaps is necessary so that they decrease the interferance to a point where it can be considered irrelvant. To achieve this 3 gaps are added into the model as can be seen below. The distance between the middle gap and the gaps at the sides will be increased by the width of one sheet pile. The scenarios are worked out for the 0.05m gap with z = (-1.5, -3). The 0.05m gap is providing the highest vertical hydraulic gradient.

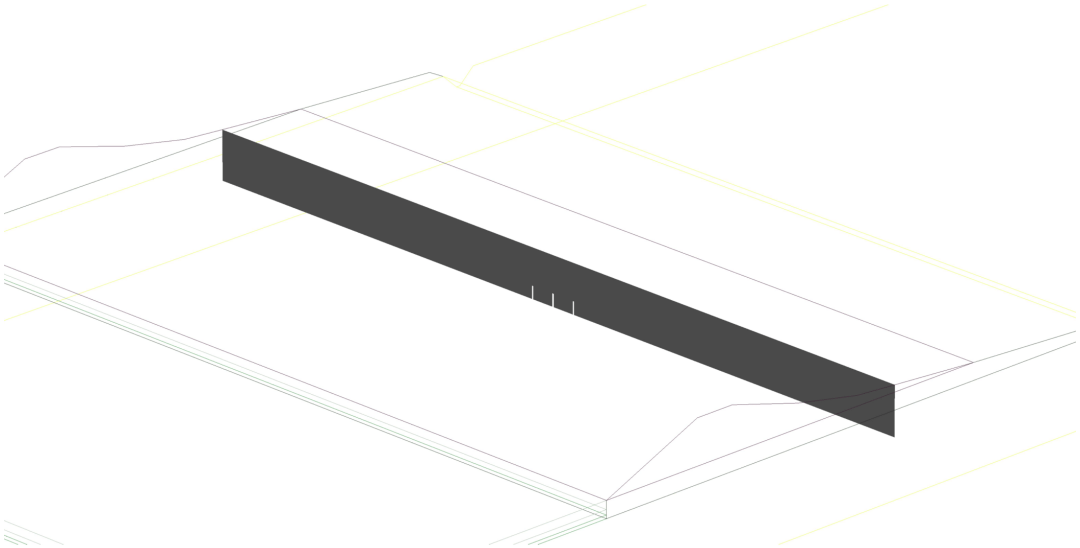

Figure 5.13: 3 gaps in the screen in 3D

The different scenarios that are computed can be seen in table 5.6. These scenarios have been analysed for both gap cases.

Table 5.6: Different scenarios for multiple gaps

Scenario	Distance between gaps
Reference	no gap
Scenario 1	1 gap
Scenario 2	1 pile in between
Scenario 3	2 piles in between
Scenario 4	4 piles in between
Scenario 5	8 piles in between

The same assumptions are valid for this model as for the reference 3D model. In reality, delocking of the screens occurs at a not predictable depth. The model uses same spacing and dimensions of the gaps, what would be a idealized scenario. However, it gives a good indication of the interference between the gaps.

6

Results

The following chapter presents the numerical and analytical findings of this thesis. The results are structured to first validate the modelling approach by comparing 2D and 3D baseline scenarios under ideal conditions. Thereafter, the impact of mandrel induced soil disturbances and localized screen defects are evaluated against heave and vertical fluidization.

6.1. Baseline and validation

For verifying the 3D model, it is compared to the 2D model. The plain-strain conditions of the 2D model are extended into 3D, so any cross-section in the y-z plain of the 3D model will look as the 2D model. The groundwater head at the bottom of the prism for both models is computed in the way it is discussed in paragraph 4.6.1. The results can be seen in figure 6.1a. The differences are smaller or equal to 0.05m, and therefore, the calculation differences will be insignificant. The difference could be explained by the finer mesh used in Plaxis 3D compared to Plaxis 2D. The line at which the groundwater head is determined can be seen in red in figure 6.1b. This red line is the bottom of the prism explained in chapter 4.6.1.

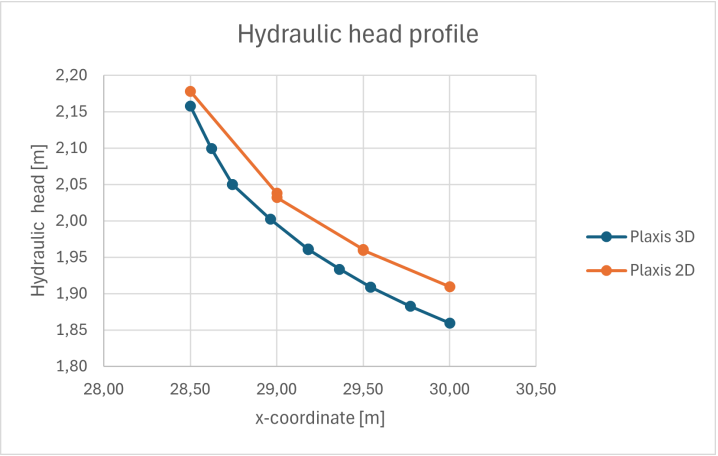

(a) Hydraulic head bottom of the prism Plaxis 2D vs. Plaxis 3D

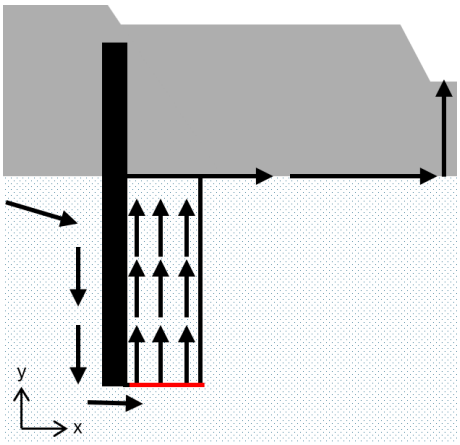

(b) Location of where groundwater head is computed

Figure 6.1: 2D vs 3D groundwater head and computation location

6.2. 2D Mandrel Induced Disturbed Zone

This section analyses the impact of the disturbed soil strip created during the installation of the steel mandrel. Using the 2D model explained in the previous chapter, the area just behind the screen is assigned changing permeability values. The result focus on how these localized changes in soil structure

influence the safety against heave, vertical hydraulic gradients and vertical flow velocities through the disturbed zone.

6.2.1. Heave

To assess safety against heave, the equilibrium method described in paragraph 4.6.1 is applied. In this approach, a soil prism is defined behind the screen, with a height equal to the penetration length of the screen into the aquifer and a width equal to half of this height. The presence of positive effective stress at the base of the prism is then evaluated. This is done by first determining the hydraulic head along the base of the prism and subsequently assessing the resulting effective stress with the use of equation 4.1.

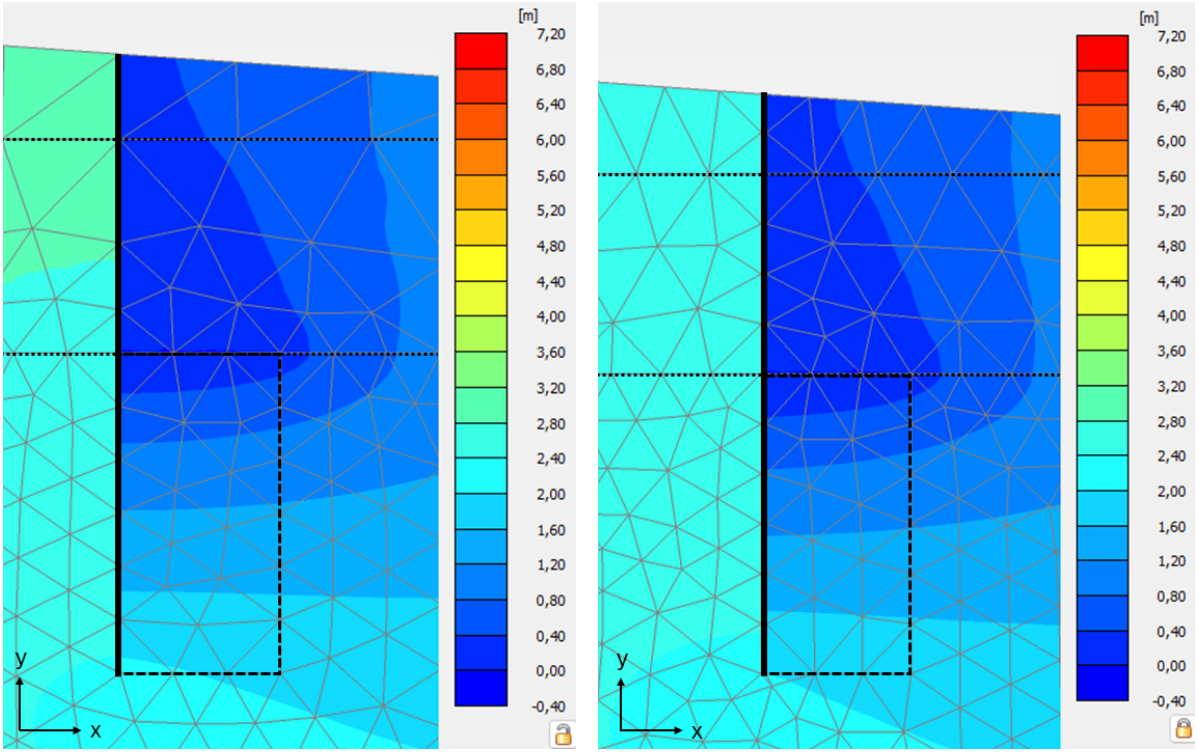

(a) Reference scenario hydraulic head

(b) 0.05m gap and 70 m/d permeability scenario hydraulic head

Figure 6.2: Visualisation heave 2D

The resulting hydraulic head at the base of the prism for each scenario from table 5.4 is presented in the graph below. The x-coordinate in model corresponds to the bottom of the prism.

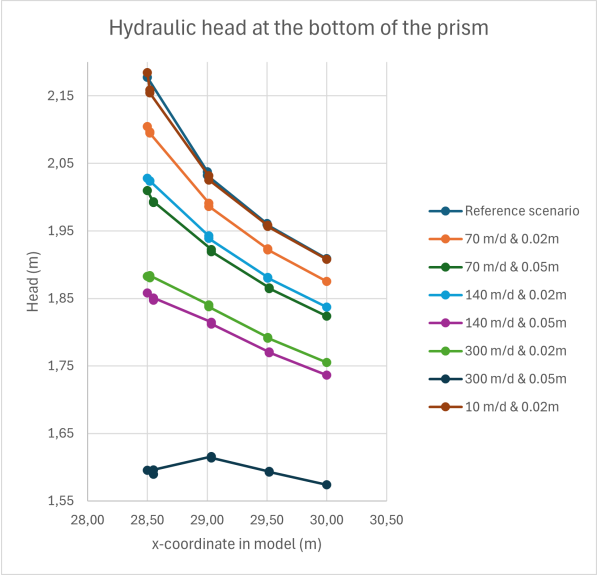

Figure 6.3: Hydraulic head bottom of the prism 2D with different gap dimensions

In figure 6.3 can be seen that both a higher permeability as a wider gap make sure that the hydraulic head at the bottom of the prism is going down. This can be explained by the gap acting as a relief well for the pressure at the bottom of the screen. A relief well makes sure the head is decreasing at and around the point where the relief well is constructed (Miranda Eguez, 2014).

Recalling equation 4.2 the effect of this decrease shows higher safety factors for the occurrence of heave, as can be seen in table 6.1:

Table 6.1: Calculated safety factors for different cases.

Scenario (hydraulic conductivity, gap)	Safety Factor	Percentage with respect to reference
Reference	2.13	-
10 m/d, 0.02 m	2.13	100%
70 m/d, 0.02 m	2.17	101.9%
70 m/d, 0.05 m	2.25	105.6%
140 m/d, 0.02 m	2.23	104.7%
140 m/d, 0.05 m	2.39	112.2%
300 m/d, 0.02 m	2.35	110.3%
300 m/d, 0.05 m	2.67	125.4%

As can be seen in the safety factors for heave the resistance against this failure mechanism is getting more favourable the wider the gap and higher the permeability in the modelled disturbed zone. The disturbed zone will act as a vent through which the high pressure at the tip of the screen can escape towards the zero head condition at the top. Purely looking at the global heave in the prism behind the screen, a higher permeability or wider gap makes this test safer.

6.2.2. Hydraulic Gradient

The vertical hydraulic gradient is evaluated directly behind the screen, along the same line which can be seen in figure 6.5. As can be seen in figure 6.2 and figure 6.6, the gap width behind the screen has only a minor influence on the vertical hydraulic gradient, except in the vicinity of the lower tip of the screen, where noticeable differences occur. Equation 4.6 is applied to compare the calculated hydraulic gradient with the corresponding critical hydraulic gradient.

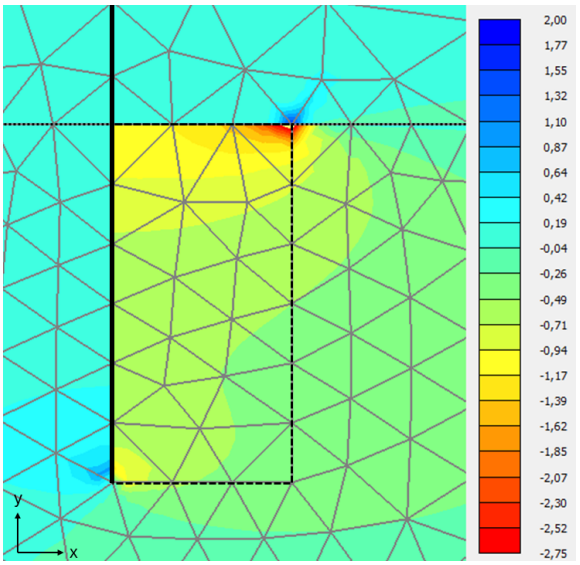

(a) Reference scenario vertical hydraulic gradient

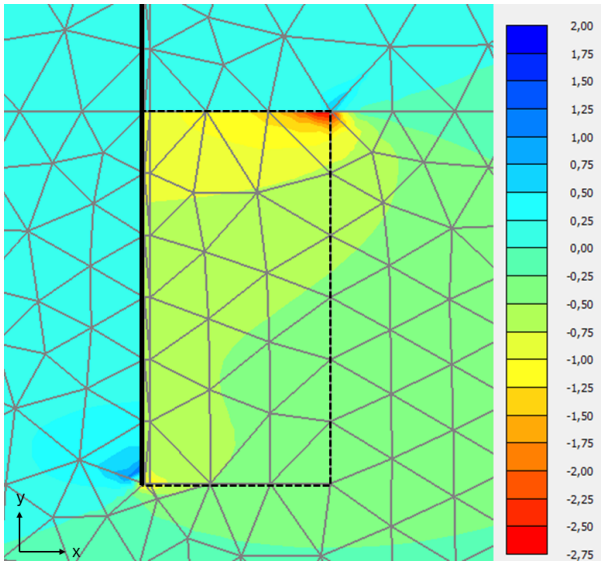

(b) 0.05m gap and 70 m/d permeability scenario vertical hydraulic gradient

Figure 6.4: Visualisation hydraulic gradient 2D

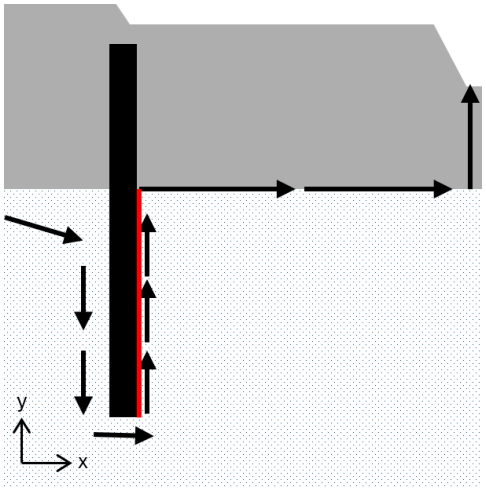

Figure 6.5: Line at which the vertical hydraulic gradient is computed

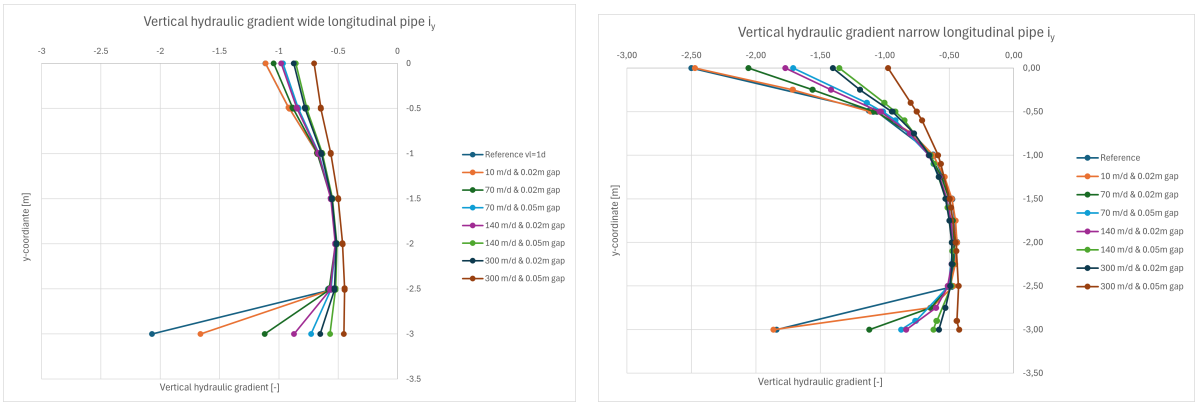

(a) Vertical hydraulic gradient wide longitudinal pipe

(b) Vertical hydraulic gradient narrow longitudinal pipe

Figure 6.6: Vertical hydraulic gradient through disturbed zone

In the table below the maximum hydraulic gradient at the top and bottom of the screen for each scenario can be seen. The critical hydraulic gradient for soil particles to start moving is dependent on the depth and therefore both the top and bottom are given. This hydraulic gradients have negative values as they are defined as moving in the opposite direction to the flow.

Table 6.2: Maximum vertical hydraulic gradient for different scenarios

Scenario (hydraulic conductivity, gap)	**Maximum hydraulic gradient Wide longitudinal pipe [m/d] top / bottom**	**Maximum hydraulic gradient Narrow longitudinal pipe [m/d] top / bottom**
Reference	-1.11 / -2.07	-2.50 / -1.84
10 m/d, 0.02 m	-1.11 / -1.66	-2.47 / -1.86
70 m/d, 0.02 m	-1.04 / -1.12	-2.06 / -1.12
70 m/d, 0.05 m	-0.96 / -0.73	-1.71 / -0.87
140 m/d, 0.02 m	-0.98 / -0.87	-1.77 / -0.83
140 m/d, 0.05 m	-0.86 / -0.57	-1.35 / -0.62
300 m/d, 0.02 m	-0.88 / -0.65	-1.40 / -0.58
300 m/d, 0.05 m	-0.70 / -0.45	-0.97 / -0.42

The critical hydraulic gradient of the soil prism can be computed with the use of equation 4.6. This gives an critical gradient for the soil section behind the screen:

$$i_c = \frac{p'_{v,avg}}{\gamma_w \cdot \Delta z} + \frac{\gamma'}{\gamma_w} \tag{6.1}$$

$$i_c = \frac{12.8}{10 \cdot 3} + \frac{10}{10} = 1.427$$

When this critical gradient is exceeded, local heave will occur making the soil unstable. If the critical gradient is to high for a larger area, the complete area will fail. For the reference model, scenario 1, and for the narrow longitudinal pipe scenario 2, the critical gradient is exceeded. However, this exceedance occurs over a very limited height. As shown in Figure 6.6, the hydraulic gradient decreases significantly with increasing distance from the ends of the heave screen.

Consequently, a reduction of effective stress is expected only locally. Since the sand is laterally confined and no continuous flow path is available, particle movement is restricted and erosion is not expected to occur.

At the upper right corner of the prism, where locally elevated vertical hydraulic gradients are observed (Figure 6.4b), a similar situation applies. Although the critical gradient may be locally exceeded, the affected zone is small and isolated, and the absence of a preferential seepage path prevents the

initiation of piping or soil transport. Furthermore, it is important to note that this zone is a side effect of the way of modelling the wide longitudinal pipe, without a pipe running back to the hinterland. If there would be flow possible towards the hinterland the gradient would decrease.

6.2.3. Flow Velocity

In contrast to the hydraulic head, the flow velocity increases with increasing hydraulic conductivity. This behaviour is expected, as the hydraulic head difference provides the driving force for flow from regions of higher pressure to regions of lower pressure. When the water encounters less resistance from the soil skeleton, the resulting flow velocity increases. An increase in hydraulic conductivity therefore corresponds to a reduction in flow resistance. The line at which the vertical flow velocity is computed is the same as for the hydraulic gradient and can be seen in figure 6.5.

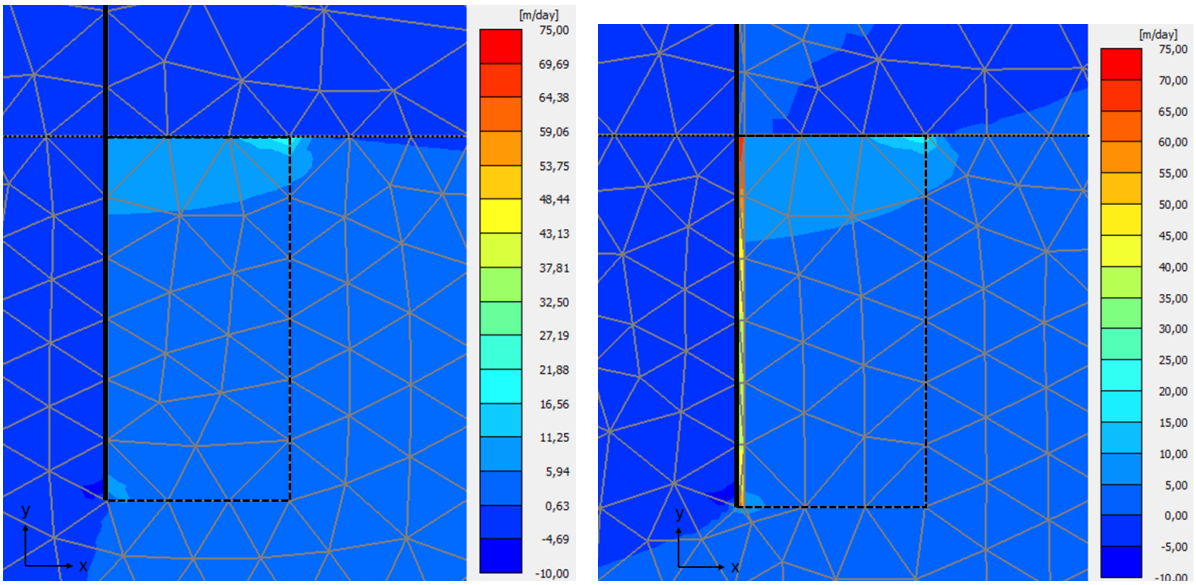

(a) Reference scenario vertical flow velocity

(b) 0.05m gap and 70 m/d permeability scenario vertical flow velocity

Figure 6.7: Visualisation flow velocity 2D

The width of the disturbed zone primarily affects the spatial distribution of the flow by spreading it over a larger area. However, the increase in cross sectional area of the disturbed zone is relatively small, and consequently the influence of the disturbed zone width on the resulting flow velocity is limited. This explains why variations in gap width do not lead to significant changes in the computed flow velocities. The difference is governed by the change in permeability. Below the results for flow velocities through the disturbed zone can be seen for both a wide- and a narrow longitudinal pipe.

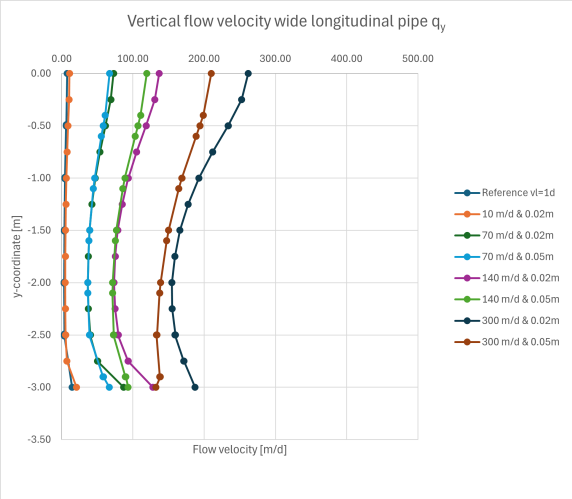

(a) Vertical flow velocity wide longitudinal pipe

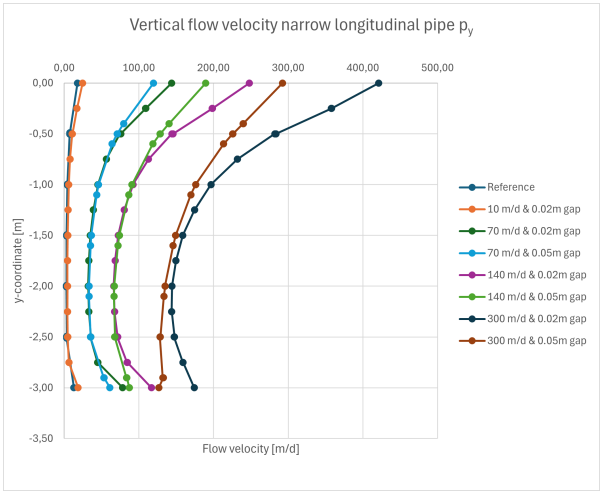

(b) Vertical flow velocity narrow longitudinal pipe

Figure 6.8: Vertical flow velocity through disturbed zone

In the table below the average flow velocities can be seen to provide an numerical overview of the magnitude of the velocities.

Table 6.3: Average flow velocity over depth for different scenarios

Scenario (hydraulic conductivity, gap)	Average flow velocity Wide longitudinal pipe [m/d]	Average flow velocity Narrow longitudinal pipe [m/d]
Reference	3.76	5.28
10 m/d, 0.02 m	5.35	8.23
70 m/d, 0.02 m	34.56	54.23
70 m/d, 0.05 m	33.60	51.87
140 m/d, 0.02 m	65.56	103.49
140 m/d, 0.05 m	60.48	94.60
300 m/d, 0.02 m	129.05	203.75
300 m/d, 0.05 m	110.50	171.63

The average flow velocity gives an indication of the differences between scenarios. High flow velocities may indicate an increased potential for soil erosion at the boundaries of the gap. Furthermore, it can be seen that, in contrast to heave, a narrow longitudinal pipe is giving higher flow velocities and so is the normative situation.

The mechanisms governing vertical fluidization behind the screen are not yet completely understood. But such high flow velocity are a clear indication of a decrease in safety against vertical erosion. A disturbed zone created by a mandrel, in the form of higher permeability, will be a safety issue. The size of the disturbed zone is not of big influence but the permeability of the disturbed zone left by retracting the mandrel should be investigated.

6.3. 2D versus 3D; Pipe to the Hinterland

This section compares the performance of 2D and 3D models in representing groundwater flow towards the hinterland. While 2D models assume an infinitely, uniform pipe, the 3D models allow for one line running back towards the hinterland, as can be seen in figure 5.11. This comparison shows the conservatism of the used 2D assessment, and shows the overestimation of a complete pipe system until the relief well.

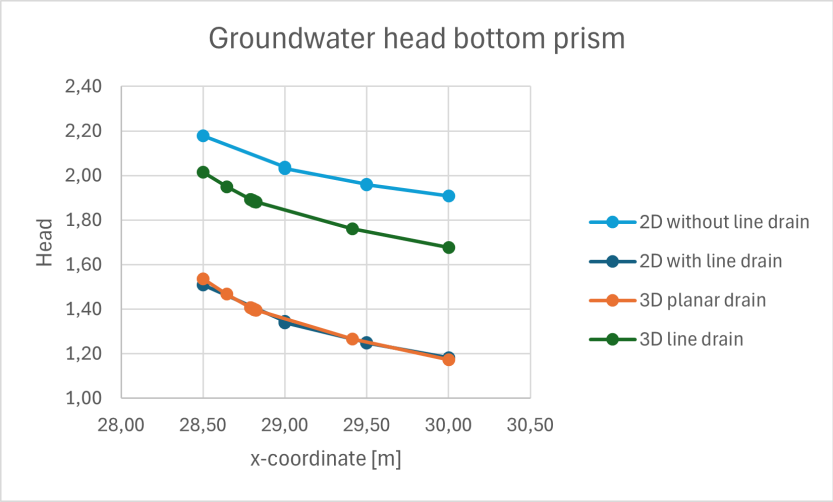

Figure 6.9: Groundwater head at bottom of prism 2D vs 3D

Figure 6.9 displays the groundwater head at the bottom of the prism, discussed in 4.6.1, for the different scenarios mentioned above. It shows that the commonly used 2D model without the pipe running to the hinterland is the most conservative for the calculation on heave. The 3D scenario with a planar drain and the 2D scenario with a line drain are overestimating the safety and should be avoided.

To see the impact of a line drain running back to the hinterland, the groundwater head at different distances from the drain is computed in 3D. The drain is situated at the middle of the model, x = 0. Then the groundwater head at x = 10, x = 20, x = 30, x = 40 and x = 50 are computed. The model can be seen in figure 5.11.

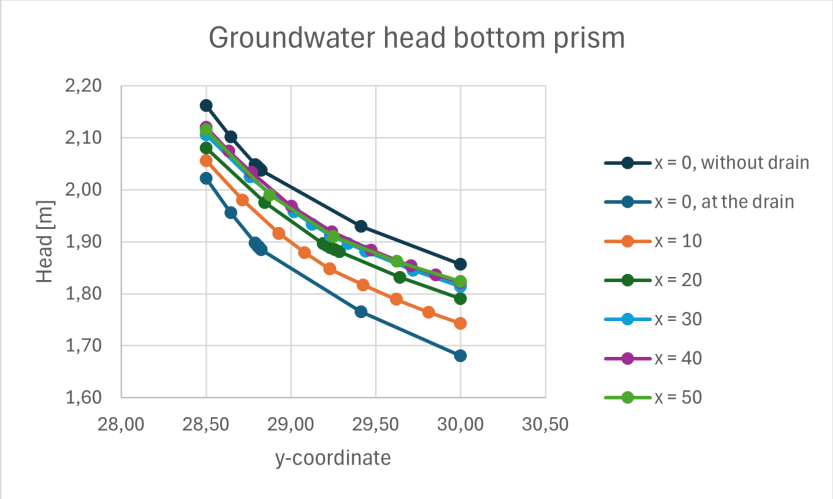

Figure 6.10: Groundwater head at bottom of prism different distances from pipe to hinterland

Adding the pipe in the model makes the head lower. The biggest difference is right at the location of the pipe, x = 0. Further away from the pipe, the head converges to a steady state which is still lower than the model where no pipe to the hinterland is implemented. This shows that not modelling a pipe running to the hinterland provides a conservative solution for heave safety.

6.4. 3D; One Gap due to Delocking

This paragraph investigates the consequences of a single gap formed by one delocked sheet pile. The 3D model is used to take the radial flow towards the fault into consideration. The analysis focuses on the heave assessment and resulting peak in the vertical hydraulic gradient at the gap.

6.4.1. Heave

The same method as in 2D is used in 3D. The most vulnerable location for heave to occur is determined to be in the middle behind the gap. At this location the hydraulic head at the bottom of the prism is computed again. This will lead to a global safety assessment. Based on the same rules the safety factors can be computed as well. The result of the head can be seen in figure D.2. The safety factors linked to the different situations can be seen in table 6.4.

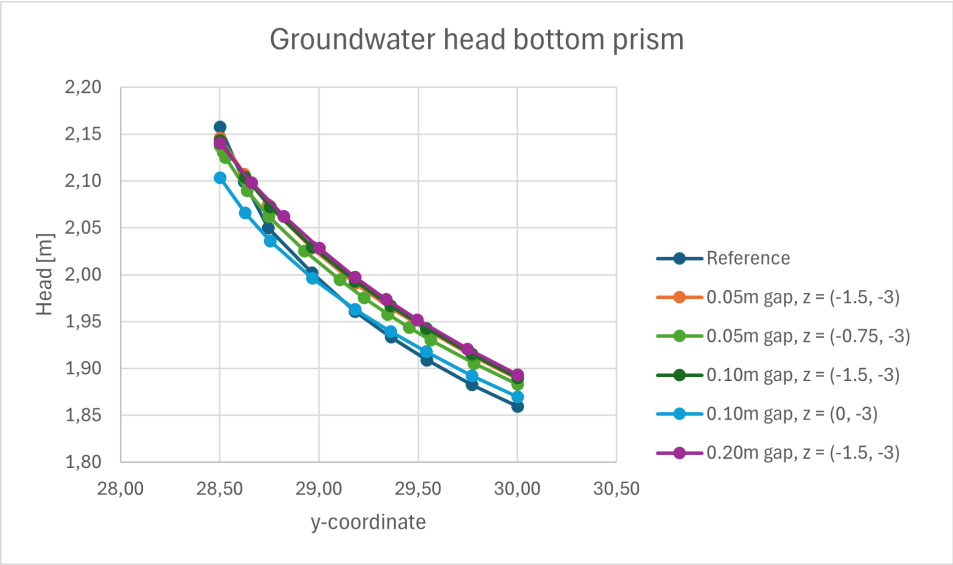

Figure 6.11: Head of wide longitudinal pipe

Table 6.4: Calculated safety factors for different gap scenarios

Scenario (gap & vertical length)	Safety Factor	Average head	Percentage with respect to reference
Reference	2.17	1.97	-
0.05m gap & z = (-1.5, -3)	2.15	1.99	99.1%
0.05m gap & z = (-0.75, -3)	2.16	1.98	99.5%
0.10m gap & z = (-1.5, -3)	2.15	1.99	99.1%
0.10m gap & z = (0, -3)	2.18	1.96	100.5%
0.20m gap & z = (-1.5, -3)	2.14	2.00	98.6%

Taking the results shown above, one gap, in the form of a dislocked screen, in the middle of a dike section does not have enough influence to increase the head difference to a level where the global safety criteria are not met any more.

However, as can be seen in figure 6.12a, the highest gradient in groundwater head difference is near the top of the gap. Therefore, a second calculation with a different reference system is made. This reference system uses a smaller, more local prism running from the top of the gap towards the interface of the aquifer and the cover layer, as can be seen in figure 6.12b. The groundwater head is computed at the red line. The dimensions of this prism are the height until where the screen delocks and the width is the half of this height.

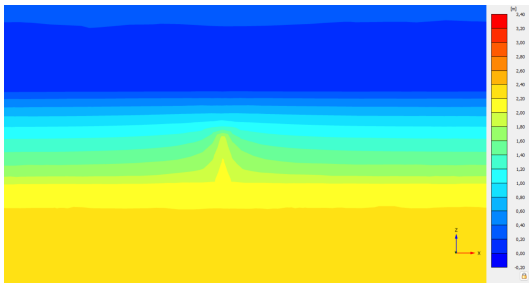

(a) Groundwater head cross section x-z plane with 1 gap

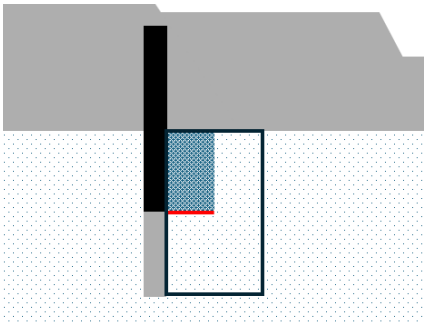

(b) Schematization local heave prism at gap

In contrast to the global heave the groundwater head for this more local situation differs significant from the reference scenario. Figure 6.13 displays the head at the bottom of the small prism, z = -1.5, for different widths of gaps. Using this head the global test on effective stress, and thus heave can be executed. The results can be seen in table 6.5.

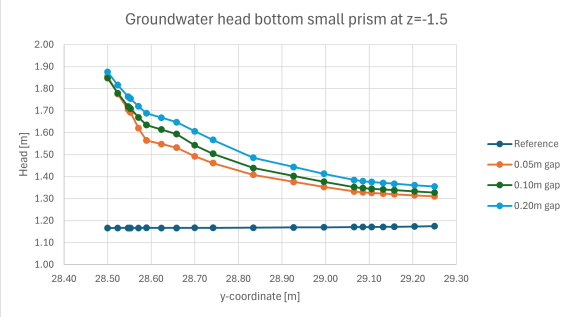

Figure 6.13: Head at z=-1.5, the bottom of the small prism

Table 6.5: Head at z=-1.5, the bottom of the small prism

Scenario	Safety factor	Average Head
Reference	2.37	1.17
0.05m gap	1.86	1.49
0.10m gap	1.83	1.52
0.20m gap	1.78	1.56

Where the safety factor of the reference scenario, without a gap is sufficient, for the scenarios where a gap has been added the safety factor goes below 2. Therefore, according to the guidelines, heave can occur and the dike is not safe. The same has been done for the 0.05m gap at z = (-0.75, -3). These results can be seen in the figure below.

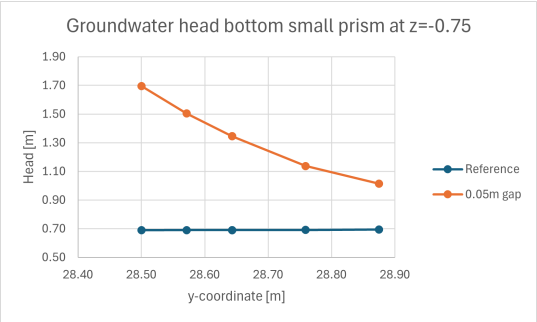

Figure 6.14: Head at z=-0.75, the bottom of the small prism

Table 6.6: Head at z=-0.75, the bottom of the small prism

Scenario	Safety factor	Average head
Reference	2.94	0.69
0.05m gap	1.51	1.34

6.4.2. Hydraulic Gradient

The same scenarios as for heave are computed for the vertical hydraulic gradient. The hydraulic gradient gives an insight about the local behaviour of the soil and flow around the gap. The hydraulic gradient is computed just behind the screen, over the length of the screen into the aquifer.

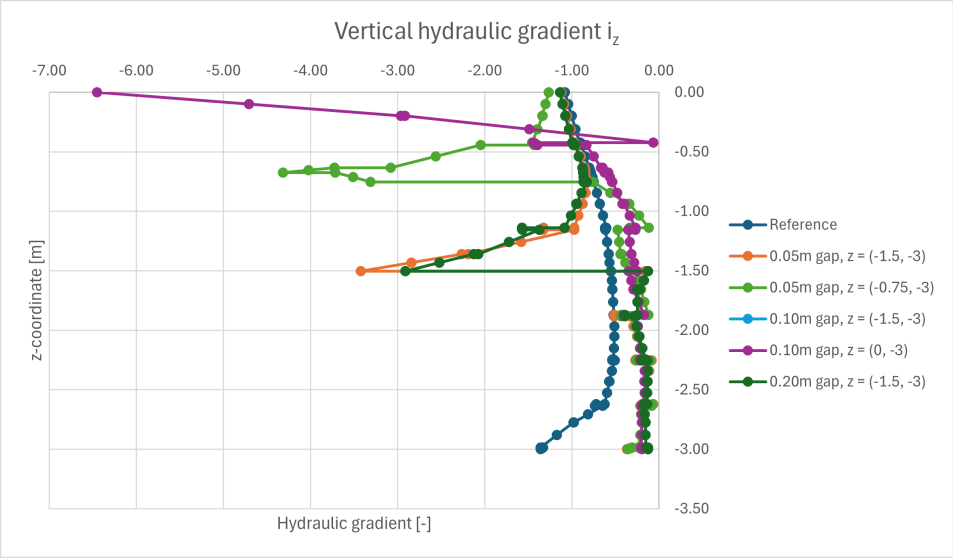

Figure 6.15: Vertical hydraulic gradient around gap in 3D

In figure 6.15 can be seen that around the gap located at -1.5m or 0m large vertical hydraulic gradients occur. These gradients exceed the critical gradient mentioned above in equation 6.1. The critical gradient doesn't change in a 3D situation compared to a 2D situation. These high gradients could imply that soil erosion is occurring. It can also be seen that the width of the gap doesn't has a big influence on the hydraulic gradient. However the location at which the gap starts, 0 or -1.5, does have a big influence.

6.5. 3D; Multiple Gaps due to Delocking

Bulding on the single gap analysis, this section evaluates the interaction between multiple delocked sheet piles. By varying the distance between the gaps along the longitudinal axis of the dike, the model identifies whether defects act independently or if there spacing leads to a positive or negative effect on the hydraulic resistance.

6.5.1. Heave

Similar as done for the heave calculation, the global safety on heave is computed using the groundwater head at the bottom of the screen z = -3 and at the top of the gaps, z = -1.5. The contours of the groundwater head around the gaps, at z = -1.5, can be seen below, in figure 6.16. In this figure can be seen that the gaps influence each other in the x-direction.

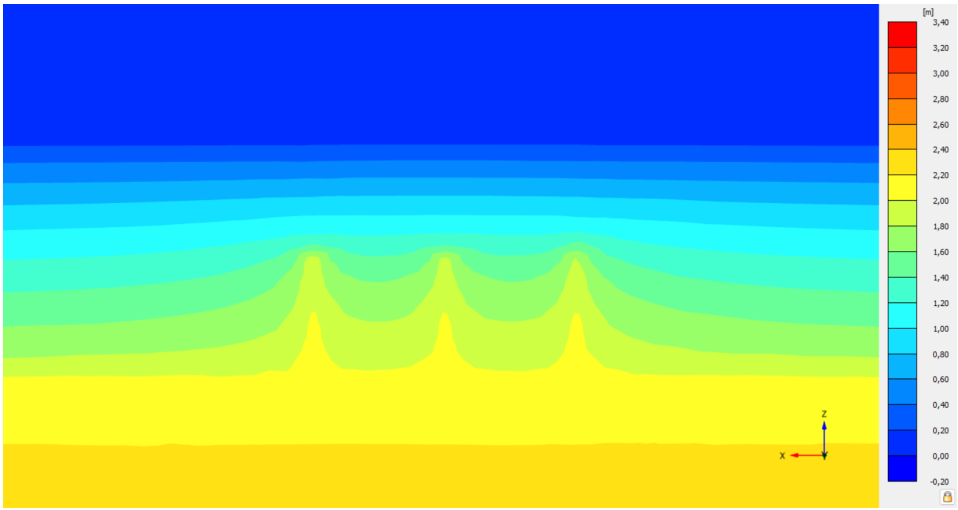

Figure 6.16: Contour groundwater head with 3 gaps

To couple numerical values to the plot, the groundwater head is computed at the start of the gap, along a line in x-direction. This because the here the difference in head will be the greatest. Further down in y-direction, towards the hinterland, the groundwater head will flatten out towards the groundwater head in the hinterland. Firstly the groundwater head at the bottom of the global prism, at the screen, is computed. This for determining the safety on global heave. In figure 6.18 the results can be seen for the different scenarios.

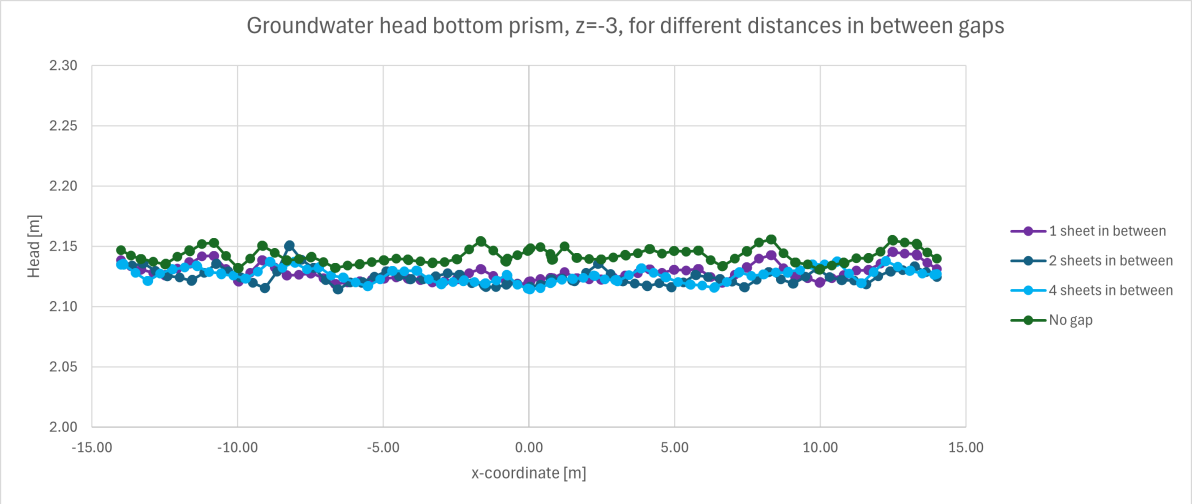

Figure 6.17: Contour groundwater head with 3 gaps at z = -3

As can be seen the gaps do not influence each other significantly. For the global safety on heave it can be concluded that multiple gaps do not influence the outcome of the safety analysis. Because of the only slight differences in groundwater head in x-direction, the head in y-direction is not computed. The differences in y-direction will level out towards the groundwater table in the hinterland.

For the local safety the groundwater head is first computed in x-direction directly behind the screen because at this location the differences will be the largest. The results for the different scenarios can be seen in figure 6.18. It can clearly be seen that the influence of that the gaps have on each other diminishes as there are more working sheets in between.

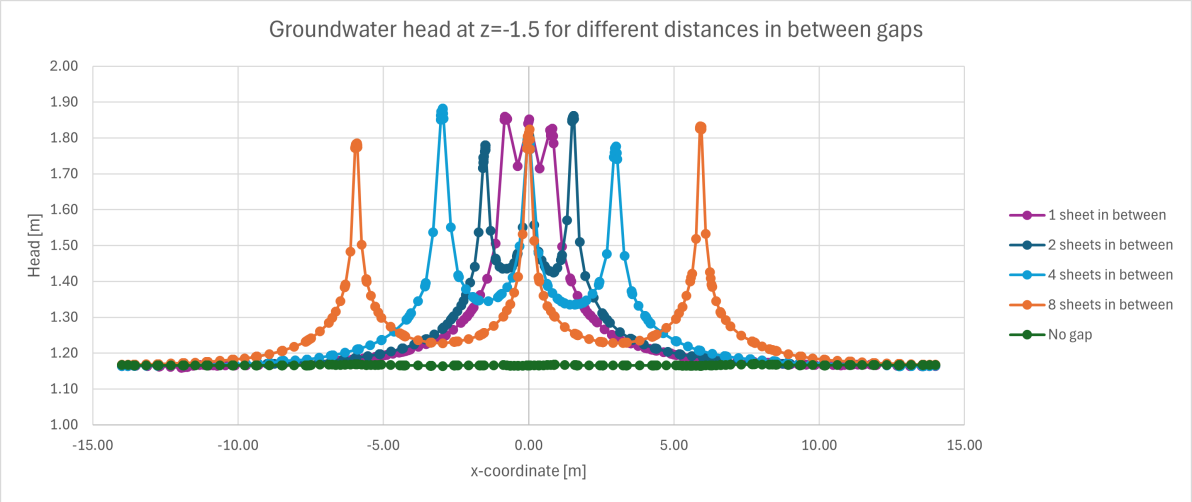

Figure 6.18: Contour groundwater head with 3 gaps at z = -1.5

In figure 6.19 the groundwater head in y-direction, at the x-coordinate of the gaps, are added to the 2D plot in figure 6.18.

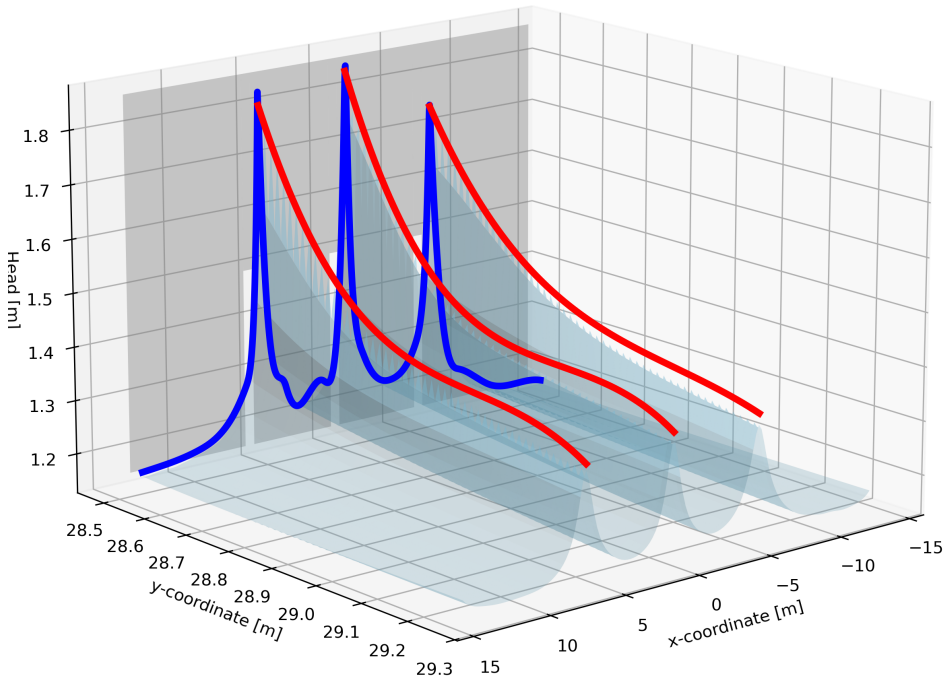

Figure 6.19: Groundwater head with 3 gaps at z = -1.5 and 8 sheets in between

Now the groundwater head is computed in the middle between the gaps to show if the zones, in which heave can occur, interfere creating a big volume in between the 2 gaps at the side where safety against heave is not guaranteed. The results can be seen in table 6.7.

Table 6.7: Groundwater head middle in between gaps at z = -1.5

Scenario	Average groundwater head	Safety factor
no gap	1.17	2.37
2 piles in between	1.44	1.93
3 piles in between	1.38	2.01
4 piles in between	1.33	2.09
8 piles in between	1.24	2.24

This means that, for the gap dimensions of 0.05m width and 1.5m height, the groundwater interferes too much if one in three sheet piles delock. Furthermore, it can be seen in figure 6.18 and figure 6.19, that in between the gaps the groundwater head decreases rapidly. For 8 working sheets in between two gaps it can be said that the area between the gaps is safe and therefore the they don't influence each other negatively. This is because for less sheet piles the influence around the gap keeps a significant width of influenced zone. With 8 gaps the influence is so little it could also be a model fault.

6.5.2. Hydraulic Gradient

The vertical hydraulic gradient is used to get insight in the local effects of the gaps formed by the sheet piles delocking. Four scenarios are created, similar to what has been done for heave.

Table 6.8: Different scenarios for vertical hydraulic gradient

Scenario	Distance between gaps
Scenario 1	1 pile in between
Scenario 2	2 piles in between
Scenario 3	4 piles in between
Scenario 4	8 piles in between

In figure 6.20 the four different scenarios are shown. The vertical hydraulic gradient is computed just behind the screen, (see figure 6.5) at the x-coordinates of the middle of the three gaps and presizely in between. This ensures an insight in the behaviour at the gap and the influence the gaps have on each other.

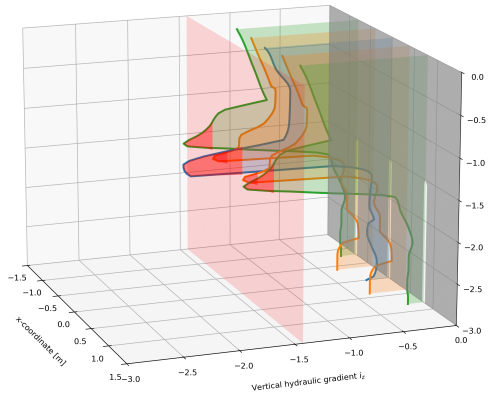

(a) Vertical hydraulic gradient 1 sheet pile in between 3D

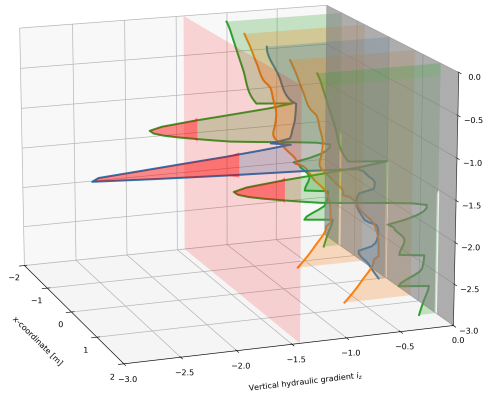

(b) Vertical hydraulic gradient 2 sheet piles in between 3D

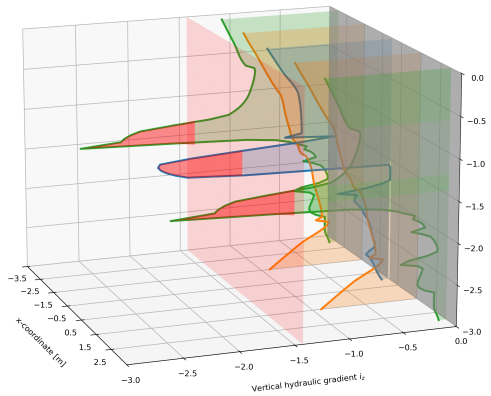

(c) Vertical hydraulic gradient 4 sheet piles in between 3D

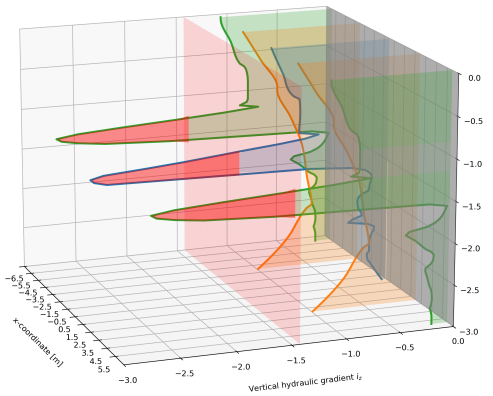

(d) Vertical hydraulic gradient 8 sheet piles in between 3D

Figure 6.20: Vertical hydraulic gradient for different distances between gaps 3D

As can be seen, for every scenario, the hydraulic gradient exceeds the critical hydraulic gradient. The critical hydraulic gradient is displayed as the red rectangle. For the first scenario, seen in figure 6.20a, at the top of the gaps, the vertical hydraulic gradient is exceeding the critical gradient in the middle between the gaps as well. For the other scenarios the hydraulic gradient in between the gaps is decreasing very quickly, ensuring that the vertical hydraulic gradient does not exceed the critical gradient in between the gaps if there are two or more working sheet piles in between. In appendix E the side views are displayed which show that the vertical hydraulic gradient is converging to reference case, without a gap, very quickly.

7

Discussion

This research provides a comprehensive insight into the hydraulic behaviour of plastic heave screens when subjected to installation-induced defects, demonstrating that installation quality is a critical hydraulic performance parameter rather than just a structural requirement. By evaluating these screens through 2D and 3D numerical models, the study reveals that while current safety assessment practices often assume an ideal, continuous barrier, realistic imperfections, such as mandrel induced soil disturbance and interlock delocking, significantly redistribute hydraulic loads and create concentrated flow paths.

A central finding of this research is that the choice of modelling framework, particularly the use of the vertical equilibrium method and the rectangular soil prism, fundamentally dictates the interpretation of safety. This standard approach provides a conservative global assessment by averaging pore water pressures across the prism's base. However, this averaging effect can be deceptive; it often masks localized hydraulic peaks, allowing global safety factors to remain above the required threshold of 2.0 even when local conditions at a specific fault have reached critical levels. Furthermore, sensitivity analysis suggests that the common assumption of a wide longitudinal pipe system may be overly optimistic compared to narrower, more realistic pipe developments which result in substantially higher groundwater heads.

The specific nature of the installation fault further influences the system's response. Mandrel induced disturbed zones create higher-permeability regions that act as localized "vents," reducing hydraulic head at the screen tip but simultaneously increasing vertical flow velocities that heighten the risk of internal vertical erosion. Conversely, 3D modelling of localized delocking captures radial flow convergence that 2D plane-strain models fail to represent. These 3D simulations confirm that while isolated gaps may not compromise global stability, the interaction between clustered defects amplifies gradients significantly. The study found that a spacing of approximately eight intact sheet piles is required for defects to be treated as independent, localized faults.

However, these findings must be interpreted within the context of the model's assumptions. The simulations consist of steady-state groundwater flow calculations, which provide a detailed look at hydraulic heads and gradients but do not include fully coupled hydro mechanical soil behaviour. Consequently, the results indicate areas of hydraulic vulnerability rather than direct predictions of time dependent erosion or failure. Furthermore, the representation of imperfections required simplification; permeability adjustments and discrete gaps capture hydraulic sensitivity but not the full mechanical complexity of soil density and stress state changes during installation.

The study also highlights significant unknowns regarding the physical causes of delocking. Whether caused by subterranean obstacles like rocks, high-resistance coarse sand layers, or false signals from lock indicators, the actual physical state of the screen may vary. For instance, a coarse sand layer causing delocking might inherently be less prone to piping, a scenario not currently implemented in the models. Additionally, the observations indicate a potential transition from horizontal backward

erosion to vertical instability or fluidization behind the screen, representing an important knowledge gap in current piping theory.

In conclusion, while plastic heave screens are an effective alternative to traditional methods, their resistance is highly sensitive to installation-induced imperfections and three dimensional flow effects. For contractors such as Heijmans, these results emphasize that small discontinuities can lead to concentrated flow paths, underlining the importance of controlling penetration depth and interlock continuity. Ultimately, a careful balance between numerical analysis, physical understanding of vertical erosion, and rigorous execution quality remains essential for the reliable performance and safety assessment of heave screen systems.

8

Conclusion

This research investigated the influence of the installation process of plastic heave screens on their hydraulic effectiveness. By using both 2D and 3D numerical models, the effects of realistic installation caused defects were quantified. The following section answers the research questions formulated in chapter 1.5.

The implementation of plastic heave screens in Dutch dike reinforcement projects represents a sustainable and cost effective alternative to traditional steel sheet piles. However, this research demonstrates that the material properties and required installation techniques for plastic, for example the use of a steel mandrel, can introduce hydraulic risks that are neglected in current safety assessment practices. Numerical analysis reveals that faults occurring during installation have a influence on the hydraulic effectiveness of the screen in preventing backward erosion piping, challenging the standard assumption of ideal, continuous conditions.

To understand these effects, the study evaluated a range of hydraulic indicators, finding that no single parameter fully captures the system's behaviour. Groundwater head distribution remains the primary tool for calculating global heave safety factors, providing insight into whether a defect reduces overall head loss across the barrier. However, it lacks the sensitivity required to detect localized instabilities. In contrast, vertical hydraulic gradients serve as a much more sensitive indicator for local soil fluidization, particularly near gaps, while vertical flow velocities highlight the specific risk of internal erosion within disturbed zones.

The impact of these installation faults is dictated by their specific physical characteristics. Two dimensional analysis of mandrel induced disturbed zones shows that higher permeability regions created during extraction act as localized relief wells or "vents". This venting effect reduces the hydraulic head at the screen tip, which increases the calculated safety factor for global heave. However, this apparent increase in safety is deceptive; the same process leads to significantly higher vertical flow velocities within the disturbed zone, heightening the risk of internal vertical erosion and potentially reducing the system's overall resistance.

When considering localized delocking, three dimensional modelling is essential for capturing radial flow convergence that standard 2D plane-strain models fail to represent. While an isolated gap caused by a delocked sheet pile may leave global groundwater head levels largely unaffected, the local head at the top of the gap increases significantly. This concentration of flow causes local heave safety factors to drop below the required threshold of 2.0, indicating that single defects can initiate localized failure.

The spatial distribution of these defects further complicates their hydraulic impact. The interaction between multiple gaps is strongly dependent on their spacing; clustered defects pose a significantly greater risk than isolated imperfections because their zones of influence overlap. This clustering amplifies both groundwater head and vertical gradients in the soil between defects, potentially leading to a

broader reduction in local safety factors. The study determined that a distance of approximately eight intact sheet piles between defects is necessary for their hydraulic influence to decrease sufficiently, allowing them to be treated as independent, localized faults.

Ultimately, the hydraulic performance of plastic heave screens is deeply interconnected with the quality and consistency of the installation process. Although global safety criteria may often remain above critical values for limited and isolated defects, improper installation redistributes hydraulic loads and creates concentrated flow paths that can reach or exceed critical values for internal soil instability. Therefore, installation quality must be recognized as a critical hydraulic performance parameter.

Moving forward, to bridge the gap between execution reality and safety assessment, research should focus on refining 3D models to replace simplified rectangular pipe representations with realistic branching pipe systems. Furthermore, a deeper physical understanding of the mechanisms governing vertical erosion and fluidization behind screens is required to establish dedicated assessment methods. Finally, validating the reliability of lock indicators is essential to ensure that detection tools used in the field accurately reflect the physical state of the installed screen.

9

Recommendations

The findings of this research include several areas where further research is necessary to better understand and manage the risks associated with plastic heave screens. It is sub divided into research recommendations and pratical recommendations.

9.1. Research recommendations

Get a good insight into how piping towards a heave screen works:
This research confirms that piping towards a heave screen is a three dimensional process, particularly when installation defects are present. Future studies should move beyond only flow calculations to include full coupled hydro mechanical soil behaviour. This would allow for the simulation of the development of erosion initiation, transport, and structural degradation, rather than relying on only hydraulic indicators. Important for this is the way in which pipes form, to be able to model a good representation of reality in 3D, pipe forming towards the screen has also a safety margin left which could lead to more economic screens.

Get a better insight into vertical erosion:
A heave screen alters the hydraulic scheme by forcing flow vertically, potentially causing vertical instability or fluidization behind the screen. The mechanism governing this vertical fluidization are currently not sufficiently understood. Dedicated research is needed to determine the critical conditions under which vertical erosion becomes the governing failure mechanism. If this known are assessment method for vertical erosion can be made.

Do tests on what happens to the soil behind the screen if the mandrel is retracted:
This research modelled the disturbances through simplified permeability adjustments. Physical testing is recommended to investigate the actual soil response during and after installation, including changes in soil density, anisotropy, and the resulting stress state. Understanding whether the ”venting effect” is observed in models occurs in practice is crucial for validating safety assessments.

Further investigation of the 2D versus 3D modelling gap:
In this research different scenarios are modelled using different models without a comparison. However, the 2D model is used as a basis for the 3D model. Future 3D models should replace current simplifications, such as modelling piping as large rectangular zones behind the screen, with more realistic representations of pipe systems consisting of several smaller, branching channels. It is important to see how the results of the 3D model of a realistic pipe system compare with the simplified 2D models. It would also be convenient, with regards to computation time, to find a way to add the 3D properties as boundary conditions to a 2D model.

Further investigation in working of delocking indicators:
While quality control currently utilizes lock indicators to verify the continuity of the plastic heave screen , the reliability of this tool remains uncertain. It is presently assumed that every trigger signifies a de-

locking event, yet it is unknown if these indicators accurately represent structural gaps or are prone to mechanical failure during the vibration installation process. A review of the design and functionality of these detection tools is recommended to distinguish between ”false positives” and genuine installation-induced defects. This validation is essential for reducing the current level of uncertainty in post construction safety assessments.

Data collection for validation:

Data need to be collected to validate the findings of the numerical model. This means finding data of the soil and hydraulic flow just behind the screen. Furthermore, soil characteristics and flow characteristics around the failed installation points is important as well to find out if the behaviour of the real situation is equivalent to the model.

9.2. Practical recommendations

Incorporating hinterland pipe systems in assessments:

The safety assessment would become more accurate with the use of a more realistic pipe system. Currently 2D representation is the standard, which may be conservative but not accuratly represent 3D piping. Incorporating more realistic hinterland pipe systems may improve the accuracy of the hydraulic prediction, reduce unnecessary conservatism and potentially lead to cost savings. However, this should only be done once validated modelling approaches are available.

Addressing the installation method:

A clear installation procedure related to the OBOR needs to be implemented. The OBOR makes assumptions based on a certain installation method, this method should be followed. If not possible, more research need to be done on this different installation method.

Bibliography

Akrami, S., Bezuijen, A., van Beek, V., Rosenbrand, E., Terwindt, J., & Förster, U. (2021). Analysis of development and depth of backward erosion pipes in the presence of a coarse sand barrier. *Acta Geotechnica*, *16*(2), 381–397. https://doi.org/10.1007/s11440-020-01053-0

Allsop, W., Kortenhaus, A., Morris Contributors Buijs, M. F., Hassan, R., Young, M., Doorn, N., van der Meer, J., Van Gelder, P., Dyer, M., Redaelli, M., Utily, S., Visser, P., Bettess, R., Lesniewska, D., & ter Horst, W. (2007). *Title Failure Mechanisms for Flood Defence Structures Lead Authors DOCUMENT HISTORY* (tech. rep.).

Beek, V. v., Rosenbrand, E., Hijma, M., & Hoogendoorn, R. (2020). Kennis voor Keringen: Syntheserapport pipingonderzoek 2018-2019.

Box, P. O., & Vrouwenvel, A. C. W. M. (1987). *Netherlands organization for applied scientific research TNO Report IBBC Tifle Probabilj-stic Design of Flood. Defences TNO Institute for Building Materials and Structures Author* (tech. rep.).

Foster, M., Fell, R., & Spannagle, M. (2000). The statistics of embankment dam failures and accidents. *Canadian Geotechnical Journal*, *37*(5), 1000–1024. https://doi.org/10.1139/t00-030

France, W. J. (2018). Seepage Rehabilitation for Embankment Dams.

Gedeon, G. (1994). *Design of Sheet Pile Walls* (tech. rep.). www.cedengineering.com

Hakkers, Van Oord, & BeensGroep. (2023, October). *Experimental Investigation Composite sheet piles* (tech. rep.).

Halter, W., Hop, M., & Wiggers, A. (2025, April). *OBOR Kunststof heaveschermen* (tech. rep.).

IKAMI, T., & MAEDA, K. (2021). Mechanism of Piping Progress in River Levee Focus on the Deformation in the Foundation Ground and the Localization of Seepage Flow by Sheet-Pile Installation. *Journal of Japan Society of Civil Engineers, Ser. B1 (Hydraulic Engineering)*, *77*(2), I_127–I_132. https://doi.org/10.2208/jscejhe.77.2{_}I{_}127

IPM-team. (2021, November). *HWBP Innovatieproject Praktijkonderzoek Opbarsten bij dijken* (tech. rep.).

Jongejan, R. B., & Calle, E. O. (2013). Calibrating semi-probabilistic safety assessments rules for flood defences. *Georisk*, *7*(2), 88–98. https://doi.org/10.1080/17499518.2013.790731

Knoeff, H., & van Bree, B. (2016, August). *Faalkansbegroting* (tech. rep.).

Koerner, R. M., & Koerner, G. R. (2013). Geotextile Filter Failures Under Challenging Field Conditions. *Sound Geotechnical Research to Practice*, 272–289. https://doi.org/10.1061/9780784412770.018

Lane, E. W. (1935). Security from Under-Seepage-Masonry Dams on Earth Foundations. *Transactions of the American Society of Civil Engineers*, *100*(1), 1235–1272. https://doi.org/10.1061/TACEAT.0004655

Lengkeek, H. J., Post, M., Breedeveld, J., & Naves, T. (2019). Eemdijk full-scale field test programme: Ground dike and sheet pile dike failure test. *17th European Conference on Soil Mechanics and Geotechnical Engineering, ECSMGE 2019 - Proceedings*. https://doi.org/10.32075/17ECSMGE-2019-0454

Li, M., & Fannin, R. J. (2012). A theoretical envelope for internal instability of cohesionless soil. *Geotechnique*, *62*(1), 77–80. https://doi.org/10.1680/geot.10.T.019

Miranda Carlos, Teixeira Ana, Huber Maximilian, & Schweckendiek Timo. (2025, February). Uncertainties Analysis and Life Cycle Costs of Piping Mitigation Measures. In *Geotechnical safety and risk v*. IOS Press. https://doi.org/10.3233/978-1-61499-580-7-855

Miranda Eguez, C. A. (2014). *Probabilistic Design of Relief Wells as Piping Mitigation Measure* (tech. rep.). http://repository.tudelft.nl/.

Oldhoff, R. (2013). *Meetkwantiteit versus toetsingskwaliteit* (tech. rep.). www.bzim.nl

Ploegam. (2020, June). Proef met kunststof damwanden.

Pol, J. C., Kanning, W., & Jonkman, S. N. (2021). Temporal Development of Backward Erosion Piping in a Large-Scale Experiment. *Journal of Geotechnical and Geoenvironmental Engineering*, *147*(2). https://doi.org/10.1061/(asce)gt.1943-5606.0002415

Pol, J. C., Noordam, A., & Kanning, W. (2024). A 3D time-dependent backward erosion piping model. *Computers and Geotechnics*, *167*, 106068. https://doi.org/10.1016/j.compgeo.2024.106068

Pol, J. (2020, October). *Shields-Darcy pipingmodel. Verschilanalyse met Sellmeijer en D-GeoFlow* (tech. rep.).

Raadschelders & Lukas. (2023). *Analysis of the effects of dike structures on heave failure at screens* (tech. rep.).

Rijkswaterstaat. (2012, March). *Zandmeevoerende Wellen* (tech. rep.). www.rijkswaterstaat.nl

Rijkswaterstaat. (2021, May). *Schematiseringshandleiding piping* (tech. rep.). www.iplo.nl

Rijkswaterstaat. (2023, December). *Handleiding Overstromingskansanalyse Piping: Dijken/Dammen Deel 2* (tech. rep.). www.iplo.nl

Rosenbrand, E., van Beek, V., Förster, U., van der Kolk, B., Wiersma, A., Terwindt, J., Peters, D., Akrami, S., Koelewijn, A., van Gerven, K., Voogt, L., & Bezuijen, A. (2019). Large-Scale Test of a Coarse Sand Barrier as a Measure Against Backward Erosion Piping. *European Working Group on International Erosion EWG-IE*, 23–25.

Salmasi, F., Nourani, B., Abraham, J., & Norouzi, R. (2021). Numerical investigation of relief well performance for decreasing uplift pressure under embankment dams. *International Journal of Environmental Science and Technology*, *18*(9), 2819–2830. https://doi.org/10.1007/s13762-020-03030-2

Schweckendiek, T., Vrouwenvelder, A. C., & Calle, E. O. (2014). Updating piping reliability with field performance observations. *Structural Safety*, *47*, 13–23. https://doi.org/10.1016/j.strusafe.2013.10.002

Sellmeijer, H., de la Cruz, J. L., van Beek, V. M., & Knoeff, H. (2011). Fine-tuning of the backward erosion piping model through small-scale, medium-scale and ijkdijk experiments. *European Journal of Environmental and Civil Engineering*, *15*(8), 1139–1154. https://doi.org/10.1080/19648189.2011.9714845

Sivakugan, N., & Das, B. M. (2010). *Geotechnical engineering : a practical problem solving approach*. J. Ross Pub.

Tauw. (n.d.). SoSEAL: Een innovatieve dijkverserkingstechniek. https://www.tauw.nl/projecten/soseal-%E2%80%93-soil-sealing-by-enhance-aluminium-and-organic-matter-leaching.html

te Riele, E. (2021, August). *Quick scan advies kunststof heaveschermen WOS* (tech. rep.).

Technical Advisory Committe on Water Defences. (1998, January). *Fundamentals on Water Defences* (tech. rep.).

Technische adviescommissie voor de waterkeringen. (2001). *Technisch Rapport Waterkerende Grondconstructies Geotechnische aspecten van dijken, dammen en boezemkaden* (tech. rep.).

Terzaghi, K. (1943, January). *Theoretical Soil Mechanics*. Wiley. https://doi.org/10.1002/9780470172766

van Beek, V. M. (2015). *Backward erosion piping initiation and progression* (tech. rep.). TU Delft.

Van Hoven, A., Noordam, A., & Wiersma, A. (2019). *POVM Opbarsten Cluster Rekentechnieken POV MACRO STABILITEIT* (tech. rep.).

Vorogushyn, S., Merz, B., & Apel, H. (2009). *Natural Hazards and Earth System Sciences Development of dike fragility curves for piping and micro-instability breach mechanisms* (tech. rep.). www.nat-hazards-earth-syst-sci.net/9/1383/2009/

Wierenga, J., Bisschop, C., van Zanten, H., & Faber, H. (2025). *Ontwikkelnotitie Waterveiligheid DO JAK* (tech. rep.).

Wiggers, A., van der Doef, L., Servais, R., Halbmeijer, L., & Nollen, R. (2025). Publicatie Heaveschermen.

Zagema, A. (2023, June). *The risk assessment of incorrectly installed vinyl heave screens in dikes* (tech. rep.).

Zwanenburg, C., & Patricia, N. (2018). Lessons Learned from Dike Failures in Recent Decades. *International Journal of Geoengineering Case Histories ©*, *4*(2). https://doi.org/10.4417/IJGCH-04-03-04

Appendix A - Countermeasures piping

In this appendix, further explanation is given about different control measures against piping. The different piping measures can prevent different aspects of piping from occurring.

Seepage berms

The seepage berm is a stabilization measure which is driven by its mass. It is primarly designed to mitigate heave and exit gradient concentration at the downstream toe. In geometries where a clay blanket overlies a aquifer, the berm acts as a physical surcharge.

Mechanically, the berm increases the total vertical stress acting on the confining layer. This makes sure that the pore pressure in the underlaying aquifer does not exceed the threshold for hydraulic heave to occur, where the effective stress reaches zero. Furthermore, by extending the horizontal seepage path, the berm reduces the average hydraulic gradient. While an impermeable berm shifts the exit point further landside, a sand berm allows controlled vertical discharge, effectively venting the pressure through a graded filter that prevents soil migration while maintaining normal pressures at the surface.

Berms require a lot of space, they are the most economical viable option but often can't be used because of the lack of space (Miranda Carlos et al., 2025).

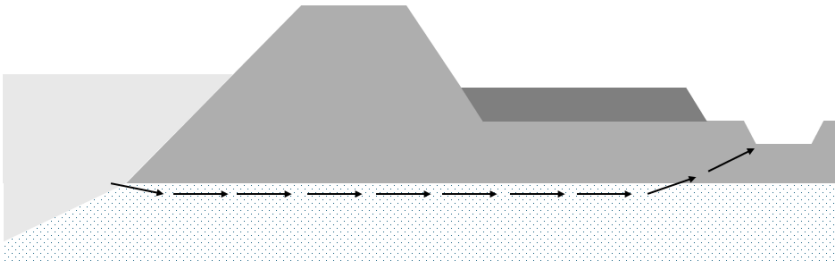

Figure A.1: Schematization piping berm

Vertical cutoff walls (heave screens)

Vertical barriers serve as physical blockage to horizontal seepage, aiming to reduce the discharge and the localized exit gradient at the toe. There are two versions:
Cutoff walls: Typically constructed via the trench method (using soil-bentonite or cement-bentonite), these barriers are digged into an underlying impermeable layer. This creates a drastic drop in piezometric head across the wall, significantly reducing the hydraulic load on the landside foundation.
Heave screens: These are partial vertical barriers, made of steel or plastic, installed at the seepage

exit. They do not block the flow entirely but force seepage streamlines to follow a deeper, more resistant full path. This vertical redirection creates a localized head loss, ensuring the vertical exit gradient remains below the critical gradient required to initiate sand boiling (Halter et al., 2025).

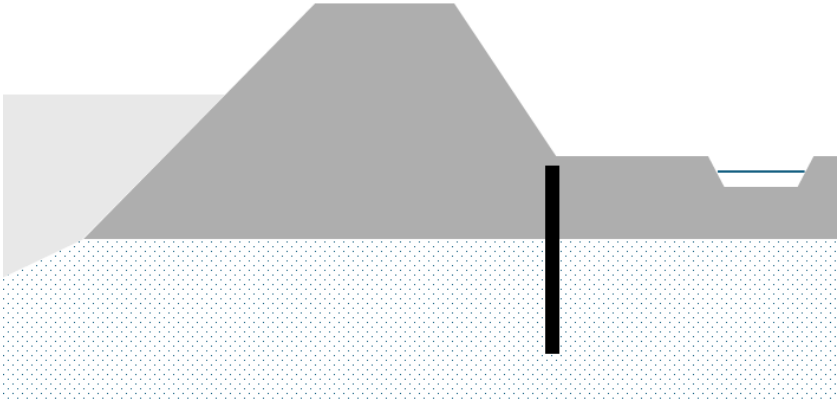

Figure A.2: Vertical cutoff wall (heave screen)

Pressure relief wells

Relief wells are active hydraulic interventions used when depth or space constraints make berms or cutoffs impractical. They function by creating a localized cone of depression in the confined aquifer's piezometric surface. The wells provide a path of least resistance. By allowing water to discharge under controlled conditions through a granular filter pack, the wells reduce the uplift pressure against the overlying cover layer. However, the efficiency of these systems is subject to clogging and incrustation (France, 2018).

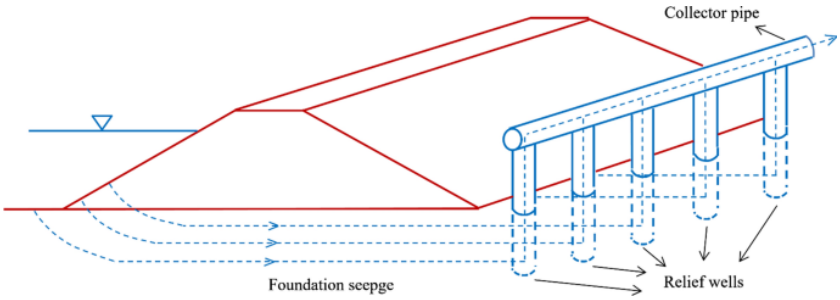

Figure A.3: Schematization relief wells (Salmasi et al., 2021)

Coarse sand barrier

The coarse sand barrier is a passive, targeted measure against piping. It involves the replacement of natural foundation sand with a trench of densified, coarser material. Its efficacy is dependent on two things:

critical gradient contrast: The larger grain size of the barrier material significantly increases the critical hydraulic gradient required to start the movement of particles. When a pipe advances upstream and reaches the barrier, the local flow velocity is insufficient to transport the coarser grains, stopping the pipe's progression.

Hydraulic conductivity contrast: The barrier is highly permeable, acting as a hydraulic bypass. This allows water to flow through the barrier with minimal head loss, which reduces the driving force at the tip of the erosion pipe (Rosenbrand et al., 2019).

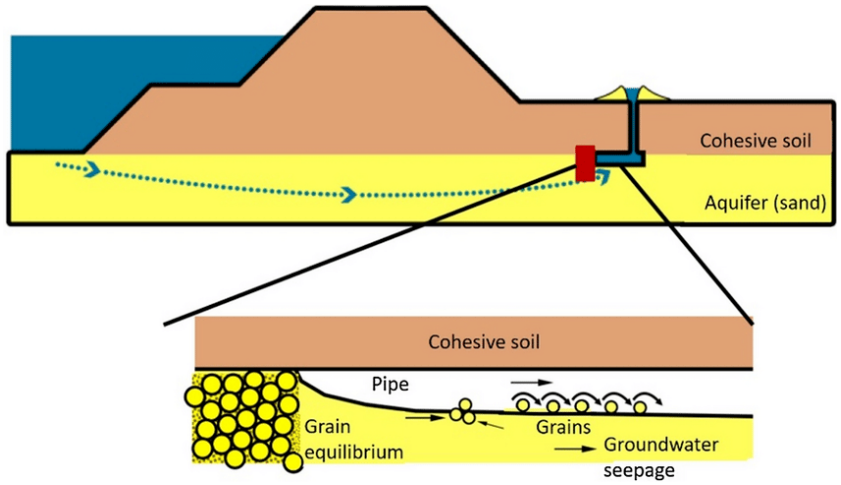

Figure A.4: Schematization coarse sand barrier (Akrami et al., 2021)

Geotextile filter layer

In drainage and slope protection, geotextiles serve as a synthetic alternative to graded granular filters. Their primary function is to maintain interfacial stability, allowing fluid flow while preventing soil movement. However, in the context of internal erosion, geotextiles face the risk of clogging or blinding. Blinding occurs when a thin layer of fine grained particles settle on the upstream surface of the fabric, creating an impermeable layer. This leads to a rapid increase in pore water pressure behind the geotextile, which can destabilize the dike. Because of this, their use in generally restricted to zones where hydraulic gradients are low or where the system is accessible for long term monitoring (Koerner and Koerner, 2013). They are placed at the same place as the cutoff walls (see figure A.2), but different to the cutoff, geotextiles let water pass.

SoSEAL

SoSEAL is an in-situ sealing technology that replicates the geological process of podzolization. By injecting a solution of dissolved organic matter (DOM) and aluminium salts into the sandy soil, a chemical reaction is triggered that forms stable flocs. These flocs accumulate in the pores of the sand, drastically reducing the hydraulic conductivity of the soil. This transforms a pervious sand layer into a low permeability barrier. The advantage of this method is the lack of structural disturbance, it avoids the vibrations and heavy equipment associated with sheet piling, making it an intervention for seepage control in environmentally sensitive or built areas (Tauw, n.d.).

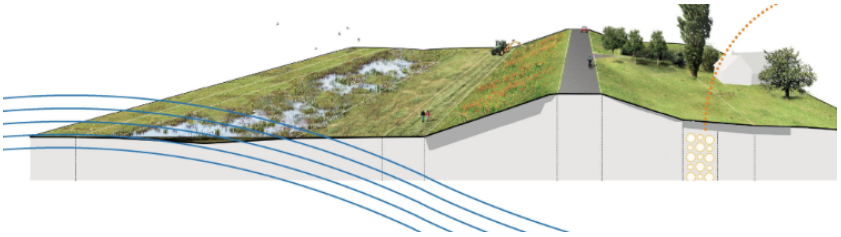

Figure A.5: SoSEAL solution (Tauw, n.d.)

B

Appendix B - Probability of failure due to piping

This provides a better insight on what probability calculation the chance of failure due to piping is based. It is provides extra information for chapter 2.

B.1. Probability of failure

The risk of backward erosion piping becomes negligible when there is a certain ratio between the seepage path length and the hydraulic head difference across the flood defense. This safe ratio depends on several factors: the thickness of the cover layer, the length of the dike section, and the applicable safety standard.

The safe ratio between seepage path length and head difference can be determined using the figures below. The technical guideline Piping Module describes how the parameters L (seepage path length), ΔH (head difference), and Dcover (cover layer thickness) should be defined.

If the ratio between the seepage path length and the head difference exceeds the values shown in the figures, the probability of backward erosion piping is considered acceptably low. However, if the ratio falls below these values, this generic decision rule indicates that the flood defence does not have evidently safe dimensions.(Rijkswaterstaat, 2023)

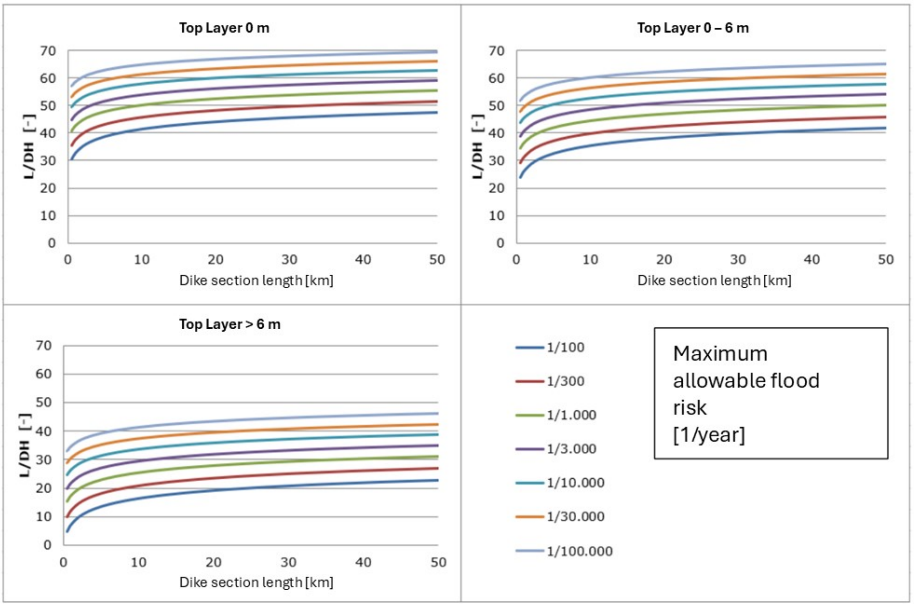

Figure B.1: Seepage length vs dike section (Rijkswaterstaat, 2023).

The calculation guide for assessing whether a dike is prone to piping is divided into three components: uplift, heave, and backward erosion piping (BEP).

For the uplift model, a probability of 1 is assumed. This is because the model only applies when the top layer is completely intact, without any cracks. However, cracks are an essential condition for piping to occur. It can be imagined that, in cases where the top layer is sufficiently thick, vertical equilibrium may be exceeded without cracks forming. This specific scenario is currently being investigated further (Rijkswaterstaat, 2023).

The calculation model for heave applies to situations where a cover layer is present. Although the model has only been partially validated through theoretical and laboratory research, exploratory studies are available in Beek et al., 2020. Therefore, for an initial estimation of flood probability, a conservative value for the critical heave gradient is used.

For BEP calculation, Sellmeijer is used. This is based on theoretical analysis, numerical calculations, and a calibration of sand properties based on physical model tests. There are conditions under which you can use this calculation method, which can be seen in table B.1, if these conditions are not met, extra explanation is needed.

Parameter	**Condition**
Grain diameter (d_{70})	150–500 µm
Relative density	> 50%
Uniformity (d_{60}/d_{10})	1.5–2.5
Fine fraction	Negligible; clean washed sand used
Aquifer composition	Homogeneous and isotropic sand, no structures
Seepage path length	0.3–15 m
Geohydrological conditions	Resistance-free infiltration at waterside, impermeable dike body and foreland, negligible influence from hinterland, no concentrated outflow to a hole
Seepage path orientation	Horizontal

Table B.1: Overview of conditions used in piping-related experiments (based on Deltares studies Rijkswaterstaat, 2012)

B.2. Uplift

As stated above, uplift is an important part of piping. If uplift does not occur, piping will not occur either. Uplift is driven by the weight of the impermeable soil layer against the uplift pressure of the water below. This can be calculated as explained below.

$$Z_u = \Delta\phi_{c,u} - (\phi_{exit} - h_{exit}) \tag{B.1}$$

with:
Z_u = Limit state function for uplift
h_{exit} = Phreatic level or height of the ground level
$\Delta\phi_{c,u}$ = Critical head difference for uplift to occur

$$\Delta\phi_{c,u} = \frac{D_{coverlayer}(\gamma_{sat} - \gamma_{water})}{\gamma_{water}} \tag{B.2}$$

with:
$D_{coverlayer}$ = Thickness of cover layer [m]
γ_{sat} = Saturated soil weight [kN/m^3]
γ_{water} = Weight of water [kN/m^3]

If the cover layer exists out of multiple layers the right part of the equation is the summation of these cover layers (Rijkswaterstaat, 2021).

B.3. Heave

Piping can only occur if the vertical exit gradient is exceeded. The limit state function for this failure mechanism is given below.

$$Z_h = i_{ch,h} - i = i_{c,h} - \frac{\phi_{exit} - h_{exit}}{D_{coverlayer}} \tag{B.3}$$

with:

Z_h = Limit state function for heave

$i_{c,h}$ = Critical heave gradient$[-]$

$D_{coverlayer}$ = Thickness of cover layer$[m]$

h_{exit} = Phreatic water table at the exit point$[m]$
(Rijkswaterstaat, 2021)

B.4. Backward erosion piping

The third condition for the occurrence of piping is the development of backward erosion piping. The stability factor, which determines this mechanism, is the ratio of he critical head difference to the actual head difference. The critical head difference is calculated using the Sellmeijer equation (Rijkswaterstaat, 2023).

$$Z_p = m_p \Delta H_c - (h - h_{exit} - r_c D_{coverlayer}) \tag{B.4}$$

$$\frac{\Delta H_c}{\gamma_n * \gamma_b} > (\Delta H - 0,3d) \tag{B.5}$$

with:

$$\Delta H_c = L \cdot F_{resitance} \cdot F_{scale} \cdot f_{geometry} \tag{B.6}$$

$$F_1 = F_{resistance} = \frac{\gamma_p^{'}}{\gamma_w}(\eta tan(\theta)) \tag{B.7}$$

$$F_2 = F_{scale} = \frac{d_{70m}}{\sqrt[3]{\kappa L}}(\frac{d_70}{d_{70m}})^{0,4} \tag{B.8}$$

$$F_3 = F_{geometry} \overset{MSeep}{=} F(G) \overset{standarddike}{=} 0,91 \cdot (\frac{D}{L})^{\frac{0,28}{(\frac{D}{L})^{2,8}-1}+0,04} \tag{B.9}$$

In which:

ΔH_c = critical hydraulic gradient

γ_n = safety factor

γ_b = schematization factor

ΔH = head loss across the water barrier [m]

d = thickness of the cover layer [m]

γ_p' = (apparent) unit weight of sand grains under water [kN/m^3]

γ_w = unit weight of water [kN/m^3]

θ = angle of repose of sand grains [°]

η = White's coefficient [-]

κ = intrinsic permeability of the piping-sensitive upper sand layer [m^2]

d_{70} = 70th percentile of the grain size distribution [m]

d_{70m} = average d_{70} in small-scale tests (2.08 × 10^{-4} m)

D = thickness of the sand layer [m]

L = horizontal length of the seepage path [m]

B.5. Combined probability

In practice, to define if a dike is safe, a parallel system is used between uplift, heave and BEP. If one of the failure probability requirement of a individual system is met, the total system is safe. The requirement, $P_{required}$, is given by the following formula:

$$P_{required} = P_{max} \cdot \omega \tag{B.10}$$

with:

$\omega = 0.24$

(Rijkswaterstaat, 2012)

To determine the safety of a complete dike trajectory, it is divided into separate cross-sections. If one cross-section fails the whole system fails. The failure probability requirement for a dike trajectory is as follows:

$$P_{required,i} = \frac{P_{max} \cdot \omega}{N} \quad \text{and} \quad N = 1 + \frac{a \cdot L_{trajectory}}{b} \tag{B.11}$$

with:

$a =$ length of dike trajectory sensitive to piping

$b =$ length of independent representative segments
(Technische adviescommissie voor de waterkeringen, 2001)

C

Appendix C - Testing method heave screens

To create the ability to use hydraulic properties to calculate soil properties, the equilibrium method explained in chapter 4.6.1 is created. Using soil weight and groundwater head the effective stress in the heave prism behind the screen can be determined. To make the use of this method easy a test sheet is made. In this test sheet all the boundary conditions added. These boundary conditions are based on the hydraulic conditions and geometry of the dike section. After filling in these conditions only the average head at the bottom of the prism needs to be computed. Using this average head, the test sheet will give the safety factor on heave.

Geometric assumptions at the uplift location

Ground level hinterland		[m NAP]	1
Bottom of cover layer hinterland		[m NAP]	0
Cover layer thickness hinterland		[m]	1
Watercourse		[-]	ja
Watercourse bed level		[m NAP]	-1.74
Watercourse depth		[m]	2.74
Water level in water course (polder level)		[m NAP]	0
		[m]	1.74
Watercourse width at ground level		[m]	8.5
Breedte waterbodem		[m]	0.5
width of canal bed	H1	[m]	1
Cover layer thickness under canal bed	H2	[m]	0
Effective cover layer thickness	H3	[m]	N.v.t.
Effective cover leyer thickness (2D effect)		[m]	0.00
Effective ground level (2D effect)		[m NAP]	-1.74
Effective watercourse width		[m]	0.00

Soil profile cover layer hinterland

Soil layer	Bottom	γ_{nat}	Eff thickness	Soil pressure
[-]	[NAP+m]	[kN/m^3]	[m]	[kPa]
Water in watercourse		10.0	1.74	17.4
Cover layer 1	0.00	16.1	0.00	0.0
			Total soil pressure	17.4

Geohydrological assumptions

River water level	$WBN_{+zet.comp}$	[m NAP]	6.79
Threshold potential	$\varphi_{grensp.}$	[m NAP]	0.00
Uplift channel resistance		[0,#d]	0
Piezometric head in longitudinal pipe	$\varphi_{langspijp}$	[m NAP]	0.00

Figure C.1: Heave test sheet part 1

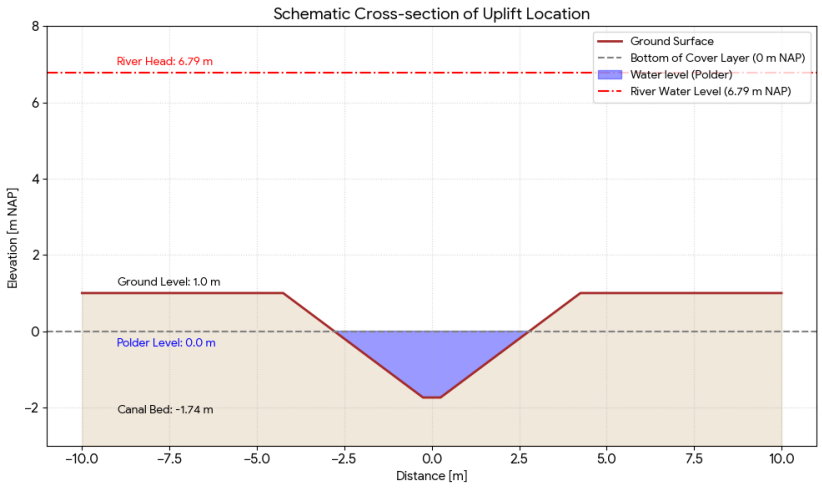

Figure C.2: Uplift location

In the two figures above the geometric and hydraulic boundary conditions for the exit location are displayed. This is used to determine the head in the pipe.

Heave test				
General				
Scenario		[-]	Brede pipe	
Remarks		[-]	25% van p' B=s/2	
Geometry				
Bottom gover layer at screen	z_3	[m NAP]	0	
Bottom screen*	z_1	[m NAP]	-3	* Derived iteratively from Plaxis
Screenlength into aquifer	s	[m]	3.0	
Prism width	B	[m]	1.5	
	B/s	[-]	0.5	
Width erosion pipe	b	[m]	1.5	
	b/s	[-]	0.5	
Hydraulic head profile at the top and bottom of the heave prism				
Average head top of prism	$\varphi_{b.k.;gem}$	[m NAP]	0.00	* Based on TUN VGO equal to the along pipe water level = ground surface level at the heave location, or polder water level
Average head bottom prism*	$\varphi_{o.k.;gem}$	[m NAP]	2.00	* This is a result from Plaxis. The average value can be determined in the 'Help' tab
Head difference	$\Delta\varphi$	[m]	2.00	
Waterpressure difference	**Δu**	**[kPa]**	**20.0**	
Vertical equilibrium method				
Surcharge				
Average surcharge*	p_{gem}	[kPa]	51	* Estimate based on an average ground surface level, taking into account possible instabilities
Average water pressure against bottom cover layer	p_{water}	[kPa]	0.00	
Average effective surcharge	p'_{gem}	[kPa]	51	
Percentage included		[%]	25%	
Included effective surcharge	p'	[kPa]	12.8	
Stress from sand				
Saturated weight sand	γ_{zand}	[kN/m^3]	20	
Effective stress from sand	p'_{zand}	[kPa]	30	
Total average effective stress (p'+p'$_{zand}$)*	**$\sigma'_{ok.hydro}$**	**[kPa]**	**42.8**	* Average effective stress at the level of the bottom of the screen, assuming hydrostatic water pressure from the underside of the cover layer
Safety factor	**SF_{VEM}**	**[-]**	**2.14**	

Figure C.3: Heave test sheet part 2

In figure C.3 the safety factor for heave is determined. The values in the light blue are the values needing to be filled in. The 2 most important values are the average head at the bottom of the

prism and the average surcharge. The first value is computed using Plaxis. This will first give you the distribution of groundwater head along the bottom of the prism. After computing the average of this distribution it can be filled in. For the average surcharge, forced by the cover layer, the thickness of the cover layer and dike at the screen is used. Because at the top of the prism the head is assumed to be the same as in the pipe, no direct vertical surcharge can be added. Therefore, they use 25% coming from the soil right of the heave prism. A schematization can be seen below.

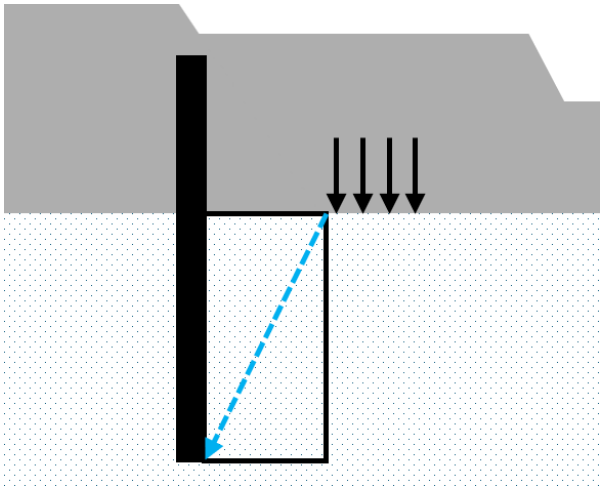

Figure C.4: Radiation of soil weight

The 25% is a conservative estimation of the spreading of soil weight over depth.

Appendix D - Different pipe systems

As addition to the wide longitudinal and narrow longitudinal pipe systems, different models were made as well. These models are not verified and therefore not mentioned in the rapport. They do however give an indication about the influence of the ways of modelling in 3D. The different scenarios are displayed in the figure below. A pipe system as shown in figure D.1a and figure D.1b are unrealistic, because if you would take a wide dike section, of 100 meters, a lot of sand need to be transported to create such a big pipe system. Therefore the other two situations are modelled. These situations are not exactly as in reality but represent it better than the other two.

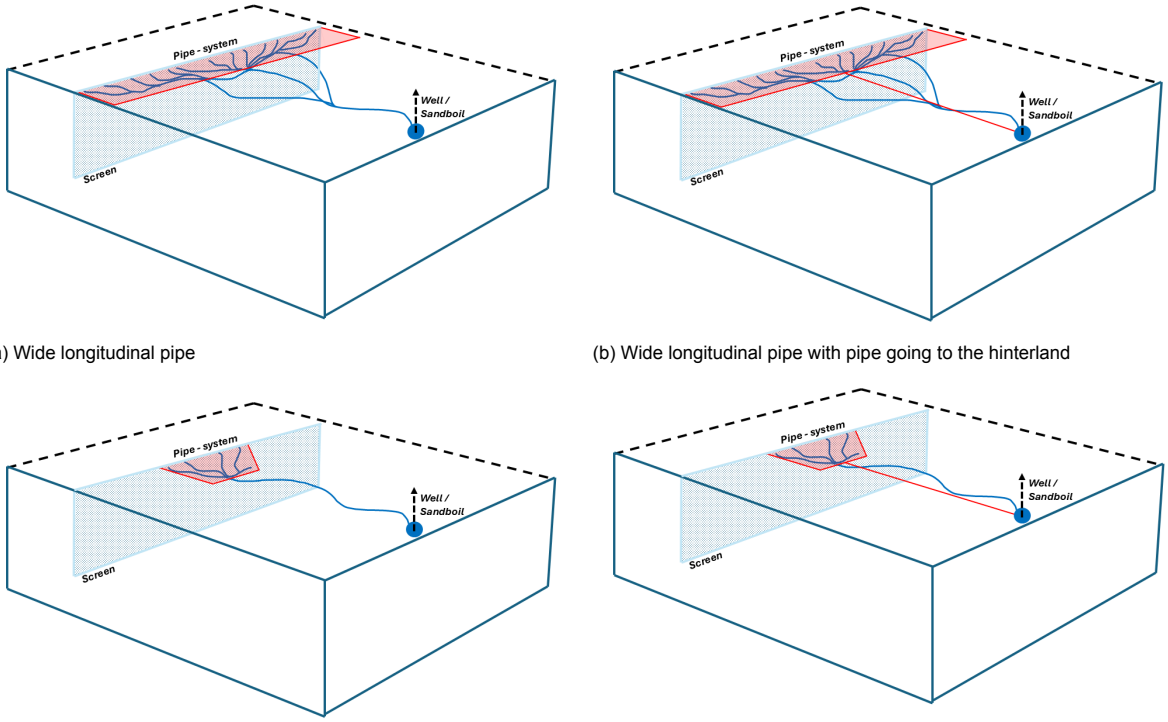

(a) Wide longitudinal pipe

(b) Wide longitudinal pipe with pipe going to the hinterland

(c) Tree like pipe system

(d) Tree like pipe system with pipe going to the hinterland

Figure D.1: Different pipe systems

The results computed can be seen in the figures below. The numerical values should not be used but it clearly shows that there is a difference in outcomes if the piping system is modelled more as in reality. More research is necessary to find a representative and tested model in 3D, to better understand the piping system in a wide dike section.

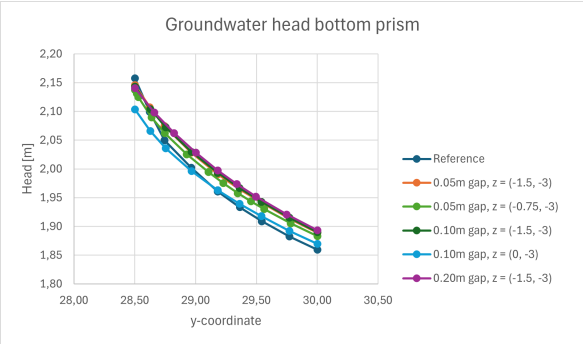

(a) Head of wide longitudinal pipe

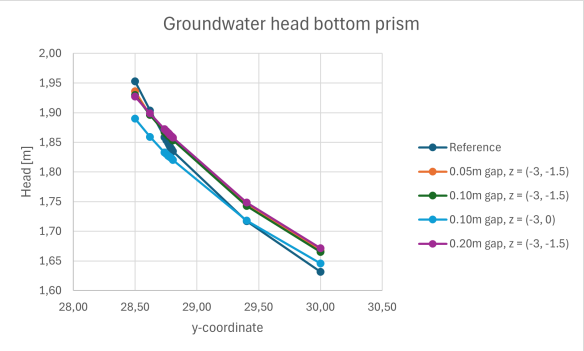

(b) Head of wide longitudinal pipe with pipe going to the hinterland

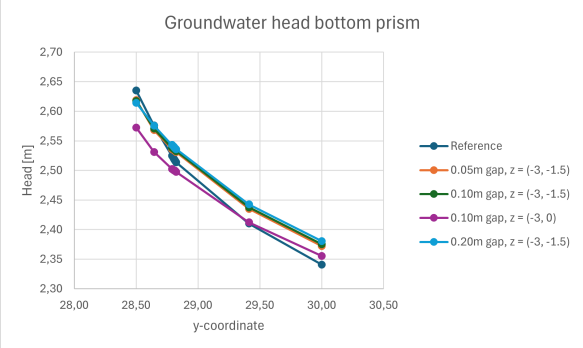

(c) Head of tree like pipe system

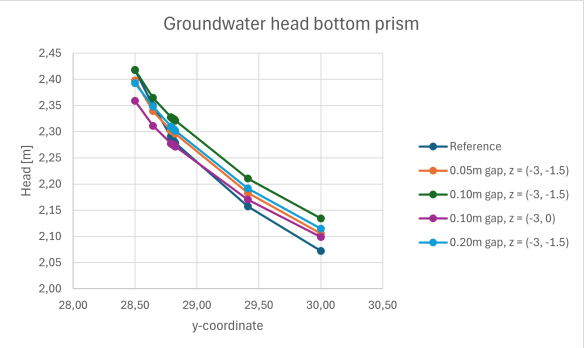

(d) Head of tree like pipe system with pipe going to the hinterland

Figure D.2: Groundwater head for different pipe systems

For the groundwater head can be seen that it increases a lot when a less wide zone is used compared to the wide longitudinal pipe over the total width of the dike section. This is concerning and therefore more research is needed on pipe development towards the screen. Furthermore, it can be seen that a pipe running to the hinterland reliefs pressure and makes it safer compared to a situation where no pipe is running to the hinterland.

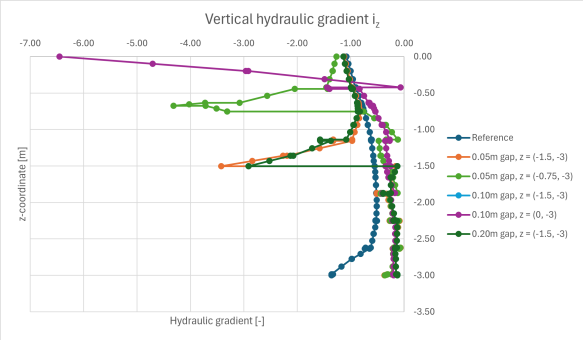

(a) Vertical hydraulic gradient of wide longitudinal pipe

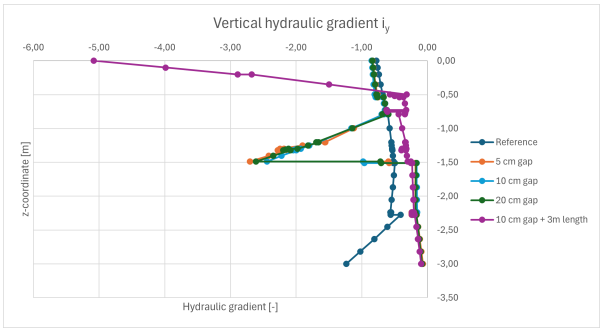

(b) Vertical hydraulic gradient of wide longitudinal pipe with pipe going to the hinterland

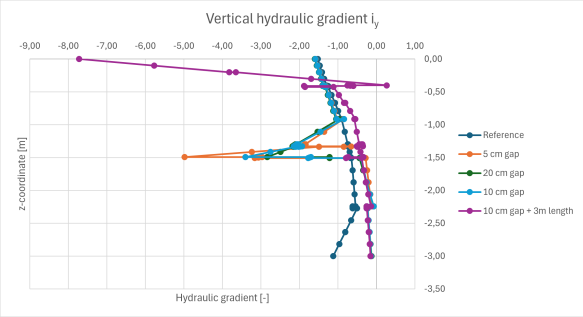

(c) Vertical hydraulic gradient of tree like pipe system

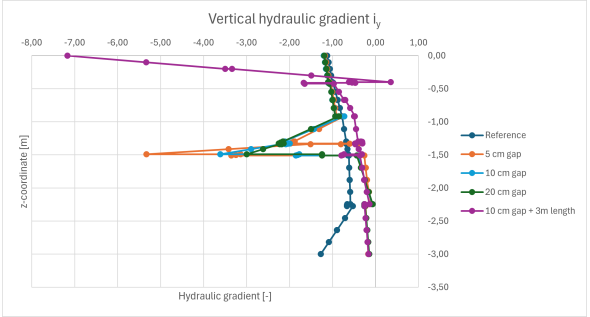

(d) Vertical hydraulic gradient of tree like pipe system with pipe going to the hinterland

Figure D.3: Vertical hydraulic gradient for different pipe systems

For the hydraulic gradient the difference is smaller. The hydraulic gradient at the gaps does change but the zone of influence does not. Therefore, it stays very local and not global. It can however still indicate vertical erosion.

Appendix E - Side view vertical hydraulic gradient 3D

In this appendix it can be seen that the vertical hydraulic gradient in between two gaps is decreasing very quickly with the amount of working sheet piles in between the gaps.

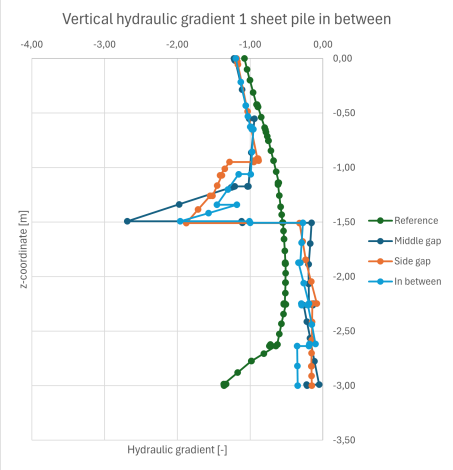

(a) Vertical hydraulic gradient 1 sheet pile in between

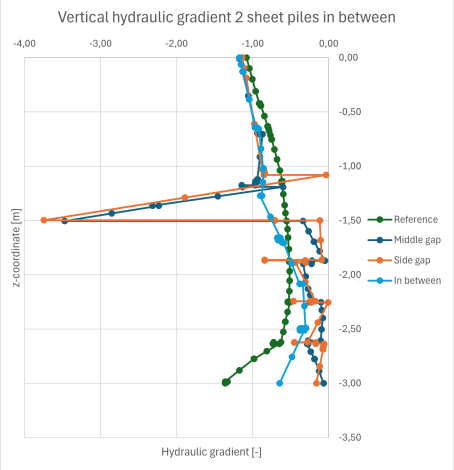

(b) Vertical hydraulic gradient 2 sheet piles in between

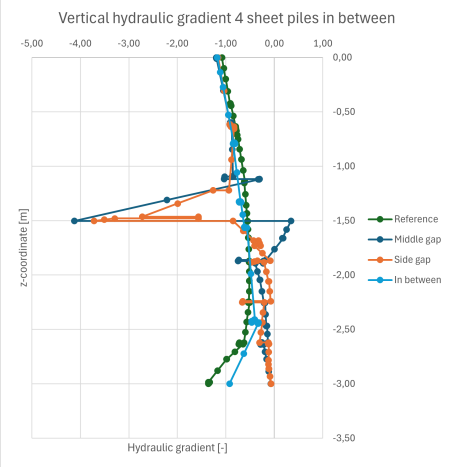

(c) Vertical hydraulic gradient 4 sheet piles in between

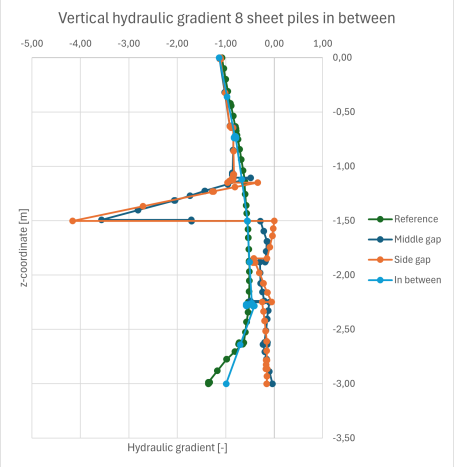

(d) Vertical hydraulic gradient 8 sheet piles in between

Figure E.1: Side view vertical hydraulic gradient different amount of working sheet piles in between